



UNIVERSIDADE D  
COIMBRA

Ariana Amorim Sena

**DEVELOPMENT AND OPTIMIZATION OF  
METHODOLOGIES TO ASSESS BUCCAL  
PERMEATION**

**Dissertação no âmbito do Mestrado em Biotecnologia Farmacêutica orientada  
pelo Doutor António Augusto Lucas dos Santos Nunes e pela Professora  
Doutora Carla Sofia Pinheiro Vitorino e apresentada à Faculdade de  
Farmácia da Universidade de Coimbra**

Julho de 2021





UNIVERSIDADE D  
COIMBRA

Ariana Amorim Sena

**DEVELOPMENT AND OPTIMIZATION OF  
METHODOLOGIES TO ASSESS BUCCAL  
PERMEATION**

**Dissertação no âmbito do Mestrado em Biotecnologia Farmacêutica orientada  
pelo Doutor António Augusto Lucas dos Santos Nunes e pela Professora  
Doutora Carla Sofia Pinheiro Vitorino e apresentada à Faculdade de  
Farmácia da Universidade de Coimbra**

Julho de 2021



***“Nothing in life is to be feared, it is only to be understood.  
Now is the time to understand more, so that we may fear less.”***

Marie Curie



## Acknowledgements

I would like to begin by thanking my mentor Dr. António Nunes, for the opportunity to grow as a professional and as a person within the team of Bluepharma. Thank you for always challenging me, for sharing your knowledge and for all the kindness shown.

To my mentor Dra. Prof. Carla Vitorino, for the constant availability and endless assistance in guiding me through this step of my academic life.

To Alain, for the tireless support along this journey. Thank you for always having the kindest words, for all the long hours, the motivational speeches and patience. For never doubting me and always inspiring me to be better.

I also thank the Research and Innovation team and all the members of Bluepharma who made me feel welcome by creating such a motivational environment in which I was glad to work; in particular to Alexandra, Andreia, Beatriz and Francisca for the words of encouragement, comprehension and all the fun moments.

To the professors who I have crossed paths with in these last few years, in particular to Dra. Prof. Ana Rita Figueiras, for the availability and interest shown in helping me achieving this goal.

I would like to thank André and Fábio, who always supported me and brought me laughter and joy through the most stressful moments. You made this year brighter.

To my parents, for being role models of humility, determination and compassion. The ones who never lost confidence in me and for whom I am very much grateful for.

To my brother, a true example of strength and persistence which I will keep admiring through our path together. For all the long night calls, the countless words of tranquilization in the most desperate moments and constant reminder to never give up.

To my friends from Celorico and Coimbra I owe a special thanks for all the encouragement, support and friendship. My life is more colorful because of the moments we share.







# Table of Contents

<b>Resumo</b> .....	<b>i</b>
<b>Abstract</b> .....	<b>iii</b>
<b>Motivation and Aims</b> .....	<b>v</b>
<b>Structure and organization of the Dissertation</b> .....	<b>vi</b>
<b>List of Abbreviations</b> .....	<b>vii</b>
<b>List of Figures</b> .....	<b>ix</b>
<b>List of Tables</b> .....	<b>xi</b>
<b>Chapter I. General Introduction</b> .....	<b>I</b>
<b>1.1. Structure of oral mucosa</b> .....	<b>3</b>
<b>1.2. Oromucosal according to oral cavity regions</b> .....	<b>6</b>
<b>1.3. Routes of permeation</b> .....	<b>8</b>
<b>1.4. Molecule parameters affecting drug permeability</b> .....	<b>11</b>
<b>1.5. Challenges to permeation</b> .....	<b>14</b>
<b>1.5.1. Saliva</b> .....	<b>15</b>
<b>1.5.2. Mucus layer</b> .....	<b>15</b>
<b>1.5.3. Enzymatic activity</b> .....	<b>15</b>
<b>1.5.4. Membrane-coating granules</b> .....	<b>15</b>
<b>1.5.5. Basement membrane</b> .....	<b>16</b>
<b>1.6. Strategies to enhance buccal permeation</b> .....	<b>16</b>
<b>1.6.1. Chemical permeation enhancers</b> .....	<b>17</b>
<b>1.6.2. Physical enhancers</b> .....	<b>19</b>
<b>1.7. Methods to assess permeability</b> .....	<b>19</b>
<b>1.7.1. In vivo methods</b> .....	<b>20</b>
<b>1.7.1.1. Buccal absorption test</b> .....	<b>20</b>
<b>1.7.1.2. Perfusion cells</b> .....	<b>21</b>
<b>1.7.1.3. Disc method</b> .....	<b>21</b>
<b>1.7.1.4. Raman probe device</b> .....	<b>22</b>
<b>1.7.2. Ex vivo methods</b> .....	<b>22</b>
<b>1.7.2.1. Porcine buccal mucosa</b> .....	<b>23</b>
<b>1.7.3. In vitro methods</b> .....	<b>26</b>
<b>1.7.3.1. Cell-based models</b> .....	<b>26</b>
<b>1.7.3.2. Artificial membranes</b> .....	<b>28</b>
<b>1.7.4. Apparatus</b> .....	<b>29</b>
<b>1.7.4.1. Franz diffusion chamber</b> .....	<b>30</b>
<b>1.7.4.2. Flow-through cell</b> .....	<b>31</b>
<b>1.7.4.3. Ussing chambers</b> .....	<b>32</b>
<b>Chapter 2. Method development</b> .....	<b>35</b>
<b>2.1. HPLC method development for content and permeation profile</b> .....	<b>37</b>
<b>2.1.1. Introduction</b> .....	<b>37</b>
<b>2.1.2. Method development</b> .....	<b>38</b>
<b>2.1.3. Assessment of results - HPLC method pre-validation</b> .....	<b>42</b>
<b>2.1.3.1. Specificity</b> .....	<b>43</b>

2.1.3.2. System precision .....	46
2.1.3.3. Detection limit (DL) and quantitation limit (QL) .....	47
2.1.3.4. Linearity .....	49
2.1.3.5. Accuracy .....	52
2.1.3.6. Stability .....	53
2.2. Franz Cell <i>in vitro</i> method development .....	54
2.2.1. Introduction .....	54
2.2.2. <i>Set-up</i> development .....	56
2.2.2.1. Temperature evaluation test.....	58
2.2.2.2. Filling procedure .....	59
2.2.2.3. Air bubbles entrapment .....	59
2.2.2.4. Collection and replacement techniques .....	60
2.2.2.5. Study conditions.....	64
2.2.2.6. Final risk assessment matrix.....	65
2.2.3. Evaluation of permeation profile of artificial membranes .....	67
2.2.3.1. Study conditions.....	68
2.2.3.2. Filters .....	68
2.2.3.3. Dialysis membrane .....	69
2.2.3.4. PermeaPad® Barrier membrane .....	70
2.2.4. Permeation studies using Permeapad® Barrier membrane.....	73
2.2.4.1. Finite dose vs infinite dose conditions .....	73
2.2.5. Inclusion of permeation enhancer.....	77
<b>Chapter 3. Concluding remarks and future perspectives .....</b>	<b>83</b>
<b>References.....</b>	<b>87</b>



## Resumo

O desenvolvimento e caracterização de formulações para administração na cavidade bucal requer uma metodologia apropriada e robusta para avaliação da permeabilidade através da mucosa bucal.

A presente dissertação teve como objetivo o desenvolvimento de um método de permeação bucal *in vitro* baseado numa membrana comercial biomimética - Permeapad<sup>®</sup> Barrier, segundo uma abordagem *Analytical quality by design* (aQbD). O trabalho experimental iniciou-se com o desenvolvimento de um método cromatográfico (cromatografia líquida de alta resolução em fase reversa) para análise do teor e perfil de permeação do composto ativo. Este processo consistiu na otimização das condições cromatográficas, com base nos parâmetros de desempenho, por meio de alterações nas condições iniciais do método analítico. Posteriormente, o método foi validado, considerando como parâmetros a seletividade, precisão, exatidão, linearidade e estabilidade, apresentando como limites de detecção e quantificação 0.0001 mg/mL e 0.001 mg/mL, respetivamente. O desenvolvimento das condições operacionais para os ensaios de permeação bucal *in vitro* foi baseado no uso de uma membrana Permeapad<sup>®</sup> Barrier, colocada numa célula de difusão de Franz. Foram aplicados elementos aQbD com o objetivo de otimizar o procedimento, com base nos parâmetros analíticos previamente identificados como críticos, especificamente, temperatura, enchimento, remoção de bolhas e colheita de amostras. Posteriormente, foram efetuados estudos de permeação para avaliação do perfil de permeação e determinação dos coeficientes de permeação através de membranas com diferentes características, incluindo a membrana de Permeapad<sup>®</sup> Barrier. Perante os perfis de permeação obtidos de forma bem-sucedida, foram realizados estudos para avaliação do impacto da dose aplicada - dose finita vs dose infinita - usando as condições operacionais previamente otimizadas. Os perfis de permeação não evidenciaram alterações significativas dos coeficientes de permeação obtidos em diferentes condições de dose aplicada. Por fim, foi avaliado o poder discriminatório da membrana Permeapad<sup>®</sup> Barrier, considerando a inclusão de um promotor de permeação na formulação. Tal conduziu a uma significativa potenciação de permeação em condições de dose infinita, o que suporta o poder discriminatório do método desenvolvido. No entanto, serão necessários mais estudos, incluindo promotores químicos que atuem segundo diferentes mecanismos de ação e variações na sua concentração de modo a possibilitar uma avaliação mais robusta da resposta do método relativamente a esta estratégia de melhoria de permeação.

Este trabalho permitiu o desenvolvimento bem-sucedido de um método de permeação bucal *in vitro* reprodutível, o qual poderá ser uma ferramenta útil a implementar na avaliação de formulações da Bluepharma.

**Palavras-chave:** mucosa oral; permeação bucal; método de permeação *in vitro*; membrana Permeapad<sup>®</sup> Barrier; promotores de permeação.

## **Abstract**

The development and characterization of formulations for administration in the oral cavity requires an appropriate and robust methodology for assessing permeability through the oral mucosa.

The present dissertation aimed the development of an *in vitro* buccal permeation method based on a biomimetic commercial membrane - Permeapad® Barrier membrane, following an analytical Quality by Design (aQbD) approach. The experimental work initiated with the development of a chromatographic method (Reverse Phase High Resolution Liquid Chromatography) for the analysis of the content and permeation profile of the active pharmaceutical ingredient (API). This process consisted in optimizing the chromatographic conditions, based on the performance parameters, by modifying the initial conditions of the analytical method. Then, the method was validated considering the parameters of selectivity, precision, accuracy, linearity and stability, presenting as detection and quantification limits 0.0001 mg/mL and 0.001 mg/mL, respectively.

The development of the *in vitro* permeation *set-up* was based on the use of a Permeapad® Barrier membrane placed in a Franz diffusion Cell apparatus. aQbD elements were applied to optimize the procedure based on analytical parameters previously identified as critical, specifically temperature, filling, bubble removal, and sampling. Permeation studies were then performed to evaluate the permeation profile and the determination of permeation coefficients through membranes with different properties, including the Permeapad® barrier membrane. Considering the successfully obtained permeation profiles, studies were performed to evaluate the influence of the applied dose - finite dose vs. infinite dose - using the previously optimized operating conditions. The permeation profiles showed no significant changes in the permeation coefficients obtained under the different conditions of applied dose. Finally, the discriminatory power of the Permeapad® barrier membrane was evaluated considering the inclusion of a permeation enhancer in the formulation. It resulted in significant permeation improvement under infinite dose conditions, supporting the ability of the developed method to discriminate regarding the inclusion of permeation enhancers. Moreover, further studies employing enhancers that act by other mechanisms of action with varying concentrations will provide a more robust evaluation of the method response to this permeation improvement strategy.

This work enabled the successful development of a reproducible and sensitive *in vitro* method for assessing buccal permeation, which could be a useful tool for the screening and characterization of Bluepharma formulations.

**Keywords:** oral mucosa; buccal permeation; *in vitro* permeation method; Permeapad<sup>®</sup> barrier membrane; permeation enhancers.



## **Motivation and Aims**

During the development and characterization of oral spray formulations, permeability across the buccal mucosa has to be considered. The buccal mucosa, although richly perfused, has a smaller surface area compared to other mucosae from the oral cavity, which is contradicted with the fact that it is considered a relatively good permeable region. In this context, the assessment of the permeation profile will allow the optimization of drug formulations as well as the comparison of formulations with different properties and, consequently, the impact of its components. Motivated to implement this capability in Bluepharma in-development formulations, the objectives of this experimental work are described below.

The major aim of the present dissertation is:

- To develop a reproducible *in vitro* permeation method able to predict permeability through the buccal region of the oral cavity and consequently enable the optimization - fine-tuning - of drug formulations.

Secondary objectives:

- To develop a selective and robust analytical method for quantification of the total amount of drug in the formulation - Content - and the amount of drug permeated - Permeation Profile;
- To assess the selectivity of the permeation method over permeation enhancers based on a biomimetic membrane - Permeapad® Barrier membrane.

Note: For confidentiality purposes, information regarding the API could not be disclosed.

## **Structure and organization of the Dissertation**

This Dissertation is divided into four chapters. **Chapter 1** reflects a literature review on the oral mucosa as a site for drug delivery, covering topics such as permeability barriers, transport pathways of permeation and existing methods to assess buccal permeation; relevant concepts for the development and assessment of the experimental work are also addressed throughout the dissertation.

As for **Chapter 2**, it presents the studies performed within the experimental work as well as the results obtained. It regards the development of an *in vitro* method for the assessment of the permeation of drug formulations, being sectioned into 2 parts: a first one (**Section 2.1.**), which includes the high performance liquid chromatography (HPLC)-based analytical method development for the quantification of the total amount of drug in the formulation - Content – and the amount permeated - Permeation Profile; while the **second one (Section 2.2.)** comprises the development of the method *set-up* and the procedure based on a Franz Cell apparatus, applying concepts of analytical quality by design.

The last chapter (**Chapter 3**) emphasizes the general conclusions of this work, and future studies that could be conducted for complementing the findings retrieved in this Dissertation.

Relevant bibliography is presented at the end of the Dissertation.

## ***List of Abbreviations***

<b>API</b>	Active Pharmaceutical Ingredient
<b>aQbD</b>	Analytical quality by design
<b>CAA</b>	Critical analytical attributes
<b>CMV</b>	Critical method variables
<b>DL</b>	Detection limit
<b>DS</b>	Drug Substance
<b>FD</b>	Finite dose
<b>HBD</b>	Hydrogen bond donors
<b>HPLC</b>	High performance liquid chromatography
<b>ID</b>	Infinite dose
<b>LogD<sub>6.8</sub></b>	Distribution coefficient at pH 6.8
<b>LogP</b>	Partition coefficient
<b>MCGs</b>	Membrane coating granules
<b>MV</b>	Molecular volume
<b>nRotBs</b>	Number of hydrogen bond donors
<b>OC</b>	Oral cavity
<b>PBS</b>	Phosphate buffered saline
<b>PDA</b>	Photo diode array
<b>QbD</b>	Quality by design
<b>QL</b>	Quantification limit
<b>RF</b>	Response factor
<b>RSD</b>	Relative standard deviation
<b>SD</b>	Standard deviation



## List of Figures

Figure 1 - Localization and extent of masticatory, lining and specialized mucosa in the oral cavity. (Adapted from (5)).....	4
Figure 2 - A. Structure of the oral mucosa and respective layers; B. Process of differentiation of oral epithelium; B. I. Layers in keratinized tissues (masticatory mucosa and specialized mucosa); B. II. Layers in non-keratinized tissues (lining mucosa). (Adapted from (9)).....	5
Figure 3 - Mechanisms of drug transport through oral mucosa. ....	10
Figure 4 - Schematic representation of the correlations between buccal permeation and significant molecular descriptors. ....	14
Figure 5 - Graphic representation of the permeation barriers. Key: MCGs = membrane coating granules.....	14
Figure 6 - Schematic representation of the available methods to assess buccal permeability.....	20
Figure 7 - Schematic representation of the procedure conditions in porcine buccal mucosa <i>ex vivo</i> permeation studies.....	23
Figure 8 - Tissue harvesting procedure (63).....	24
Figure 9 - MatTek EpiOral™ (78).....	27
Figure 10 - Permeapad® Barrier membrane (95).....	28
Figure 11 - Liposomal gel-like structure of Permeapad® Barrier membrane.....	28
Figure 12 - Schematic representation of available impregnated artificial membranes: type of membrane and impregnated solutions. ....	29
Figure 13 - A. Standard vertical Franz Cell; B. Side-by-side Franz Cell (94).....	30
Figure 14 - Schematic representation of a flow-through diffusion cell (1).....	32
Figure 15 - Ussing Diffusion Chamber (88). ....	32
Figure 16 - Schematic representation of HPLC-PDA.....	37
Figure 17 - Schematic representation of the separation process within the HPLC column. A. Mixture entering the column with the stationary phase; B. Analytes separated by polarity.....	38
Figure 18 - Chromatogram of API solution at 0.05 mg/mL in the solvent described in Table 10.....	39
Figure 19 - Chromatogram of API standard solution at 0.05 mg/mL in PBS pH=7.4 and instrumental conditions described in Table 10.....	39
Figure 20 - Chromatogram of API standard solution at 0.6 mg/mL in PBS pH=7.4 with the new mobile phase.....	40
Figure 21 - Chromatogram of API standard solution at 0.2 mg/mL in PBS pH=7.4 with the new method conditions.....	41
Figure 22 - Chromatograms obtained from specificity method assessment: a) Selectivity: Blank Solution (PBS pH=7.4) (zoomed chromatogram); b) Selectivity: Placebo at content concentration (zoomed chromatogram); c) Formulation after permeation in set-up with Permeapad® membranes (zoomed chromatogram); d) Selectivity: Standard solution at 100% ( $C_{API} \approx 0.20$ mg/mL); e) Selectivity: Standard solution at 100% ( $C_{API} \approx 0.20$ mg/mL) (zoomed chromatogram).....	45
Figure 23 - Linear regression for API in theoretical content concentration ( $C_{API} \approx 0.20$ mg/mL).....	50
Figure 24 - Linear regression for API in theoretical permeation concentration ( $C_{API} \approx 0.33$ mg/mL). 51	51
Figure 25 - Representation of the Ishikawa diagram. ....	56
Figure 26 - Sequence representation of air bubbles removal process. A. Franz Cell removal of the stirring system; B. Start of turning the Franz Cell; C. Franz Cell turned at a ~90-degree angle; D. Franz	

Cell turned at a ~100-degree angle, air bubbles being released through the sampling port while tapping on the bottom.....	60
Figure 27 - Needle plus a tube technique.....	60
Figure 28 - Micropipette plus a tube technique.....	60
Figure 29 - Micropipette tip plus a small-caliber tube technique.....	61
Figure 30 - Receptor solution replacement tip.....	62
Figure 31 - Permeagear® micropipette tips assembly (94).....	62
Figure 32 - Permeation profile phases: Lag time, Steady-State and 'plateau' phase.....	67
Figure 33 - Permeation profile using (a) 0.2 µm polypropylene filters and (b) 80 µm nylon filters.....	69
Figure 34 - Representation of the (a) Permeation profile and (b) Steady-State slope from the permeation study using a dialysis membrane.....	70
Figure 35 - Representation of the (a) Permeation profile and (b) Steady-State slope from the permeation study using a PermeaPad® Barrier membrane.....	71
Figure 36 - Representation of the (a) Permeation profile and (b) Steady-State slope from the permeation study (#2) using a PermeaPad® Barrier membrane.....	72
Figure 37 - Representation of the (a) Permeation profile and (b) Steady-State slope from the permeation study using a PermeaPad® Barrier membrane under finite dose conditions.....	74
Figure 38 - Representation of the (a) Permeation profile and (b) Steady-State slope from the permeation study using a PermeaPad® Barrier membrane under infinite dose conditions, collecting 500uL of receptor solution.....	75
Figure 39 - Representation of the (a) Permeation profile and (b) Steady-State slope from the permeation study using a PermeaPad® Barrier membrane under FD conditions collecting 0.2mL and ID conditions collecting 500uL of receptor solution.....	76
Figure 40 - Representation of (a) permeation profile and (b) apparent permeability ( $P_{app}$ ) from the permeation study applying the formulation without permeation enhancer (FT) and upon the inclusion of permeation enhancer A. (FT with Permeation Enhancer A.); under FD conditions collecting 200µL of receptor solution. Results are expressed as mean ± standard deviation.....	79
Figure 41 - Representation of (a) permeation profile and (b) apparent permeability ( $P_{app}$ ) chart from the permeation study applying the formulation without permeation enhancers (FT) and upon the inclusion of permeation enhancer A. (FT with Permeation Enhancer A.); under ID conditions collecting 500µL of receptor solution. Results are expressed as mean ± standard deviation, n=6. Apparent permeability ( $P_{app}$ ) values were considered significantly different ( $p<0.05$ ) based on a Student's <i>t</i> -test analysis.....	80

## List of Tables

Table 1 - Types of oral mucosa: function, regions covered and relative extent in the oral cavity. ....	4
Table 2 - Characteristics of oromucosal sites of the oral cavity. ....	8
Table 3 - Definitions of molecular descriptors significant for buccal permeation. ....	13
Table 4 - Classes and examples of permeation enhancers employed in buccal mucosal permeation..	18
Table 5 - Schematic representation the <i>in vivo</i> buccal absorption test with the related advantages and limitations (I). Key: OC = Oral Cavity. ....	20
Table 6 - Schematic representation of the <i>in vivo</i> perfusion cell test with the related advantages and limitations (I). Key: OC = Oral Cavity. ....	21
Table 7 - Advantages and disadvantages of the disc <i>in vivo</i> method. ....	22
Table 8 - Schematic representation of the <i>in vivo</i> Raman probe device with the related advantages and limitations. ....	22
Table 9 - Main processing tissue methods comparison. ....	25
Table 10 - Initial analytical method conditions for development. ....	38
Table 11 - Performance parameters for API standard solution at 0.05 mg/mL. ....	39
Table 12 - Performance parameters for API standard solution at 0.05 mg/mL in PBS pH=7.4 and instrumental conditions described in Table 10. ....	40
Table 13 - Performance parameters for API standard solution at 0.6 mg/mL in PBS pH=7.4 with the new mobile phase. ....	41
Table 14 - Performance parameters for API standard solution at 0.2 mg/mL in PBS pH=7.4 with the new method conditions. ....	41
Table 15 - Analytical method conditions for pre-validation. ....	42
Table 16 - Parameters and respective acceptance criteria for analytical method development. Key: RSD = relative standard deviation; DL = Detection limit; QL = Quantification limit; S/N =signal/noise ....	43
Table 17 - Performance evaluation results of API peak. ....	46
Table 18 - System precision results for API standard solution at 100% of the theoretical content concentration ( $C_{API} \approx 0.20$ mg/mL). Key: RF = response factor; RT = retention time; SD = standard deviation; RSD = Relative standard deviation. ....	47
Table 19 - System precision results for API standard solution at 100% of the theoretical permeation concentration ( $C_{API} \approx 0.33$ mg/mL). Key: RF = response factor; RT = retention time; SD = standard deviation; RSD= relative standard deviation. ....	47
Table 20 - System precision results evaluation. Key: RF = response factor; RSD = relative standard deviation. ....	47
Table 21 - Detection Limit and Quantitation Limit by S/N ratio. ....	48
Table 22 - API permeation accuracy results at 0.3%. Key: RSD = relative standard deviation; CI = confidence interval. ....	48
Table 23 - Evaluation of API accuracy at 0.3% (0.001 mg/mL). Key: RSD = relative standard deviation. ....	49
Table 24 - Linearity results for API in theoretical content concentration ( $C_{API} \approx 0.20$ mg/mL). Key: RF = response factor. ....	50
Table 25 - Linearity results for API in theoretical permeation concentration ( $C_{API} \approx 0.33$ mg/mL). Key: RF = response factor. ....	50

Table 26 - Linearity results evaluation for API in theoretical content concentration ( $C_{API} \approx 0.20$ mg/mL). .....	51
Table 27 - Linearity results evaluation for API in theoretical content concentration ( $C_{API} \approx 0.33$ mg/mL). .....	51
Table 28 - Evaluation of accuracy results. Key: RSD = relative standard deviation; CI = confidence interval. ....	52
Table 29 - Results evaluation for $C_{API}$ standard solution in vials kept inside the autosampler at 20°C. .....	53
Table 30 - Assessment of results from HPLC Method Pre-Validation. Key: RSD = relative standard deviation, CI = confidence interval; S/N = signal-to-noise.....	54
Table 31 - Initial risk assessment for IVPT method optimization. Criticality was assessed based on the impact of CMV on CAAs, i.e., permeability flux at steady state ( $J_{ss}$ ), apparent permeability ( $P_{app}$ ) and lag time. ....	57
Table 32 - Temperature (°C) of the set-up components.....	58
Table 33 - Collection techniques precision and accuracy results. ....	60
Table 34 - Precision and accuracy of the micropipette tips collecting 100µL.....	61
Table 35 - Precision and accuracy of the micropipette tips collecting 200µL.....	61
Table 36 - Precision and accuracy results of the micropipettes collecting 200µL from 19/10/2020 and 16/12/2020.....	62
Table 37 - Precision and accuracy of the PermeGear® micropipette tips collecting 100µL. ....	63
Table 38 - Precision and accuracy of the PermeGear® micropipette tips collecting 200µL. ....	63
Table 39 - Precision and accuracy of the PermeGear® micropipette tips collecting 500µL.....	63
Table 40 - API concentration saturation in the receptor medium (PBS pH=7.4).....	65
Table 41 - Final risk assessment for IVPT method optimization. Criticality was assessed on the basis of the impact of CMV on CAA i.e. permeability flux at steady state ( $J_{ss}$ ), apparent permeability ( $P_{app}$ ) and lag time. ....	66
Table 42 - Final risk assessment matrix from analytical quality by design approach. ....	66
Table 43 - Permeation Studies summary using different artificial membranes.....	72
Table 44 - Assessment of sink conditions at time points 240min, 360min and 480min from collecting 200µL of the receptor solution under Finite dose conditions. Key: SS = steady-state. ....	74
Table 45 - Assessment of sink conditions at time points 240min, 360min and 480min from collecting 500µL of the receptor solution under infinite dose conditions.....	76
Table 46 - Permeability coefficients results from Finite Dose (FD) conditions collecting 200µL; Infinite Dose (ID) conditions collecting 500µL.....	77
Table 47 - Permeability coefficients results from the permeation study with i) formulation and ii) formulation including permeation enhancer A.; under finite dose conditions. Results are expressed as mean ± standard deviation, n=2* and n=3** . ....	78
Table 48 - Permeability coefficients results from the permeation study with i) formulation and ii) formulation including permeation enhancer A, under infinite dose conditions. Results are expressed as mean ± standard deviation, n=6. ....	80







# *Chapter 1.*

## *General Introduction*



## 1.1. Structure of oral mucosa

The **oral cavity** (OC) corresponds to the region within the mouth and has an estimated surface area of 200 cm<sup>2</sup> (1). OC is comprised by the lips and teeth; the cheeks, that form the lateral wall of the buccal cavity; the palate, situated between the buccal and nasal cavity, which can be divided into hard palate (bony partition) and soft palate (muscular back portion); and lastly, the floor of the mouth, beneath the tongue.

All these regions are coated by a protective mucous layer denominated oral mucosa and surrounded by the environment of the oral cavity. Its physiological environment - pH, fluid volume and composition - is mainly regulated by the secretion of saliva. **Saliva** is a moderately viscous aqueous fluid secreted by the major salivary glands (parotid, submandibular and sublingual glands) and other minor gland of the submucosa (2). It is composed mostly of water and a much lesser percentage of organic and inorganic materials. This oral fluid is constantly being secreted and removed from the OC, maintaining a moist oral cavity with a pH close to neutrality (6.7 to 7.3) (3), as well as a daily volume of between 1 L and 1.5 L (4), which is the amount of fluid that is available to hydrate oral mucosal dosage forms.

As part of saliva, a viscoelastic adhesive intercellular substance identified as mucus is synthesized, surrounding the cells of the oral epithelium. **Mucus** binds to the epithelial cell surface as a continuous gel layer with an average thickness of 50-450 μm (5), and provides both protection and lubrication to the mucosal membrane. Its main components are mucins and carbohydrates. Mucins are highly glycosylated large glycoproteins, which can assemble into three-dimensional mucus network (6). At physiological salivary pH, this network is negatively charged due to the presence of sialic acids and sulfate residues, leading to the formation of a strongly cohesive gel structure, which in turn plays a role in cell-cell adhesion (7). Also, as part of the oral cavity environment, some proteolytic enzymes are present on the mucosal surface such as carboxypeptidases, aminopeptidases, endopeptidases, and esterases (8).

Furthermore, the biological environment of the OC is constantly changing and being exposed to potentially damaging external factors. In this context, the primary and essential function of the **oral mucosa** is to protect the underlying tissues from microorganisms, while offering resistance to mechanical injury. **Oral mucosa** can be classified according to its location and respective function within the OC into: masticatory, lining and specialized mucosa. All of these types of mucosa are characterized in Figure 1 and Table I, in terms of their function and the regions covered (including the percentage of coverage):

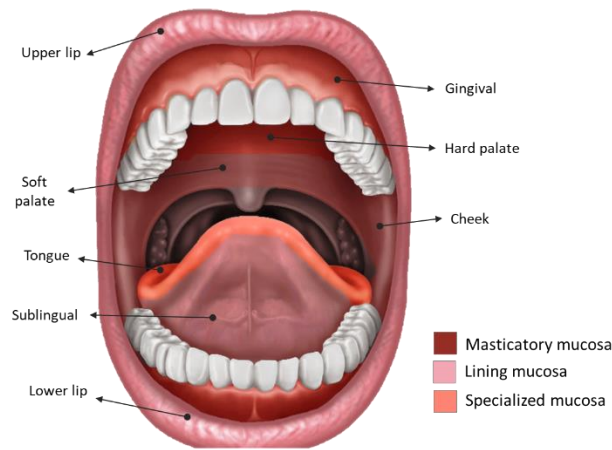


**Figure I** - Localization and extent of masticatory, lining and specialized mucosa in the oral cavity. (Adapted from (5))

**Table I** - Types of oral mucosa: function, regions covered and relative extent in the oral cavity (6, 11, 10).

Type of oral mucosa	Function	Regions covered within oral cavity	Relative extent in the oral cavity
<i>Masticatory mucosa</i>	Chemical resistance and mechanical strength	Gingiva Hard palate	25%
<i>Lining mucosa</i>	Elasticity for movements such as mastication and speech	Lips Cheeks Sublingual Soft palate	60%
<i>Specialized mucosa</i>	Sensorial system by the presence of taste buds	Dorsal surface of the tongue	15%

Regarding the **structure** of the oral mucosa, three layers can be distinguished: oral epithelium, lamina propria and submucosa (Figure 2).

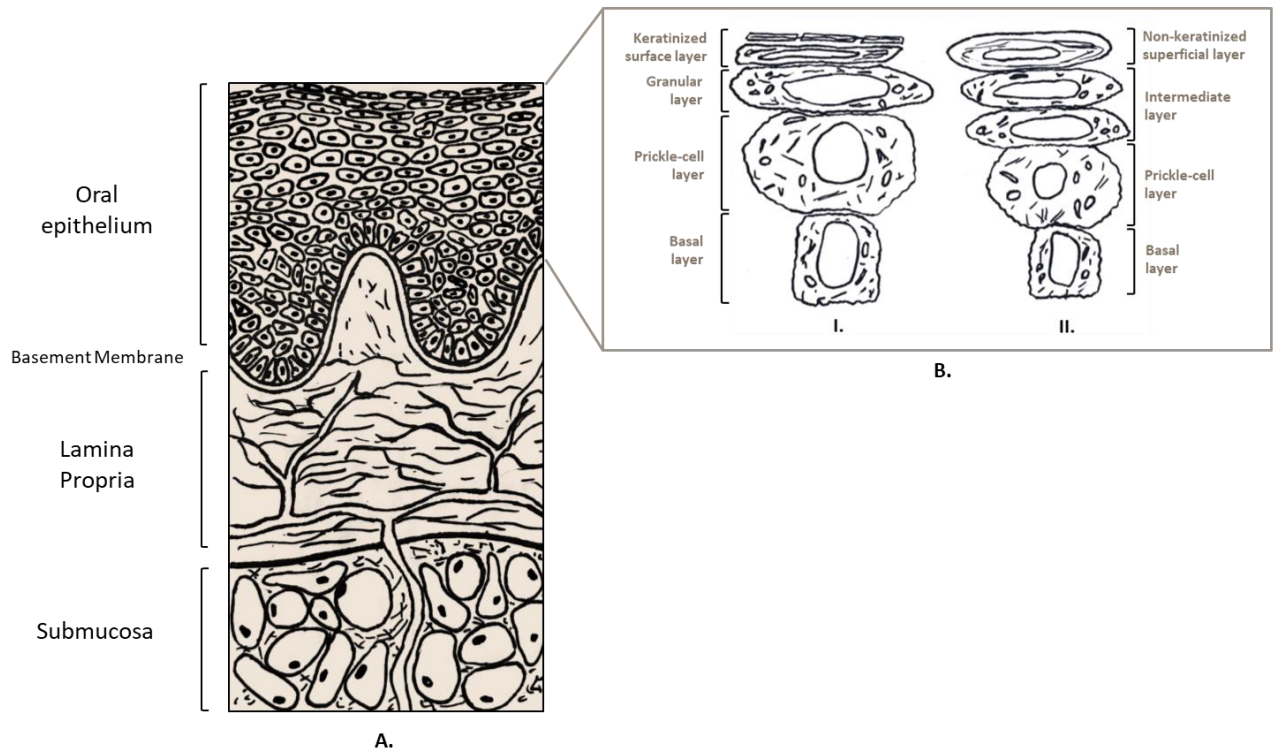


**Figure 2 - A.** Structure of the oral mucosa and respective layers; **B.** Process of differentiation of oral epithelium; **B. I.** Layers in keratinized tissues (masticatory mucosa and specialized mucosa); **B. II.** Layers in non-keratinized tissues (lining mucosa) (9,10,11,12). (Adapted from (9)).

The **oral epithelium** is the most superficial layer of the oral mucosa and acts as a mechanical barrier, protecting the underlying tissues and glands of the oral cavity and providing a barrier against toxins and microorganisms (10). It consists of a basal cell layer with mitotically active cells that differentiate into larger and flatter cells (11) as they begin to accumulate lipids that progress through intermediate layers to reach the superficial layer of the epithelium (6). The process of differentiation itself and the lipid composition varies along the different regions of the oral mucosa, resulting in two types of epithelium: keratinized (as in the masticatory and specialized mucosae) and non-keratinized (as in the lining mucosa) (see Figure 2.). Each type of oral mucosa has different epithelium structural features.

In all types of oral mucosa, as cells reach the prickle cell layer, small organelles known as membrane-coating granules (MCGs) are formed (10), as a result of lipid accumulation. MCGs are oval intracellular vesicles which, based on the oral mucosal site, produce distinct types of lipids (5).

Common to all types of OM is a continuous elastic membrane of extracellular material of about 1-2  $\mu\text{m}$  thickness that connects the epithelium to the lamina propria - the basement membrane (11). The **basement membrane** appears as an undulating boundary being considered the most stable layer of the oral mucosa, providing strength to the structure and adherence between the epithelium and lamina propria (9). It is a trilaminar structure composed of collagen arranged as a highly ordered network (9), glycoproteins and lipids (12).

Below the basement membrane lies the **lamina propria** which contains collagen and elastic fibers in a hydrated ground substance rich in blood capillaries and nerve fibers (9), providing support and nutrients to the mucosa (10). While in the masticatory mucosa this layer is thick and connects the oral mucosa directly to the underlying periosteum of the bone, the lamina propria in the lining mucosa is particularly thin and elastic in comparison. These differences are related to the fact that the masticatory mucosa has no other layers beneath these regions, whereas in the lining mucosa its function is critical to provide elasticity for movements.

In certain types of oral mucosa (lining and specialized mucosa), one can identify an innermost layer called the **submucosa**. It is formed by arteries, veins, capillaries, nerves, and lymphatic vessels, which extend through the overlying layer to supply nutrients to the tissues (13).

## 1.2. Oromucosal according to Oral cavity regions

Each of the three types of functional mucosae (masticatory, lining and specialized mucosa) can be found covering different regions of the oral cavity and are therefore classified as buccal, sublingual, gingival and palatal (from either soft and hard palate) mucosa. Each of these mucous membranes, has considerable differences in structure, blood flow and environmental pH, which in turn leads to distinct applications.

The **buccal mucosa** is identified as the coating of the cheeks as well as the area between the gums and back of the lips, and represents the largest of all sites, with an area of  $50\text{ cm}^2$  (1). It is characterized by a 500-600  $\mu\text{m}$  thick non-keratinized epithelium with an estimated turnover time of 5-7 days (14). The blood flow of the buccal mucosa is of the order of  $2.4\text{ mL}\cdot\text{min}^{-1}\cdot\text{cm}^{-2}$  (11), and in the Rhesus monkey was observed to be  $20.3\text{ mL}/\text{min}/100\text{ g tissue}$  (15). Moreover, the average pH in this region is approximately 6.7 to 7.3 (3).

The buccal mucosa has a rich blood supply, high accessibility, and relatively rapid cellular recovery after local stress and damage (14). Based on these characteristics, it is considered to be the preferred route for the administration of molecules with slower onset but longer duration of action, i.e., when sustained and systemic transmucosal drug delivery is required



(6). Moreover, it is considered the most appropriate site for the treatment of chronic disorders.

The **sublingual mucosa** delineates the floor of the mouth with an average surface area of 26.5 cm<sup>2</sup> (16). The respective epithelium is non-keratinized and has a thickness of approximately 100-200 μm (17). The blood flow of the sublingual mucosa is slower compared to the buccal mucosa and is of the order of 1.0 mL.min<sup>-1</sup>.cm<sup>-2</sup> (11); in the Rhesus monkey it was observed to be 12.2 mL/min/100 g of tissue (15). In addition, the average pH in this region is approximately 6.5±0.3 (18).

Being relatively thin and owing to its non-keratinized structure, it has been demonstrated to have the highest permeability to drugs of all the routes (19). For this reason, it is the most appropriate route when rapid onset of action is desired, as it provides rapid access to the systemic circulation, and is therefore generally suitable for highly permeable drugs with an infrequent dosing regimen, i.e., for the treatment of acute disorders (14).

The **gingival and palatal mucosa** (soft and hard palatal mucosa) delineates the gingiva and palatal tissues, respectively. Both epithelia are keratinized and similar in thickness: gingival has 250 μm and palatal mucosa 200 μm (11). The blood flow of these mucosae in Rhesus monkey was 19.5 mL/min/100 g tissue for gingival mucosa; and in the case of palatal mucosa, it was 7.0 mL/min/100 g tissue (15). The mean pH values in gingival and palatal mucosa are 6.8±0.26 and 6.28±0.36, respectively (18). The palatal mucosa has the lowest blood flow of all regions, especially the hard palate, while the gingival region has high blood flow, although slower than the buccal mucosa (15).

These are less permeable than the buccal and sublingual areas (20). The gingival and palatal mucosae keratinized epithelium is considered inappropriate to the systemic drug delivery of drugs, being useful only for the treatment of oral disease localized at the gingiva or palate.

Table 2 shows the characteristics of the oromucosal sites of the oral cavity: buccal mucosa, sublingual mucosa, gingival mucosa, and palatal mucosa.

**Table 2** - Characteristics of oromucosal sites of the oral cavity (6, 1, 14, 15).

	Buccal mucosa	Sublingual mucosa	Gingival mucosa	Palatal mucosa
Epithelium Thickness	500-600 $\mu\text{m}$	100-200 $\mu\text{m}$	250 $\mu\text{m}$	200 $\mu\text{m}$
Degree of Keratinization	Non-Keratinized	Non-Keratinized	Keratinized	Hard palate: Keratinized  Soft palate: Non-Keratinized
Expected Permeability	Sublingual>Buccal>Palatal>Gingival			
Blood Flow	Buccal>Gingival>Sublingual>Palatal			
pH value	6.7-7.3	6.5 $\pm$ 0.3	6.8 $\pm$ 0.26	6.28 $\pm$ 0.36

Both the degree of keratinization and epithelium thickness have been negatively correlated with oromucosal permeation. The sublingual and buccal mucosae, being non-keratinized, are expected to display a higher permeability in comparison to the gingival and palatal higher degree of keratinization. Also, as the sublingual mucosa is characterized by the thinnest epithelium, it is expected to have the highest permeability of all mucosae.

Comparing the buccal mucosa with the gingival and palatal mucosae, it can be assumed that the degree of keratinization has a greater influence on oromucosal permeability than epithelium thickness itself, as the buccal mucosa has a higher permeability despite its thicker mucosa. Moreover, a higher epithelium thickness has been associated with higher blood flow in the respective mucosa (21).

### 1.3. Routes of permeation

There are two possible routes by which drugs can pass through the oral mucosa: the paracellular and the transcellular routes. The **paracellular route**, also known as the intercellular route, involves passage between cells through the intercellular spaces of the extracellular lipid domain, whereas the **transcellular route** or intracellular route involves transversing the epithelium through the membrane cells (22).

As the epithelial layer of the oral mucosa is both hydrophilic and lipophilic (6), the permeation route will be influenced by the properties of the drug. The more polar route characterized by dispersed and loose intercellular lipids, that is the **paracellular route**, is the main route for

hydrophilic (water-soluble) drugs which traverse this route via aqueous channels associated with the polar head groups of lipids; as for the lipophilic (lipid-soluble) drugs, these may permeate by diffusion through the lipid intercellular matrix (14). The main limitation of this route is the small area available (23).

The **transcellular route** is the pathway preferred for lipophilic drugs because the cell membrane is lipophilic in nature. Hydrophilic compounds can pass through the intracellular matrix through aqueous pores of individual epithelial cells (23), which is probably limited to small molecules (9). This non-polar route requires the drug to alternatively cross the hydrophilic and lipophilic phases of the epithelial cell, i.e., considerable and significant aqueous and lipid solubilities is required (9). As a result, this pathway offers significant diffusional resistance despite having a greater surface area available (14).

Overall, both routes can be an option for drug absorption, although depending on the physicochemical properties of the drugs, the one that offers the least penetration resistance for passage is usually preferred (7).

The flux of drug through the membrane under sink conditions for paracellular route can be written as *Equation 1*:

$$J_p = \frac{D_p \varepsilon}{h_p} C_d \quad (\text{Equation 1})$$

Where,  $D_p$  corresponds to the diffusion coefficient of the permeate in the intercellular spaces,  $h_p$  is the path length of the paracellular route,  $\varepsilon$  stands for the area fraction of the paracellular route and  $C_d$  is the donor drug concentration (21,24).

The flux of drug through the membrane under sink conditions for transcellular route can be written as *Equation 2*:

$$J_c = \frac{(1 - \varepsilon) D_c K_c}{h_c} C_d \quad (\text{Equation 2})$$

Where,  $K_c$  corresponds to the partition coefficient between lipophilic cell membrane and the aqueous phase,  $D_c$  is the diffusion coefficient of the drug in the transcellular spaces and  $h_c$  stands for the path length of the transcellular route (21,24).

The **mechanisms** by which drugs are transported into or across the mucosal membrane are passive diffusion, carrier-mediated transport, or endocytosis (Figure 3).

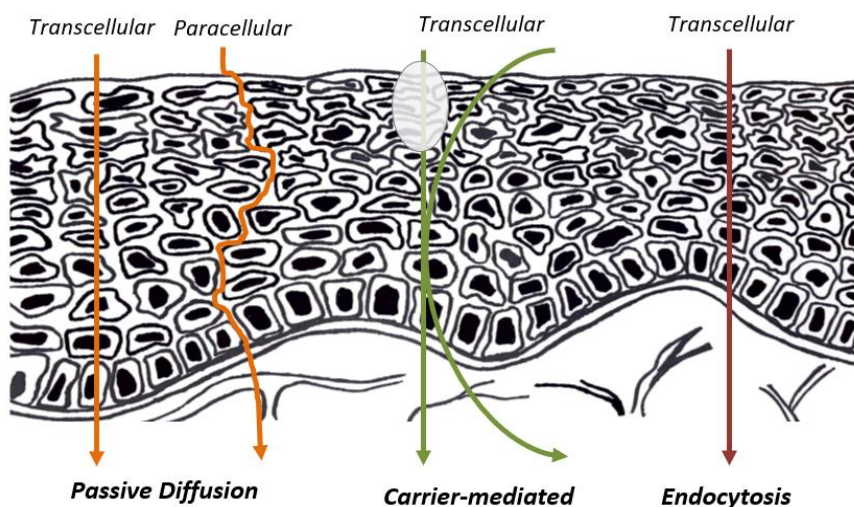


**Figure 3** - Mechanisms of drug transport through oral mucosa.

Most compounds are absorbed into the buccal epithelium by **passive diffusion**, which in turn may follow the paracellular or the transcellular route (25). Authors suggested that passive diffusion is governed by a concentration gradient (23) and that this transport is unidirectional, maintaining a concentration gradient as the drug is carried away from the inner compartment by the blood (26). This process can be explained by the Fick law of diffusion (*Equation 3*) that states the drug molecule moves in favor of a concentration gradient, from a higher concentration to a low concentration environment until equilibrium is reached.

The Fick's first law of diffusion is given by the following *Equation*:

$$J_{SS} = \frac{DK_p}{h} C_D \quad (\text{Equation 3})$$

Where D is the diffusion coefficient of the drug within the buccal mucosa,  $K_p$  is the partition coefficient between the buccal mucosa and the donor chamber buffer solution, and h is the length of the pathway through which the drug must traverse (paracellular or transcellular)(27).

According to Henry J. A. (28) on his study on buccal absorption of propranolol, passive transfer across membranes will only occur when sufficient drug is present on one side of the membrane. On removal of the drug from the buccal cavity, the concentration gradient is altered, and back-partitioning into the mouth may occur. Passive diffusion is, therefore, estimated to happen in favor of a concentration gradient.

Although the former is considered the primary mechanism of drug absorption, there is evidence for the existence of specific receptors on the membrane that recognize and transport target molecules across the membrane. This transport is termed **carrier-mediated transport**, which can be subdivided into facilitated diffusion or active transport, although it does not seem possible to distinguish between the two. Absorption of some sugars, such as D-glucose and L-arabinose (29) was found to be both stereospecific and saturable, which indicated the presence of a carrier-mediated process as these are not characteristics of passive diffusion. Yujito O. (30) investigated the glucose transport system using isolated oral mucosal cells it concluded the existence of, not only Na<sup>+</sup>/glucose co-transportation but also facilitative glucose transporters in the oromucosal cells. GLUT1, GLUT2, GLUT3, and SGLT1 were determined as the molecule transporters present. In addition to sugars, monocarboxylic and salicylic acids (31), cephadroxyl (32), L-ascorbic acid (33), nicotinic acid and nicotinamide (34) were also reported to permeate via a carrier.

In very few cases, absorption by the process of **endocytosis** may occur. Endocytosis is considered active transport wherein the molecule permeates through the transcellular route. It consists on the engulfment of molecules by the cells after its uptake. The usage of this mechanism across the entire stratified epithelium is improbable as well as the feasibility of the active transport in this environment (35).

#### **I.4. Molecule parameters affecting drug permeability**

As previously mentioned, the physicochemical properties of the drugs have an impact on the mechanism as well as the extent of permeation. In this regard, several molecular parameters are associated with permeability across biological barriers.

##### ***Lipophilicity and ionization degree***

Lipophilicity is a relevant molecular physical property when predicting active compounds behavior in drug discovery. Lipophilicity is represented by the descriptors log P and log D; both measure the differential solubility in two immiscible solvents, where the most commonly used solvent system is octanol/water. However, the partition coefficient (log P) is a lipophilicity descriptor for neutral compounds or when the compound exists in a single form, while the distribution coefficient (log D) takes into consideration the degree of ionization, as it measures the differential solubility as a function of pH. Therefore, log D is nowadays considered to be the appropriate descriptor when measuring ionizable compounds' lipophilicity (36).

Furthermore, the ionization of a compound strongly affects the octanol-water partitioning and consequently the affinity towards the lipophilic membrane. According to the pH-partition hypothesis characteristic of passive diffusion, the non-ionized form of an ionizable compound has a higher lipid solubility and is therefore expected to penetrate the oral mucosal membrane to a greater extent than the ionized hydrophilic fraction, due to the hydrophobic characteristic of the membrane. In this context, pKa and pH values have a direct effect on the dissociation form, which is governed by the acid/base compound profile. Therefore, pH dictates the charge state and log D value and consequently the compound absorption. Negative log D values indicate that the molecule has higher aqueous solubility and poor membrane permeability, whereas positive log D values reflect higher lipid solubility and thus higher affinity for the oral mucosa membrane (36).

### ***In silico models- key physicochemical properties***

In addition to lipophilicity, several other physicochemical properties have been suggested to be relevant. Lipinski *et al.* proposed five key physicochemical parameters - the 'Rule of Five' - related to absorption rates of orally administered drugs: besides partition coefficient (Log P), molecular weight, hydrogen bonding, number of rotational bonds, polar surface area were also included in this rule. Moreover, despite the considered importance of these parameters, it should be highlighted that the 'Rule of Five' being applied to the oral route considers the gastrointestinal tract and hepatic first-pass metabolism the molecules are subjected. To this end, *in silico* models were used to assess the importance of these molecular properties in relation to oromucosal drug delivery. *In silico* models, often based on multiple linear regression (MLR), represent a fast and cost-effective approach as an initial assessment tool, avoiding the limitations of *in vitro* and *ex vivo* studies. Kokate *et al.* (37) developed a model for drug permeability across buccal mucosa using fifteen model drugs. The molecular descriptors selected for these studies were molecular volume (MV), molecular weight (MW), log P (octanol-water partition coefficient), logD<sub>6.8</sub> (distribution coefficient at pH 6.8), pKa, total polar surface area (TPSA), hydrogen bond acceptors (HBAs), hydrogen bond donors (HBDs), number of rotatable bonds (nRotB), solubility (at pH 6.8), and melting point (mp), see Table 3 (37). For the prediction of drug permeation across buccal mucosa, **MV**, **logD<sub>6.8</sub>**, **HBDs**, **nRotB**, were identified as the most significant descriptors (P<0.001, Q<sub>2</sub>=0.882). The definitions of the former are indicated in Table 3.

**Table 3** - Definitions of molecular descriptors significant for buccal permeation.

Molecular Descriptor	Definition
Molecular Volume (MV)	Expresses molecular size, being a better descriptor for the former than molecular weight. It can be defined according to the molecular surface, e.g., the Van der Waals volume.
Distribution Coefficient at pH 6.8 (LogD <sub>6.8</sub> )	Measure of pH-dependent differential solubility of all species of a compound in the octanol/water system, being the most appropriate descriptor to predict ionizable compounds' lipophilicity.
Number of hydrogen bond donors (HBD)	Calculated based on the number of oxygen and nitrogen atoms connected to nitrogen atoms in a molecule.
Number of rotational bonds (nRotBs)	"Any single bond, not in a ring, bound to a non-terminal heavy (i.e., non-hydrogen) atom". It reflects conformation changes of molecules; a molecule with higher number of rotatable bonds, exhibit larger conformational flexibility.

The resulting *in silico* model to predict buccal permeation is expressed as the following Equation (37):

$$\log K_p(cm/s) = -3.13(\pm 0.95) - 0.0128(\pm 0.0051) \times MV - 0.617(\pm 0.170) \times HBD + 0.263(\pm 0.110) \times nRotB + 0.654(\pm 0.200) \times \log D_{6.8} \quad (\text{Equation 4})$$

Based on Equation (4) and the overall study, a positive correlation was found between logD<sub>6.8</sub> and permeability, indicating that an increase in lipophilicity leads to an improvement in permeation, i.e., lipophilic compounds cross the biological membranes easier than hydrophilic molecules. It was also demonstrated that an increase in H-bonding groups results in a decrease in the diffusion coefficient, which shows a negative correlation. Moreover, molecules with greater flexibility favor buccal mucosa permeation as the number of rotational bonds (nRotB) is positively correlated with permeability. Furthermore, the positive dependence on logD<sub>6.8</sub> and the negative dependence on hydrogen acceptability reflect that permeation through the buccal mucosa favors hydrophobic compounds, as well as the hydrophobicity characteristics of the membrane (Figure 4).

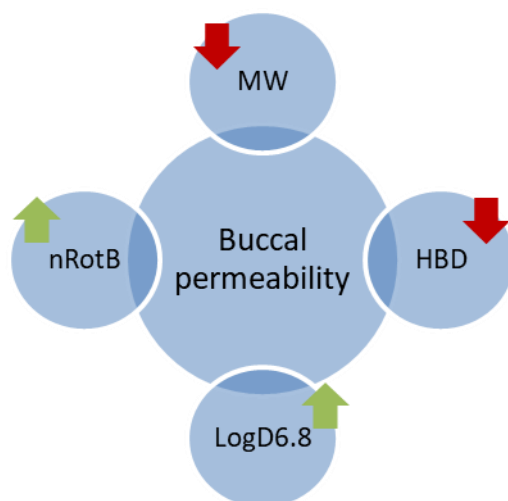


**Figure 4** - Schematic representation of the correlations between buccal permeation and significant molecular descriptors.

Smaller molecular size, high lipophilicity, lower hydrogen bond capability and greater flexibility are hence important features when considering buccal mucosa drug permeation.

Moreover, the literature describes a series of experimental studies using the same model drugs (38–42), that when analyzed by the previously described *in silico* model yielded a quite similar  $\log K_p$  value, making this *in silico* model presents a reliable alternative for predicting buccal permeation.

### 1.5. Challenges to permeation

For successful oromucosal drug delivery, the drug must overcome potential adverse conditions of the oral environment such as saliva, mucus, and enzymes that can retard the rate and extent of drug absorption. It must also partition into and diffuse across the mucosal layers, which in turn may create resistance to drug passage (Figure 5).

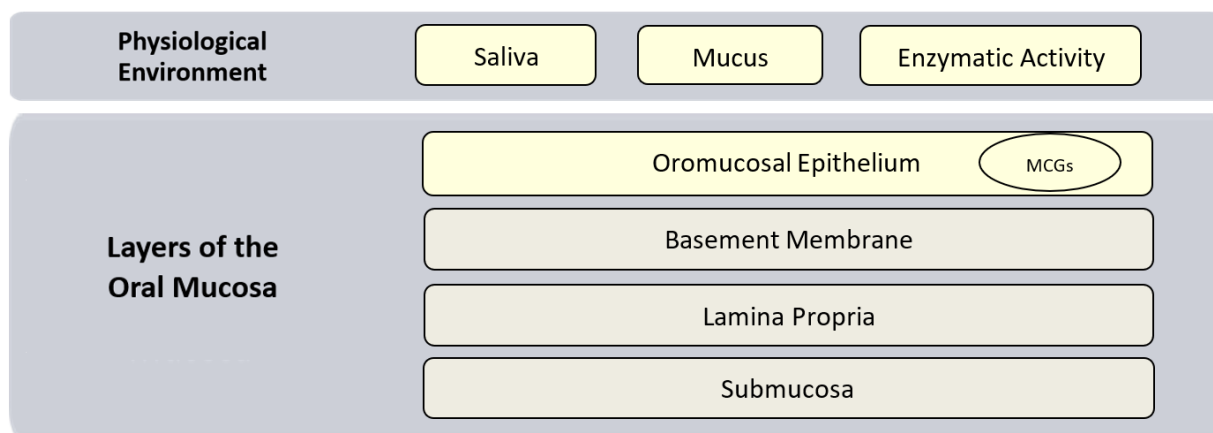


**Figure 5** - Graphic representation of the permeation barriers. Key: MCGs = membrane coating granules.



### **1.5.1. Saliva**

The oral mucosa is constantly washed by salivary flux, a phenomenon known as “saliva wash-out”, which facilitates the dissolution of the drug but can often represent an obstacle to drug delivery, especially for locally applied drug systems. In addition, as previously mentioned, the salivary flow rate varies with the time of the day, different stimuli and food intake.

Premature involuntary swallowing of saliva can lead to drug loss and a rapid decrease in drug concentration to below therapeutic levels (43). Also, the uneven distribution of drug within saliva makes it difficult to deliver therapeutic drug concentrations to all the sites (7). In order to increase the time the drug is retained, adhesive drug delivery systems for local drug delivery have been developed.

### **1.5.2. Mucus layer**

The mucus layer can be a barrier to drug passage as its thickness increases the depth of the diffusion barrier, especially for large molecules. However, it is not considered a significant challenge to permeation unless specific binding of the drug with the glycoproteins occurs. Numerous anionic and cationic functional groups are attached to the mucins, with which charged molecules can interact through hydrophobic, electrostatic or hydrogen bonding interactions, retaining its transport through the epithelial layer (6).

On the other hand, interaction with the mucus - mucoadhesion - may reveal as advantageous since it improves the time the drug is adhered to the mucus layer and consequently the absorption rate; however, the short turnover time characteristic of this layer may be a limitation if sustained drug release is desired (14).

### **1.5.3. Enzymatic activity**

As also part of the oral cavity environment, some proteolytic enzymes are present on the mucosal surface, such as carboxypeptidases, aminopeptidases, endopeptidases, and esterases (8). Although OC is considered to have a relatively low enzymatic activity, they can become a barrier to overcome by protein and peptide drugs, as these enzymes, together with their presence in saliva, may cause peptide degradation (22).

### **1.5.4. Membrane-coating granules**

The permeability barrier of keratinized and non-keratinized oral mucosal epithelium has been associated with the membrane coating granules (MCGs), evidenced in the prickle cell layer. At the final stages of the epithelial cells differentiation process, MCG's fuse with the cell

membrane and consequently extrude the lipid contents into the intercellular spaces of the upper three-quarters of the epithelium (6).

Squier *et al.* (44), evaluated the permeability barrier of the oral epithelium to lanthanum in rabbits and rats. In both keratinized and non-keratinized tissues, this tracer protein was evident in the intercellular spaces of the epithelium in the layers where the membrane coating granules appeared, suggesting that these organelles may be the reason for an intercellular barrier. Similar results have been demonstrated to different sizes and chemical properties of the tracer protein, horseradish peroxidase (45).

### ***Intercellular lipid content***

The intercellular barrier may then originate from the lipid content present in the intercellular spaces, which is derived from the lipids extruded from the MCGs. These differ in keratinized and nonkeratinized epithelium. The lamellar MCGs in keratinized epithelium extrude mostly non-polar lipids such as sphingomyelin, glucosylceramides, and ceramides; whereas the intercellular spaces of non-keratinized epithelium contain large amounts of polar lipids including phospholipids, triglycerides, glycosilceramides and small amounts of ceramides derived from the non-lamellar MCGs (4,5).

Furthermore, intercellular lipid content was shown to be inversely correlated with permeability, i.e., nonkeratinized epithelium exhibited higher permeability than keratinized epithelium, which was associated with lower percentage levels of ceramides (6).

### **1.5.5. Basement membrane**

The basement membrane of non-keratinized oral epithelium has been associated with limiting the passage of some compounds into the deeper layers of the oral mucosa.

Diffusion of compounds such as endotoxins (46), drugs such as chlorhexidine (47), and proteins such as albumin (12) through non-keratinized guinea pig oral epithelium, demonstrated an accumulation of the drug on the basal layers of the epithelium. Based on these studies, the basement membrane is generally considered a limiting barrier, offering resistance to the diffusion of molecules to larger molecules (12).

## **1.6. Strategies to enhance buccal permeation**

Permeation through the oral mucosal is the main factor for the successful delivery of drugs applied to the oral cavity, and the oral epithelium is the main obstacle to this performance. Several factors need to be considered in order to achieve drug oromucosal permeation, such

as oromucosal site and respective characteristics; the physiological environment (saliva, mucus, and enzymatic activity); and the physicochemical properties of the drug, which will influence the penetration pathway and its extent. Therefore, based on the physicochemical properties of the drug and the barriers often required to surpass, strategies can be used to promote permeation. These include the use of chemical enhancers and physical enhancers. **Chemical enhancement** involves the inclusion of certain excipients in the formulation, known as 'permeation enhancers' or 'absorption enhancers' that improve the undesirable molecule properties or act on the membrane itself reducing its barrier. On the other hand, **physical enhancement** is achieved by temporarily altering membrane properties upon application of an electric current - electrical-induced enhancement - or for example application of ultrasounds - mechanically-induced. Despite existing studies reporting physical enhancement success in increasing transmucosal drug delivery; evidence of its applicability to the oral mucosa is relatively limited and focused on skin permeation (48,49). Therefore, the addition of chemical permeation enhancers is still the most used strategy when improving permeation, particularly regarding oromucosal drug delivery.

#### 1.6.1. Chemical permeation enhancers

Permeation through the buccal mucosa is drug-specific, i.e. the selection of an appropriate permeation enhancer and its effectiveness depend on the physicochemical properties of the drug, nature of the vehicle, and other excipients (50). Moreover, the permeation enhancer should be safe, non-toxic and non-irritating; pharmacologically and chemically inert; the absorption-enhancing action should be immediate and unidirectional and the effect of the permeation enhancer reversible, allowing the membrane tissue to immediately recover to its barrier property without suffering any toxicity or damaging effects.

Classes of permeation enhancers employed in buccal mucosal permeation and respective examples are shown in Table 4.

**Table 4** - Classes and examples of permeation enhancers employed in buccal mucosal permeation (50, 52).

Classes of Permeation Enhancers	Examples
<b>Surfactants</b>	Anionic: Sodium lauryl sulfate, Sodium laurate Nonionic: Polysorbate 80 (Tween80) Cationic: Cetylpyridinium chloride, Benzalkonium chloride
<b>Bile salts</b>	Sodium glycodeoxycholate (GDC) Sodium cholate (SC) Sodium deoxycholate (SD)
<b>Fatty acids</b>	Oleic acid Lauric acid (C12)
<b>Chitosan and derivatives</b>	Trimethyl chitosan 5-methyl-pyrrolidinone chitosan
<b>Cyclodextrins</b>	$\beta$ -cyclodextrin Hydroxypropyl- $\beta$ -cyclodextrin (HP $\beta$ CD) Methyl- $\beta$ -cyclodextrin Randomly methylated $\beta$ -cyclodextrin
<b>Terpenes</b>	Menthol

**Co-enhancers**, such as ethanol and propylene glycol (PG) are also relevant, as they are added as a vehicle in combination with a previously described permeation enhancer to improve overall permeability.

Permeation enhancers are thought to improve the penetration of substances across the oromucosal barrier through several mechanisms of action. Although not all mechanisms of action of permeation enhancers have been unveiled, it is known that each permeation enhancer may have more than one specific mechanism, which will differ mainly according to the physicochemical properties of the drug and the presumed pathway.

Some mentioned mechanisms of action include (50, 51):

- Alteration of mucus rheology

The viscoelastic layer of mucus hinders drug absorption and creates an additional layer on the oral mucosa as an obstacle. Some permeation enhancers act by decreasing mucus viscosity.

- Extraction of intracellular lipids

A common mechanism of action of permeation enhancers is the disturbance of the intracellular lipid packing after interaction with lipids, which leads to an increase in the lipid bilayer membrane fluidity.

- Interaction with protein domains

Some compounds also interact with protein domains, inhibiting and reducing the enzymatic barrier. Furthermore, inhibition of peptidases and proteases may also result from an alteration in the membrane fluidity, promoting drug absorption by an indirect route.

- Increase in thermodynamic activity of the drug

Some compounds affect the solubility of the drug and act by micellization, which will influence the thermodynamic activity of the drug by altering the drug partition coefficient.

### **1.6.2. Physical enhancers**

Enhancement by physical methods can be obtained by mechanical or electrical techniques. Mechanically by the removal of the outermost layers of the epithelium to decrease the barrier thickness; or the use of sonophoresis, which consists on the application of ultrasounds to temporarily reduce the density of lipids in the intercellular domain, as a result of a combination of thermal, chemical and mechanical effects (53). Electrically induced transport refers to the application of an electric current to induce the movement of ions through direct interactions of the electric field with the charge of an ionic compound (Iontophoresis) or based on the process by which charged particles tend to migrate toward a less charged area (Electro-osmosis). A third option refers to the process of Electroporation, in which short pulses of high-voltage current disturb the phospholipid bilayer of the membrane and promote the transport of neutral molecules (54).

Although some studies successfully reported the use of the aforementioned strategies, the existing possibility of irreversible membrane damage leads most researchers to resort to the introduction of chemical enhancers rather than applying physical enhancers. In addition, studies using a combination of chemical and electrical enhancement have recently emerged (54, 55), and may be an alternative to be considered.

### **1.7. Methods to assess permeability**

The evaluation of drug permeability through oral mucosa has been carried out by different methodologies, which may be labeled as *in vivo*, *ex vivo* or *in vitro* methods. *In vivo* studies are performed on humans or animals, thus these are suitable for later stages of development, while preliminary formulation data are collected by *ex vivo* and *in vitro* methods where the conditions and variables such as temperature, pH and osmolarity are controlled (1). The latter methods mostly regard the placement of a tissue from animal origin - *ex vivo* - or an artificial membrane - *in vitro* - on a permeability chamber. In addition, *in vitro* methods may also include cell-based models, which consist of a cell cultured representation of the epithelium.

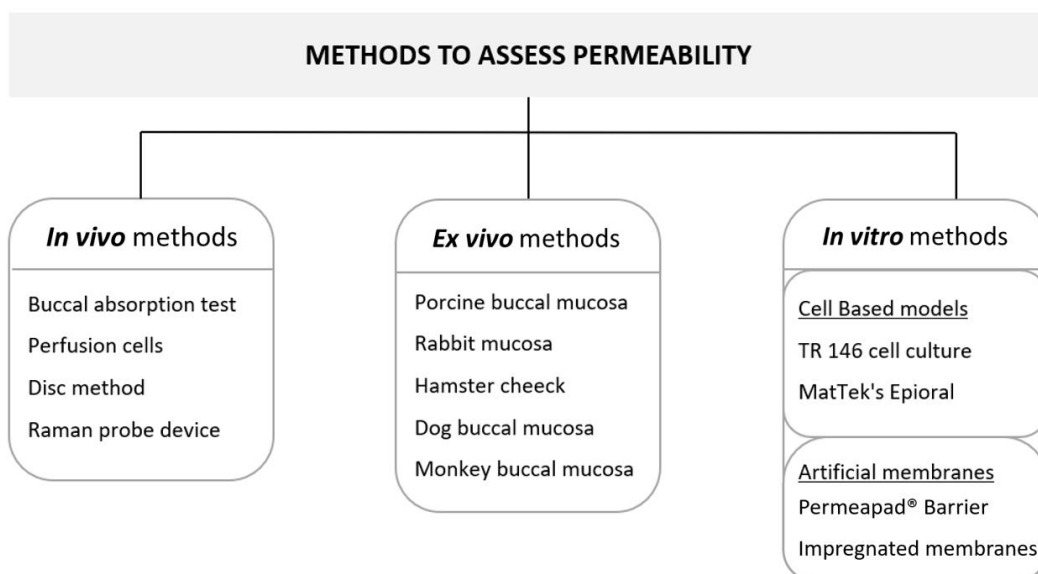


**Figure 6** - Schematic representation of the available methods to assess buccal permeability (62, 64, 87).


### 1.7.1. *In Vivo* methods

*In vivo* methods are commonly performed to assess the bioavailability of drugs administered through the buccal mucosa. As it resorts to trials in humans, they are applied at a further stage in the development of the drug, where safety is assured.

#### 1.7.1.1. Buccal absorption test

The buccal absorption test refers to an *in vivo* method in which a known volume of a drug solution is swirled around in the mouth of a subject for a specified time and then expelled. The difference between the initial and final drug concentrations (post-rinsing with distilled water) in the solution is considered as the amount of drug taken up into the oral mucosa (56), (40). The related advantages and disadvantages are listed in Table 5.

**Table 5** - Schematic representation the *in vivo* buccal absorption test with the related advantages and limitations (1). Key: OC = Oral Cavity.

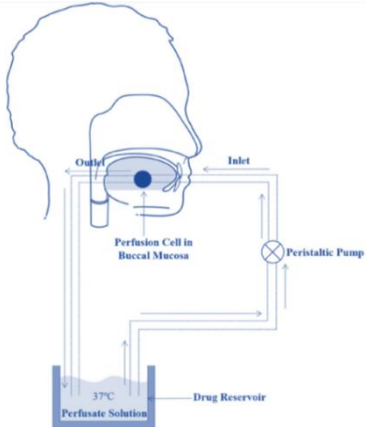
	<b>Advantages</b>	<b>Limitations</b>
	Easily performed.  Collection of quantitative data (rate and extent of drug loss).  Non-invasive.	The amount of drug absorbed is measured based on disappearance from the OC.  It does not consider other influencing factors such as pH, interference from salivary secretions, drug swallowing.  Not possible to assess site specific absorption as it may occur through various regions of the OC.

Despite its limitations, this method is useful for relating drug structure and rate constants for drug absorption and, consequently, identifying those factors that influence absorption across biological membranes.

### 1.7.1.2. Perfusion cells

Perfusion cells involve the use of an *in situ* perfusion cell, which can be attached to specific mucous membranes in the oral cavity (9). As the drug solution is continuously perfused through the cells, it is collected at different time intervals, as well as blood samples for pharmacokinetic data. The related advantages and disadvantages are mentioned in Table 6.

**Table 6** - Schematic representation of the *in vivo* perfusion cell test with the related advantages and limitations (1). Key: OC = Oral Cavity.

	Advantages	Limitations
	<p>Continuous perfusion of drug solution.</p> <p>Isolation from interference of saliva and pH.</p> <p>It allows to study regional variations.</p>	<p>The amount of drug absorbed is measured based on disappearance from the OC.</p> <p>It does not consider other influencing factors, such as swallowing and membrane storage.</p>

Despite overcoming some limitations of the buccal absorption test, drug absorption, as in the previously mentioned method, is determined by the loss of drug from the cell and hence the actual amount of drug that permeates through the buccal mucosa is not measurable (57).

### 1.7.1.3. Disc method

The disc method consists of an airtight sampling chamber comprising a drug-loaded disc, which is placed in a specific area of the mucosal membrane as a vehicle for drug delivery. The system is removed after 30 minutes of contact with the oral mucosa, and blood samples are then collected to determine the amount of drug absorbed by the mucosa. The related advantages and disadvantages are mentioned in Table 7.

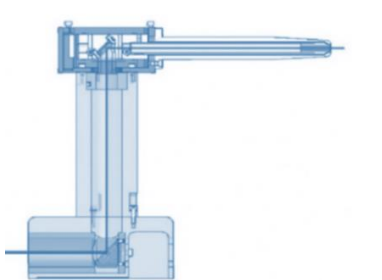
**Table 7** - Advantages and disadvantages of the disc *in vivo* method (1).

Advantages	Limitations
It allows for assessment of site-specific drug absorption.  Measures the actual amount of drug absorbed into the systemic circulation.	Interference from salivary secretions.  Low disc adherence.  Risk of drug leakage.

#### 1.7.1.4. Raman probe device

An *in vivo* Raman probe was presented by Pudney P. A. (58) that can be used to obtain *in vivo* confocal Raman spectra from difficult-to-access areas of the body, allowing depth profiling of the oral epithelium. It consists of a long pen-shaped device comprising a small external optical window at the end, which can be maneuvered against the oral epithelium. The device is externally connected to a Raman spectrometer through which is obtained a spectrum composed of a series of peaks or bands, each one corresponding to a characteristic vibrational model that provides a fingerprint for a molecule (1). The related advantages and disadvantages are listed in Table 8.

**Table 8** - Schematic representation of the *in vivo* Raman probe device with the related advantages and limitations (1).

	Advantages	Limitations
	Non-invasive.  Screening and diagnosis of oral diseases.	Qualitative method, does not provide quantitative data.  Complexity in data interpretation.

Although *in vivo* methods provide the more bio-relevant responses, the costly and burdensome experiments related to unethical considerations limits their application, being associated with the final stages of drug formulation assessment. For that reason, *ex vivo* methods have been commonly used, overcoming some of the previous limitations also ensuring good correlation *with in vivo* methods.

#### 1.7.2. Ex Vivo methods

*In vivo* studies are not feasible at the early experimental stage, whereas *ex vivo* methods based on dissected tissues represent a more appropriate and cost-effective approach. They allow the study of specific areas of the oral cavity under controlled experimental conditions, such as



temperature, pH and osmolarity, using buffers instead of blood as samples (1), and successfully provide data on the possible pathways of drug transport across the oral epithelium, which are directly related to the physicochemical properties of the drug (59).

Due to the limited availability as well as ethical issues with the use of human oral mucosa (60) most researchers rely on the use of a freshly excised mucosa from an animal model that should be as similar as possible to the human mucosa in terms of structure and permeability. Regarding the assessment of buccal mucosa permeability, various animals have been suggested and studied as possible models: rats, rabbits, dogs, monkeys and pigs (60).

Moreover, porcine buccal mucosa has been generally accepted as the most suitable tissue model for the assessment of oromucosal drug delivery, not only because of its easier and cheaper tissue acquisition, but most importantly because it resembles human buccal tissue in structure, morphology, thickness, and composition (59, 60).

#### 1.7.2.1. Porcine buccal mucosa

The use of porcine buccal mucosa as a model for drug permeation studies, as with all *ex vivo* methods, requires consideration of various conditions regarding the harvesting of the tissue, preparation of the epithelium in the apparatus, and preservation, since tissue viability is time-dependent and loss of viability will directly introduce biased results.

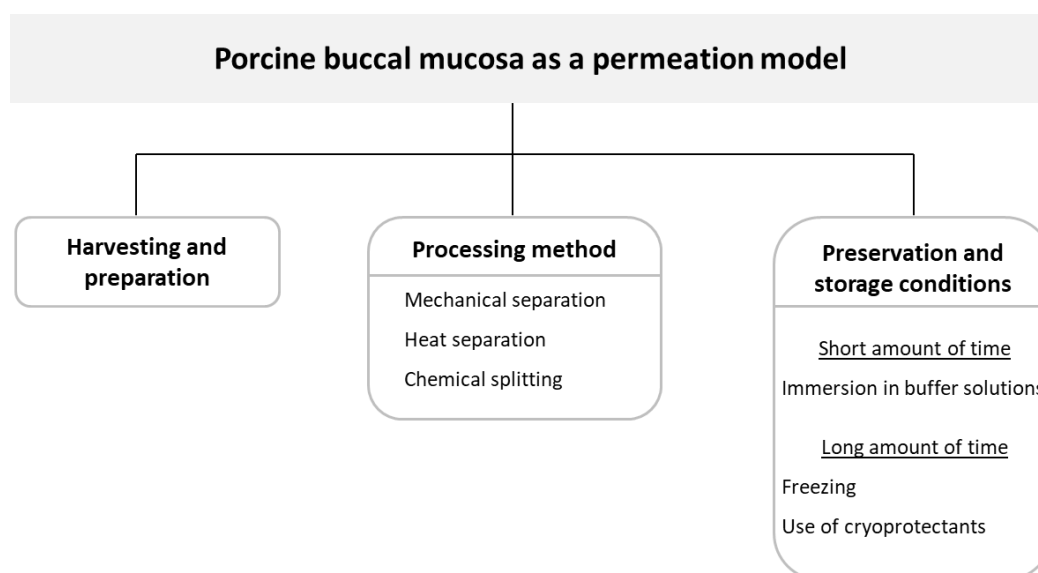


**Figure 7** - Schematic representation of the procedure conditions in porcine buccal mucosa *ex vivo* permeation studies.

#### ***Tissue harvesting and preparation***

The buccal tissue of domestic pigs is usually obtained from a slaughterhouse, where the harvesting should be performed as soon as possible after the animal is slaughtered. Throughout this process, the area of the parotid glands ducts below the ears noticeable by a papilla adjacent to the maxillary second molar, should be avoided, as this surface is associated with permeation variability (62).



**Figure 8** - Tissue harvesting procedure (63).

The buccal mucosa is then transported in containers in ice-cold isotonic buffer, for example Krebs-Ringer buffer (KBR) or isotonic phosphate buffer (PBS pH 7.4), and used within 6 h, as tissue viability is time-dependent (1). The porcine buccal mucosa is then prepared for permeability studies. The buccal epithelium is approximately 250  $\mu\text{m}$  thick and lies on a 150  $\mu\text{m}$ -450  $\mu\text{m}$  thick layer of connective tissue (lamina propria). Overall, the buccal mucosa can range from 400  $\mu\text{m}$  to 700  $\mu\text{m}$  in thickness (64). The buccal mucosa is processed to obtain 250  $\mu\text{m}$  to 500  $\mu\text{m}$  as within this range the epithelium is considered the major permeability barrier, whereas at 600  $\mu\text{m}$ , the higher presence of connective tissue acts as a barrier affecting permeability coefficients of the compounds tested. Furthermore, the recommended thickness for permeation studies is 500  $\mu\text{m}$  as 250  $\mu\text{m}$  is technically difficult to obtain.

### ***Tissue processing method***

During tissue processing, excess fat and connective tissue should be trimmed with the help of scalpels and scissors. Consecutively, the epithelium needs to be separated from the connective tissue in a precise manner. This separation stage can be performed by mechanical separation, heat treatment or chemical splitting.

Mechanical separation refers to the use of a dermatome or other surgical equipment to remove connective tissue. The main advantage is the maintenance of structural integrity as the epithelium is not subject to any treatment (60); therefore, dermatomization is one of the most used techniques, which consists of an electrodermatome (Figure 9) cutting through the tissue with a thickness previously defined (62). Nonetheless, it is a more expensive approach; and the use of surgical scissors instead is cheaper but, on the other hand, it requires extremely

high skill. In addition, none of these mechanical techniques allows the complete removal of the connective tissue (60).

A simpler and more suitable alternative to surgical trimming is a heat separation method by dipping the porcine buccal mucosa into a 0.9% NaCl solution for 60-90s at 60-70°C. It does not affect tissue integrity and has been shown to display no significant difference in permeability coefficients to surgically split tissues (64). It is considered the best method (60), due to being time-saving, less expensive, and technically easier to handle.

Moreover, chemical splitting of the epithelium refers to the incubation of buccal mucosa in 20 mM ethylenediaminetetraacetic acid disodium salt (EDTA- 2Na) PBS solution for 50 min at 60°C. Despite some authors have used this technique (65,66), it has been reported to, in some cases, affect tissue activity (64,67), possibly due to the permeation promoting effect of EDTA-2Na (60). Therefore, its applicability requires caution.

The previous described methods are summarized in Table 9, including the advantages and limitations of each processing method.

**Table 9 - Main processing tissue methods comparison (60, 62).**

<b>Processing Method</b>	<b>Procedure</b>	<b>Advantages</b>	<b>Limitations</b>
Mechanical method	<i>Dermatomization</i>	Maintenance of structural integrity	Relatively expensive; Incomplete removal of connective tissue.
	<i>Surgical scissors</i>	Maintenance of structural integrity	Time consuming; High skill required; Incomplete removal of connective tissue.
Heat separation	<i>Soak in 0.9% NaCl solution for 60–90 seconds at 60–70°C.</i>	Does not affect tissue integrity; Simple and time-saving.	-
Chemical splitting	<i>Soak in 20 mmol EDTA-2Na PBS solution for 50 min at 60°C.</i>	Simple	Detachment may affect tissue activity; EDTA-2Na promotes penetration.

**Preservation and storage conditions**

After epithelium splitting procedure, the tissue may be placed in the diffusion cell and after temperature equilibration, permeation studies may be conducted (8). On the other hand, if

the experiment is not possible to be conducted immediately, the buccal tissue remains viable postmortem for 6 h if immersed in PBS 7.4 at room temperature, reaching 8 h of integrity at 4°C; and until 24 h in KBR pH 7.4 (4°C)(64). Moreover, due to the limited availability of fresh buccal tissues, in some cases, it is required to store the tissue for a prolonged number of days. However, tissue freezing has been associated with superficial epithelium damage (64), and in a way of avoiding the formation of ice crystals, cryoprotectants, such as DMSO, glycerin, ethylene glycol, among others, have been mentioned by some authors (1,63,68).

Tissue-based models (*ex vivo* methods) are complex but in addition, very accurate regarding evaluation of drug permeability. Nevertheless, to obtain reproducible results, the process from harvesting to permeability study has to be thoroughly controlled, which may result in time-consuming methods. Moreover, the impracticality of using tissue models to assess a large number of compounds is making researchers to develop *in vitro* methods.

### **1.7.3. *In Vitro* methods**

The convenience of *in vitro* methods and less labor-intensive characteristics reflect them as an option for preclinical drug screening, where conditions are controlled and may allow elucidation of mechanisms of buccal transport. In this category, 1) cell-based models, including cell cultures and 2) non-cell-based models, such as artificial membranes, have been investigated as alternative permeation assessment methods.

#### **1.7.3.1. Cell-based models**

Few models based on cell culture have been described for initial assessment of compounds buccal permeation: TR146 cell culture and a 3D model of cultured epithelium (69). Despite the advantage of being able to test a large number of compounds, these are still the least used models regarding oral mucosal permeation.

#### ***TR146 cell culture***

TR146 cell culture is derived from human buccal metastases and has been used to assess drug transport across the human oral epithelium. After 23 days of growth on filters, TR146 cells are able to form stratified epithelial-like cells consisting of 4-7 cell layers expressing keratins, with flattened cells on the surface that are clearly distinct from the lower cells, the absence of tight junctions, and the presence of organelles resembling the membrane-coating granules of human buccal mucosa (41); hence, they have the potential to be used as a model for human buccal epithelium.

This cell line has been frequently used to evaluate the permeability of different compounds, (70–72). It is considered selective for ionization and pH-dependent permeability of drugs (71), as well as a valuable *in vitro* model for metabolism studies with enzymatically labile drugs (42). On the other hand, the barrier function of the TRI46 model was reported to be lower than that of porcine and human buccal mucosa, as evidenced by significantly higher permeability to tritiated water, mannitol, testosterone, and nicotine (42,70). This may be related to the cell cancerous nature and its failure to fully differentiate (73). In addition, the high cost of this model and the time required for cultures may limit its usage (74).

### **MatTek EpiOral™**

Recently, a new cultured human buccal epithelium model EpiOral™ has become commercially available (MatTek, Ashland, MA, USA). MatTek EpiOral™ is a metabolically and mitotically active 3D model consisting of human-derived epithelial cells (keratinocytes) cultured to form a three-dimensional 8-11 cell layered highly differentiated tissue. It is formed by an organized basal layer and multiple non-keratinized layers with identical histological and differentiation characteristics to the human buccal epithelium.

This 3D model has mostly been applied for cytotoxicity, irritancy and, more recently, permeability assessment (75–77). Rao *et al.* (75) reported similar permeability parameters for naltrexone hydrochloride using this model and porcine buccal tissue. Tissue-engineered oral mucosa seems then to be a promising approach for *in vitro* studies.

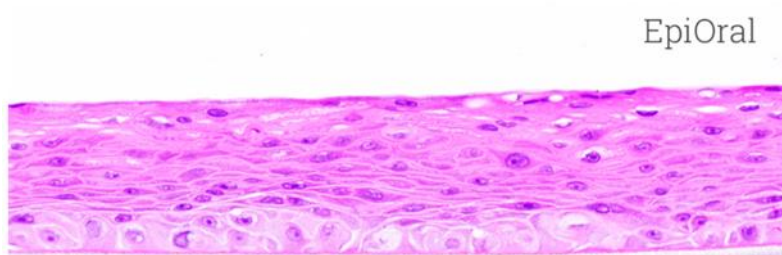


**Figure 9 - MatTek EpiOral™ (78).**

In conclusion, despite the practicability compared to the use of animal tissues, more reliable and time-efficient cell-based methods are desired, as variability between batches of cells is still limiting despite the reduced steps compared to *ex vivo* methods.

### 1.7.3.2. Artificial membranes

In vitro methods based on the use of artificial membranes may represent attractive alternatives to the cell- or tissue- based models described above as they appear less expensive, simpler, with a shorter duration of experiments and better reproducibility of results. In the present sub-chapter some biomimetic systems are reviewed.

#### **Permeapad<sup>®</sup> Barrier membrane**

Permeapad<sup>®</sup> Barrier (Figure 10) is a 'ready-to-use' biomimetic artificial membrane consisting of phosphatidylcholine layer (Lecithin (S-100)) placed between two low retention cellulose-based layers. Once the barrier is hydrated, it spontaneously forms a liposomal gel-like structure (79), that mimics passive diffusion transport. The interstices formed between the liposomes (Figure 11) upon hydration, grants this barrier the ability to mimic paracellular transport, in addition to the transcellular route, contrarily to most artificial models.



**Figure 10** - Permeapad<sup>®</sup> Barrier membrane (95).

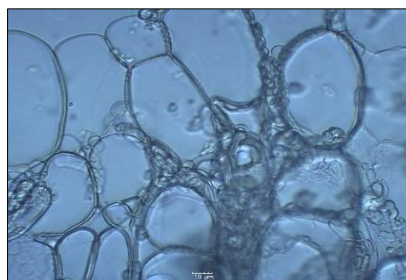


**Figure 11** - Liposomal gel-like structure of Permeapad<sup>®</sup> Barrier membrane.

Permeapad<sup>®</sup> Barrier is easy to perform maintaining its functionality over time and allowing the predictability of pH-dependent permeation over a wide pH range (pH 1-10) (80). Moreover, according to Bibi *et al.* (81) it is functionally stable even in the presence of co-solvents, surfactants and biomimetic media. Regarding permeability, Bibi (80) showed excellent correlations with porcine buccal mucosa upon metoprolol permeation across Permeapad<sup>®</sup> Barrier.

Therefore, this artificial membrane is considered a less laborious as well as cheaper alternative in comparison to cell- and tissue- based systems for fast and reliable preliminary prediction of passive drug permeability (82).

### ***Impregnated artificial membranes***

In order to study oromucosal permeation, a “PAMPA variant” method has been suggested. This comprises the preparation of artificial membranes by impregnating a porous filter with a solution of lipid mixture to be further inserted in a diffusion cell apparatus.

The materials by which these artificial membranes are made and the respective solvents (lipidic solution) may vary. These are resumed in Figure 12.

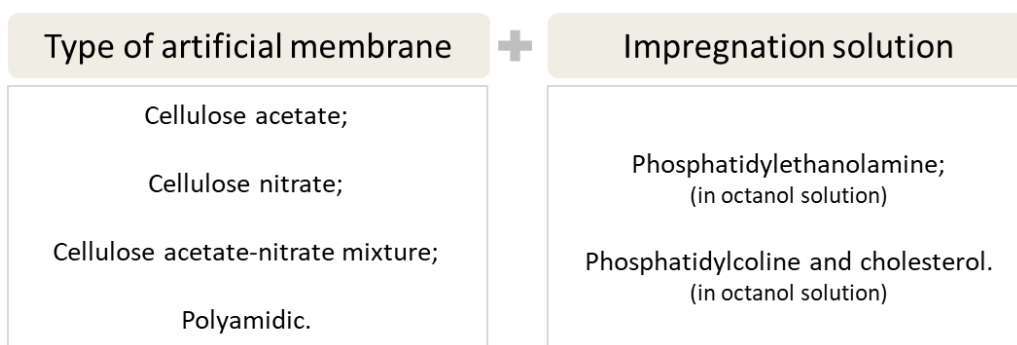


**Figure 12** - Schematic representation of available impregnated artificial membranes: type of membrane and impregnated solutions.

A. Khdair (83) demonstrated good correlation of both cellulose acetate and cellulose acetate nitrate mixture membranes with freshly excised natural porcine and rabbit buccal mucosa. Moreover, cellulose acetate nitrate mixture membrane (0.025  $\mu\text{m}$  pore size, 100  $\mu\text{m}$  thickness and 72% porosity) was considered by P. Mura (84) to be the most suitable for buccal drug absorption studies due to its smallest variability in the amount of impregnated lipid phase and the greatest reproducibility of permeation data.

Furthermore, not many researchers have resorted to the impregnated membranes as artificial barriers to oral mucosal permeation. Nevertheless, they have been reported as useful in predicting drug permeation, and A. Khdair showed selectivity for permeation enhancers (83).

#### **1.7.4. Apparatus**

Permeability studies of drug molecules across the buccal mucosa are commonly conducted using various types of diffusion cells, such as Franz-type diffusion cells, flow-through cells, and modified Ussing chambers. These apparatuses typically consist of a donor and a receiver compartment, a sampling port, and a heater to regulate set-up temperature (59). Between the compartments is placed a barrier membrane, which can be an excised tissue of animal origin (*ex vivo*) or artificial membranes (*in vitro*). Moreover, these set-up components reflect *in vivo*

conditions: the drug formulation is applied on the donor chamber (site of drug delivery) and the amount of drug diffusing across the membrane into the receptor chamber (*in vivo* plasma) is determined over time, by periodically collecting samples of the receptor solution through the sampling port, replacing with fresh buffer to maintain experimental conditions. Based on the fluid refreshment in the acceptor compartment, diffusion cells can be classified as static or flow-through. In static diffusion cells, the receptor medium is stirred continuously in the compartment, but is not refreshed, except to compensate for the volume reduction due to the collection of samples; in flow-through cells, on the other hand, the acceptor medium continuously flows through the acceptor compartment and consequently, the medium is refreshed continuously (85). The *set-up* temperature is maintained at  $37\pm 0.5^{\circ}\text{C}$  to mimic *in vivo* environment by a heated water-bath that usually undergoes the apparatus through connecting jackets.

#### 1.7.4.1. Franz diffusion chamber

The Franz diffusion chamber is a static cell that may be vertical or side-by-side (horizontal) (Figure 16). In a standard vertical cell, the membrane barrier is sandwiched between the donor and receptor chambers, so that the epithelium is faced to the air and the respective connective tissue faces the receptor chamber. The receptor medium is constantly being stirred keeping a stable receptor temperature as well as a homogeneous distribution of receptor fluid. In turn, in side-by-side diffusion cells, both donor and receptor chambers are stirred.

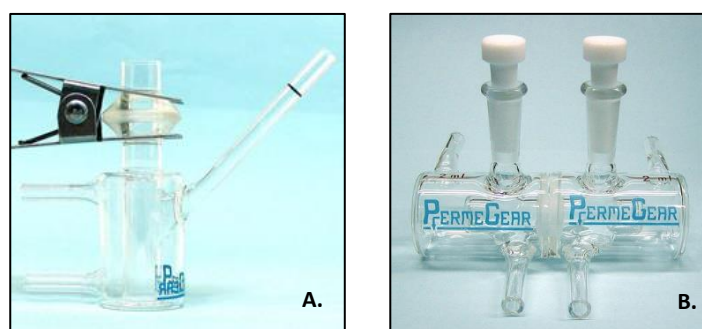


**Figure 13 - A.** Standard vertical Franz Cell; **B.** Side-by-side Franz Cell (94).

Regarding the circulation of heated water through the *set-up*, vertical Franz diffusion cells are available with integrated heating jackets (Jacketed Cell), and as Unjacketed Cells, which do not present a heating jacket and are placed in a temperature-controlled environment (thermocirculator) instead (94).



Franz diffusion cells are one of the most used and reliable apparatus; nonetheless, some limitations need to be accounted for, such as the receptor chamber limited volume capacity, which may present as an obstacle to solubility of poorly soluble drug compounds. In addition, in vertical Franz cells, the possible tissue drying from air exposure as well as the formation of air bubbles prior throughout the conduction of the permeation study are some other common disadvantages (1).

Membranes that can be used in this apparatus include porcine mucosal tissue (24,83); rabbit buccal mucosa (83); Permeapad® (80); and lipid-impregnated membranes (83).

#### **1.7.4.2. Flow-through cell**

The flow-through diffusion cell consists of a vertical chamber and its application is similar to the Franz diffusion chamber. A temperature of 37°C is maintained by placing the chamber on a heated aluminum block. Each chamber has a tube attached to an inlet port from where the donor or receptor fluid is pumped. The effluent from the receptor solutions is collected to determine the drug amount. The larger capacity of the donor compartment ensures a suitable loading of the drug solution however, a low volume of the receptor compartment and a much higher fluid volume pumped into the chamber is required. Thus, in a flow-through system, the volume and flow rate are critical (85).

Moreover, this apparatus presents several advantages compared to the static Franz diffusion cells. Being a flow-through cell, receptor fluid continuously flows beneath the tissue at a specified rate closely mimicking the blood flow and maintaining sink conditions while allowing automatic sampling, which saves time and costs. As membranes are placed between the chambers in the vertical orientation, potential for air bubble formation is minimized. Also, the tissue surface is not exposed to air, avoiding the drying of the tissue and consequent loss of validity.

On the other hand, this type of diffusion cell is a complex system (1) and requires a high amount of solution and formulation.

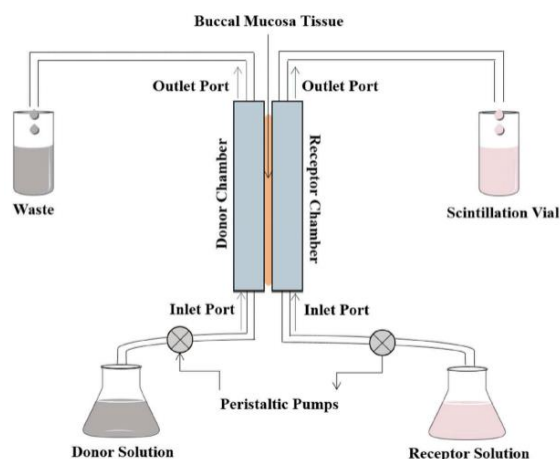


**Figure 14** - Schematic representation of a flow-through diffusion cell (1).

### 1.7.4.3. Ussing chambers

Ussing Chambers consists of two half-chambers, a perfusion system, an amplifier, and a data acquisition system. One half-chamber has stainless-steel pins that connect to the corresponding holes in the other half chamber face, placing the membrane in between to then be clamped together. The donor is filled with the drug solution and an equal volume of buffer is placed in the receptor chamber. Each half-chamber has an inlet or outlet for access to the water jacket, which allows thermoregulation, and a separate inlet port to where the circulation system pumps carbogen gas (95% O<sub>2</sub> and 5% CO<sub>2</sub>), that ensures stirring in the chamber and maintains the tissue viability (1). A solution of drug in physiological buffer is applied to the donor chamber and the same volume of this buffer is placed in the receptor chamber. Moreover, each chamber as a set of two electrodes for voltage and potential difference determination, and two more for the current (86). The carbogen gas provided to the chambers consists of a major advantage when compared to the previous type diffusion cell; however, Ussing chamber has a relatively low throughput as it does not allow a large set of segments to be analyzed. Membranes that can be applied to this apparatus include porcine mucosal tissue (87).

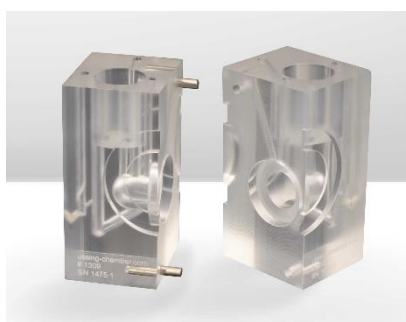


**Figure 15** - Ussing diffusion chamber (88).

This bibliographic survey provided knowledge upon the need to develop a method capable of optimizing Bluepharma's drug formulations based on buccal permeation, which will be addressed in Chapter 2.



# *Chapter 2.*

## *Method Development*



## 2.1. HPLC method development for content and permeation profile

This chapter regards the development of a High-Performance Liquid Chromatography (HPLC) based analytical method in order to quantify the total amount of drug in the formulation (Content) and the amount of drug permeated through the permeation profile (Permeation profile).

### 2.1.1. Introduction

HPLC is an advance form of liquid chromatography, an analytical technique used to separate a mixture of molecules into its individual components. The separation relies on the use of different phases or immiscible layers, one of which is held stationary while others move over it. A schematic diagram of a basic HPLC system as well as its main components - pump, injector, column, detector, and data processor - are shown in Figure 16.

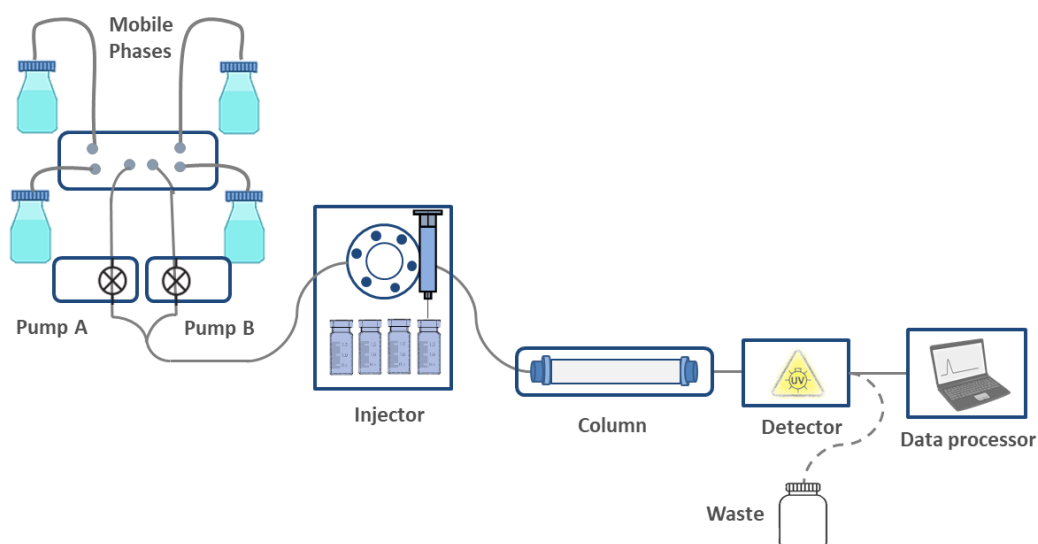


**Figure 16** - Schematic representation of HPLC-PDA.

In HPLC, a liquid mobile phase is mechanically delivered from the reservoirs by a **pump** through the system in which an **injector** places the sample into the flowing mobile phase to undergo the separation process in the **column** comprising the stationary phase. This molecular separation is conducted through reversed-phase chromatography, which involves the use of a moderately polar mobile phase and a non-polar stationary phase, ranking molecules based on their hydrophobicity through interactions with the non-polar stationary phase, i.e., molecules with polar characteristics reflect inferior retention times whilst retention time is superior for apolar molecules, see Figure 17.

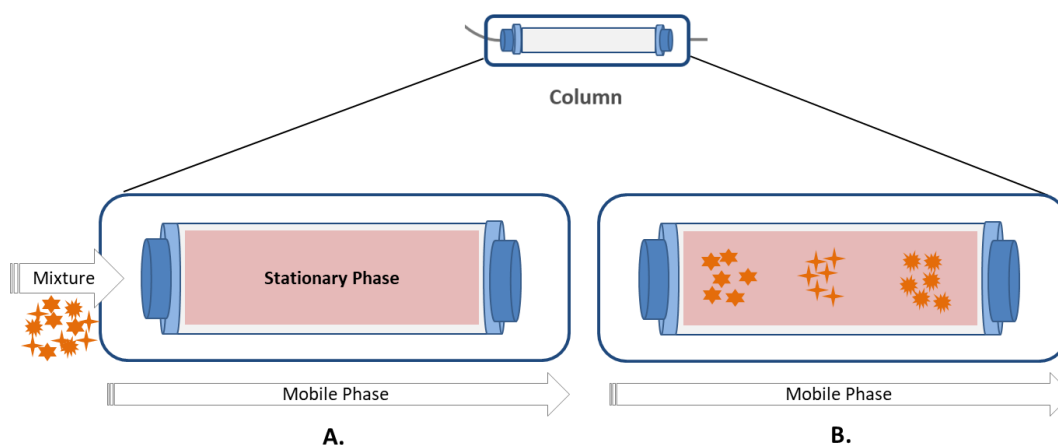


**Figure 17** - Schematic representation of the separation process within the HPLC column. **A.** Mixture entering the column with the stationary phase; **B.** Analytes separated by polarity.

After passing through the column, the separated components are sensed by a detector, in our case, a **photodiode array (PDA) detector**. PDA is an UV-VIS detector which consists in a flux cell placed at the end of the column where a ray of light goes through the cell. These detectors employ a deuterium discharge lamp (emission in the UV range) as a light source and an additional tungsten lamp (emission in the visible range) and so, as the molecules reach the detector they absorb the radiation, resulting in measurable chromatographic peaks which data is controlled through adequate computer data acquisition software.

### 2.1.2. Method development

The initial analytical method conditions, described in Table 10, were based on the HPLC-PDA pre-validated method for assay of the API.

**Table 10** - Initial analytical method conditions for development.

<b>Equipment</b>	Shimadzu UFLC with SPD-M20A PDA Detector
<b>Column</b>	YMC Pack ODS-A/S5 $\mu\text{m}/12\text{nm}$ (250 mm x 4.6 mm; 5 $\mu\text{m}$ )
<b>Mobile phase</b>	A mixture of 1.36 g of sodium 1-octanesulfonate (anhydrous), 1.0 g of sodium chloride, 580 mL of water, 420 mL of methanol, and 1.0 mL of phosphoric acid.
<b>Flow</b>	1 mL/min
<b>Column Temperature</b>	30°C
<b>Detection</b>	UV 229 nm
<b>Injection volume</b>	5 $\mu\text{L}$
<b>Solvent</b>	150 mg of edetate disodium to a 2000 mL volumetric flask and add 0.9 mL of hydrochloric acid. Make up to volume with water, and mix.
<b>Run time</b>	15 min.
<b>API Concentration</b>	0.05 mg/mL



At 0.05 mg/mL as theoretical concentration, the API peak obtained with the chromatographic conditions described in the following Figure 18 and Table 11 presents good performance.

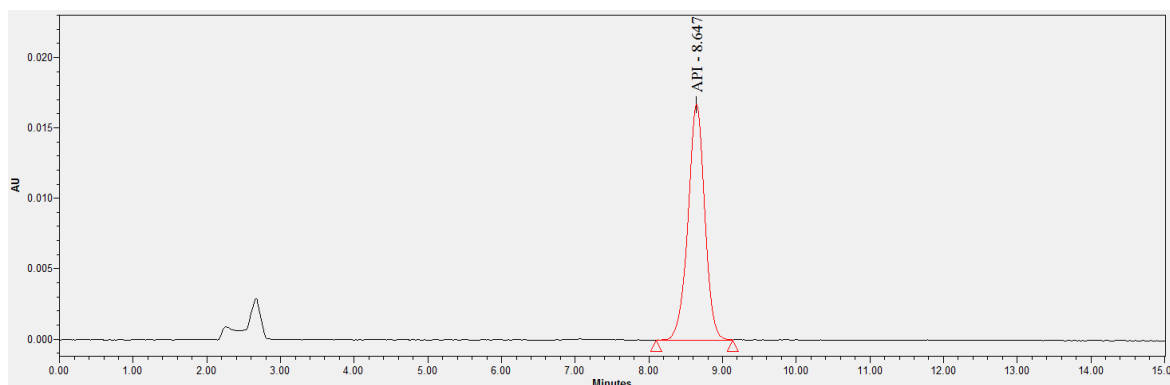


**Figure 18** - Chromatogram of API solution at 0.05 mg/mL in the solvent described in Table 10.

**Table 11** - Performance parameters for API standard solution at 0.05 mg/mL.

Test solution conc. (mg/mL)	Injection volume ( $\mu$ L)	RT (min)	Area	Resolution	Symmetry Factor	EP Plate count
0.05	5	8.65	261115	-	0.97	7.55E+03

In the permeation test, the API diffuses to phosphate buffered saline pH=7.4 solution (PBS pH=7.4). A standard solution of API at 0.05 mg/mL was made in PBS pH=7.4 and injected in the HPLC-PDA (same instrumental conditions as described in Table 10). The chromatogram can be seen in Figure 19 and the chromatographic performance can be seen in Table 12.

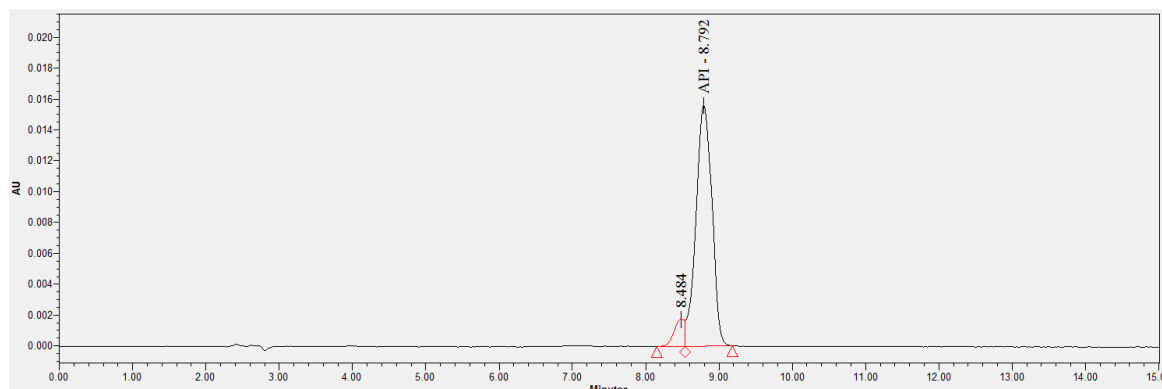


**Figure 19** - Chromatogram of API standard solution at 0.05 mg/mL in PBS pH=7.4 and instrumental conditions described in Table 10.

**Table 12** - Performance parameters for API standard solution at 0.05 mg/mL in PBS pH=7.4 and instrumental conditions described in Table 10.

Test solution conc. (mg/mL)	Injection volume (µL)	RT (min)	Area	Resolution	Symmetry Factor	EP Plate count
0.05	5	8.79	238349	-	-	7.17E+03

In PBS pH=7.4, it was clear the influence of an interfering peak in the peak of API. This influence can be verified through the analysis of Figure 19.

In order to remove the interfering peak, several changes were tested:

- Change in solvent:
  - PBS pH=7.4 and adjustment of pH before injection to pH=2.3;
  - PBS pH=7.4 and addition of EDTA;
  - NaCl 0.9%;
  - Ultrapure water.
- Change in chromatography column:
  - YMC-Triart C18/S-5µm/12nm (150mm x 4.6mm; 5µm).

The variations introduced in the methodology did not provide a reasonable separation of interfering peak, which led to the need of further adjustments.

Afterwards, a new mobile phase was tested, using the column YMC-Triart C18/S-5µm/12nm (150 mm x 4.6 mm; 5 µm). The new mobile phase is a mixture of 50 mM Ammonium Acetate Buffer pH=9.0 and Acetonitrile (44:56 v/v).

A standard solution of the API at 0.6 mg/mL was made in PBS pH=7.4 and 10 µL was injected in the HPLC-PDA. The chromatogram can be seen in Figure 20 and the chromatographic performance is displayed in Table 13.

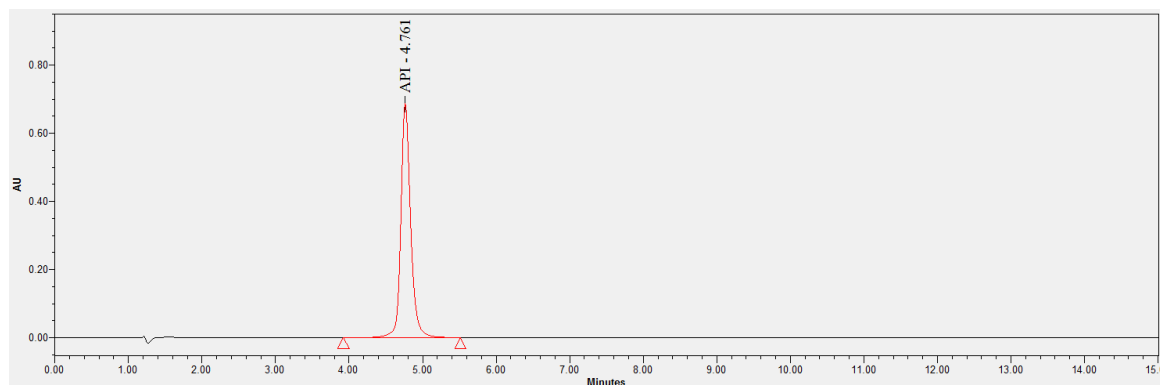


**Figure 20** - Chromatogram of API standard solution at 0.6 mg/mL in PBS pH=7.4 with the new mobile phase.

**Table 13** - Performance parameters for API standard solution at 0.6 mg/mL in PBS pH=7.4 with the new mobile phase.

Test solution conc. (mg/mL)	Injection volume (µL)	RT (min)	Area	Resolution	Symmetry Factor	EP Plate count
0.60	10	4.76	6428408	12.2	1.22	7.06E+03

As it can be seen in Figure 21 and Table 14, API peak complies with performance parameters in the new conditions; nevertheless, the chromatogram and method were optimized by changing:

- Injection solution concentration,
- Mobile phase ratio between 50 mM Ammonium solution pH=9.0 and Acetonitrile,
- Mobile phase flow.

A standard solution of API at 0.200 mg/mL was made in PBS pH=7.4 and 10 µL was injected in the HPLC-PDA with the optimized changes. The chromatogram can be seen in Figure 21 and the chromatographic performance is detailed in Table 14.

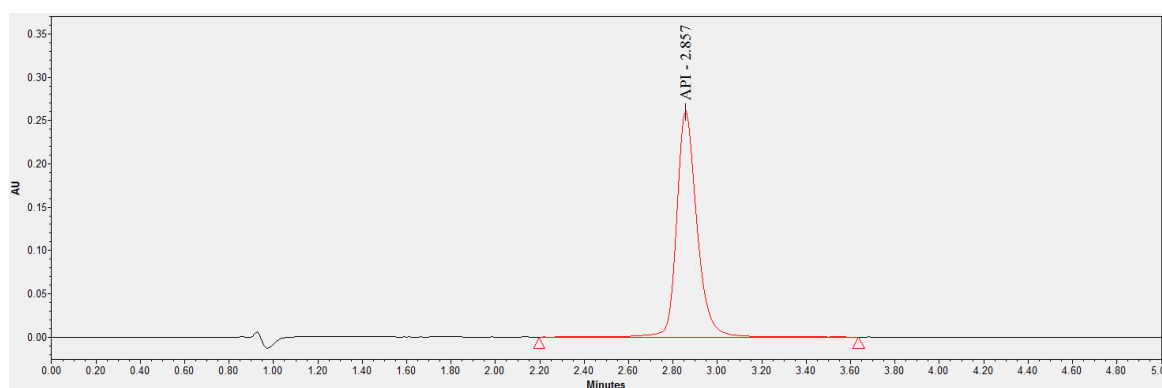


**Figure 21** - Chromatogram of API standard solution at 0.2 mg/mL in PBS pH=7.4 with the new method conditions.

**Table 14** - Performance parameters for API standard solution at 0.2 mg/mL in PBS pH=7.4 with the new method conditions.

Test solution conc. (mg/mL)	Injection volume (µL)	RT (min)	Area	Resolution	Symmetry Factor	EP Plate count
0.20	10	2.857	1629138	-	1.25	5.27E+03

Considering the results obtained - good performance for the API peak in what concerns suitable areas and short run time, it was decided to proceed to the pre-validation of content and permeation profile analysis of the API with the chromatographic conditions described in Table 15.

**Table 15** - Analytical method conditions for pre-validation.

<b>Equipment</b>	Shimadzu UFLC with SPD-M20A PDA Detector
<b>Column</b>	YMC-Triart C18/S-5µm/12nm (150 mm x 4.6 mm; 5 µm).
<b>Mobile phase</b>	50 mM Ammonium Acetate buffer pH 9.0: ACN (44:56 v/v)
<b>Flow</b>	1.3 mL/min
<b>Column Temperature</b>	30°C
<b>Detection</b>	UV 229 nm
<b>Injection volume</b>	10 µL
<b>Solvent</b>	Phosphate Buffered saline (PBS) pH 7.4
<b>Run time</b>	7 min.
<b>API Concentration</b>	0.2 mg/mL

### 2.1.3. Assessment of results - HPLC method pre-validation

Regarding analytical method development, several parameters are required to be followed and comprised within certain acceptance criteria according to ICH Q2 (R1) guideline (89) , as presented in Table 16.

**Table 16** - Parameters and respective acceptance criteria for analytical method development. Key: RSD = relative standard deviation; DL = Detection limit; QL = Quantification limit; S/N =signal/noise.

Parameter	Acceptance Criteria
<b>Selectivity</b> (Content and Permeation profile)	The presence of excipients should not interfere with API peak. Peak performance should comply. % interference $\leq 2\%$
<b>System Precision</b> (Content and Permeation profile)	RSD (n=6) $\leq \pm 0.85\%$
<b>Detection and Quantification Limits</b> (Permeation profile)	DL:S/N ratio $\geq 3$ QL: S/N ratio $\geq 10$
	Recovery QL (n=3) 90-110% RSD $\leq 7\%$
<b>Linearity</b> (Content)	y-intercept $\leq \pm 3\%$ r $\geq 0.997$
<b>Linearity</b> (Permeation profile)	y-intercept $\leq \pm 10\%$ r $\geq 0.99$
<b>Accuracy</b> (Content)	Recovery of API 98-102% RSD $\leq 2\%$
<b>Stability</b> (Content)	% change on average concentration from t=0h: $\leq 2\%$ t-test: p-value $> 0.05$

### 2.1.3.1. Specificity

Specificity, also termed selectivity, refers to the ability of producing a signal unequivocally due to the active ingredient, in the presence of other compounds and under the instrumental conditions of the method. A selective method is capable of recognizing the peak of the active pharmaceutical ingredient (API) discriminating between the analyte and other closely related structures present in the sample matrix (inactive ingredients) and the set-up used in permeation studies.

The solutions below were prepared once at the theoretical concentration levels (content and permeation profile), in volumetric flasks or from the Franz-Cells and analyzed according to the analytical method:

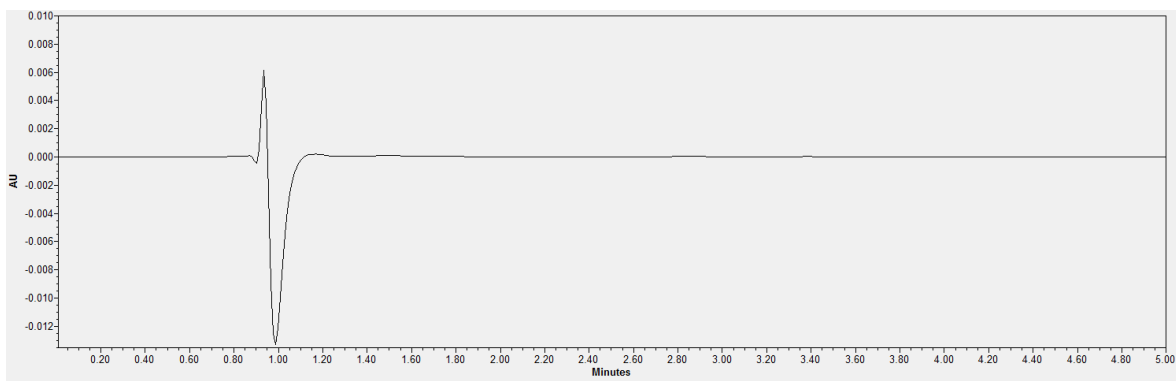
- Blank solution - solvent PBS pH=7.4,
- Formulation excipients after permeation in *set-up* with Permeapad<sup>®</sup> membranes,
- Formulation excipients (at 100 % content and permeation profile),
- Reconstituted formula: API at 0.3% (QL) for the permeation profile ( $C_{API} \approx 0.001$  mg/mL) + formulation excipients,

- Standard solution at 100% ( $C_{API} \approx 0.20$  mg/mL),
- Reconstituted formula: DS at 100% ( $C_{API} \approx 0.20$  mg/mL for content and  $C_{API} \approx 0.33$  mg/mL for permeation profile) + formulation excipients,
- Real Sample - Content,
- Real Sample - Permeation profile.

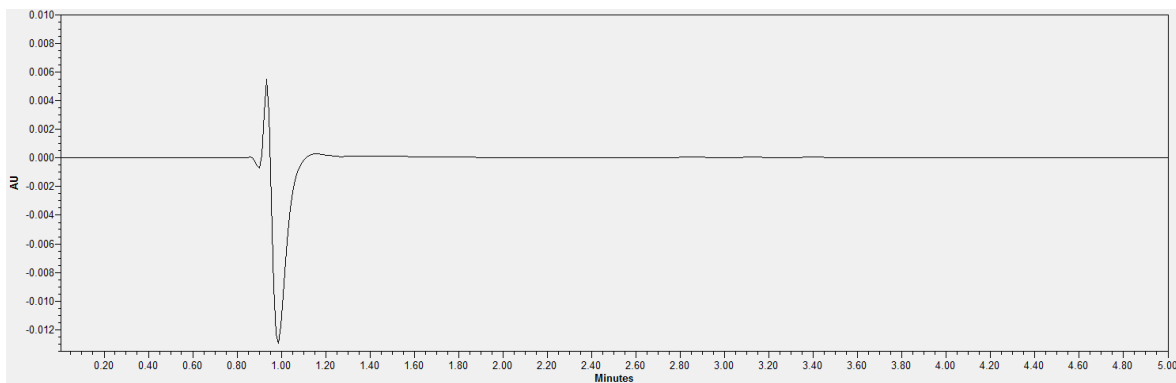
Performance parameters were evaluated for API peak in standard solution, reconstituted formula and test sample: resolution, peak symmetry and theoretical plate number.

**Chromatograms obtained from selectivity:**

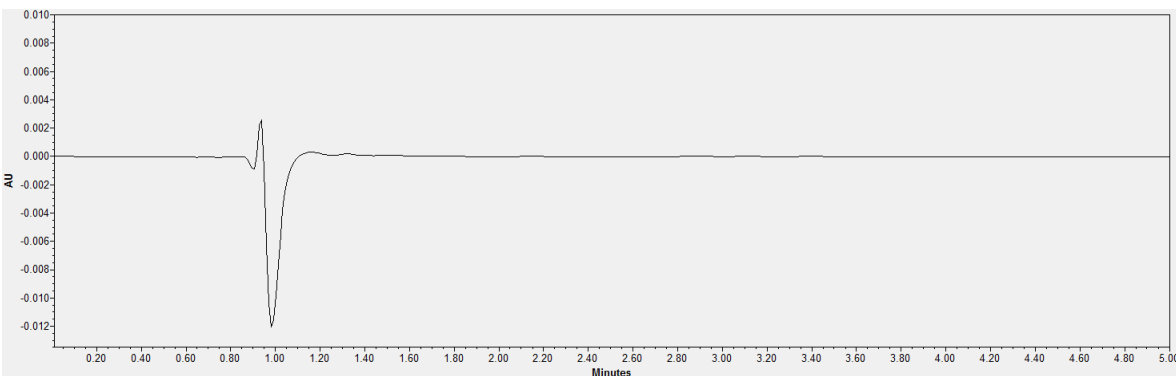
a)



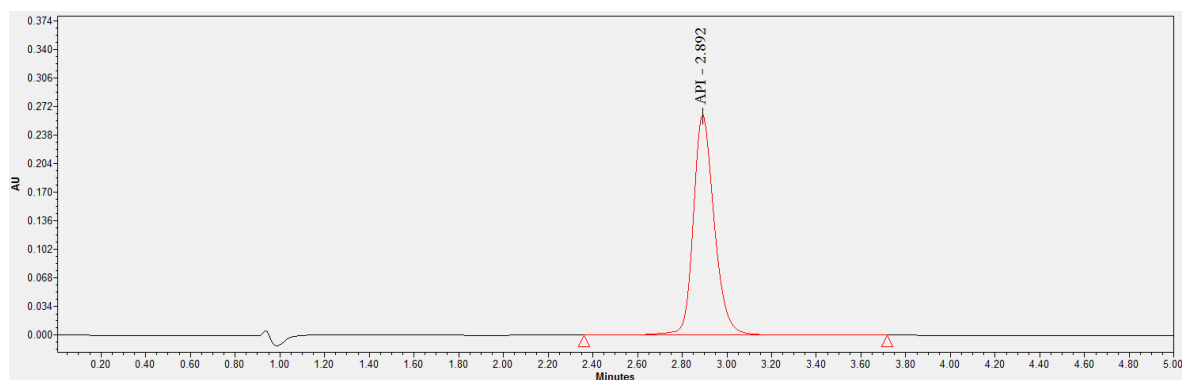
b)



c)



d)



e)

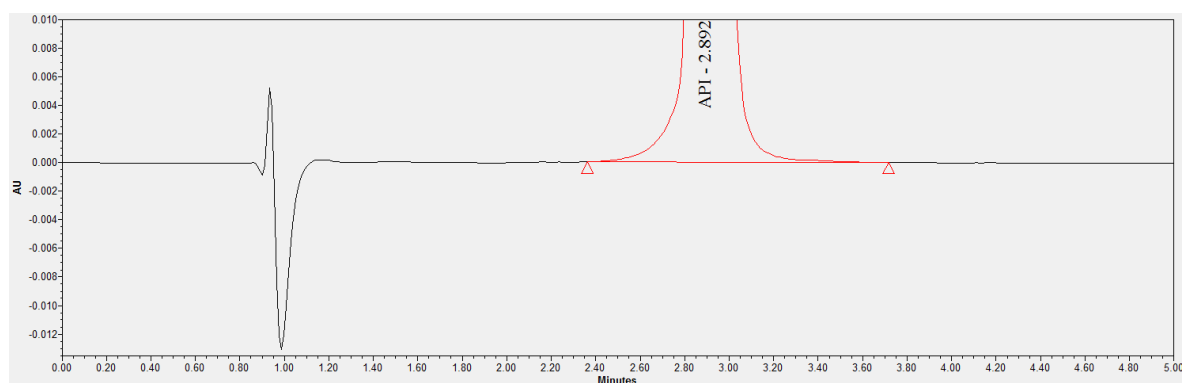


**Figure 22** - Chromatograms obtained from specificity method assessment: **a)** Selectivity: Blank Solution (PBS pH=7.4) (zoomed chromatogram); **b)** Selectivity: Placebo at content concentration (zoomed chromatogram); **c)** Formulation after permeation in set-up with Permeapad® membranes (zoomed chromatogram); **d)** Selectivity: Standard solution at 100% ( $C_{API} \approx 0.20$  mg/mL); **e)** Selectivity: Standard solution at 100% ( $C_{API} \approx 0.20$  mg/mL) (zoomed chromatogram).

The evaluation of the method performance is expressed in Table 17. All test samples comply with the limits established for retention time, resolution, theoretical plate number and symmetry factor.

**Table 17** - Performance evaluation results of API peak.

Sample	Retention Time (min)	Resolution	Theoretical Plate Number	Symmetry Factor (S)
<b>Standard Solution</b> - Content 100% - ( $C_{API} \approx 0.20$ mg/mL)	2.89	a)	4718	1.23
<b>Standard Solution</b> - Permeation 100% - ( $C_{API} \approx 0.33$ mg/mL)	2.89	a)	4625	1.23
<b>Reconstituted Formula FT22</b> (permeation profile 0.30% - $C_{API} \approx 0.0010$ mg/mL)	2.89	a)	4432	1.14
<b>Reconstituted Formula FT22#1</b> (content 100% - $C_{API} \approx 0.20$ mg/mL)	2.89	a)	4601	1.24
<b>Reconstituted Formula FT22#1</b> (permeation profile 100% - $C_{API} \approx 0.33$ mg/mL)	2.89	a)	4680	1.23
<b>Reconstituted Formula FT22#2</b> (content 100% - $C_{API} \approx 0.20$ mg/mL)	2.89	6.9	4587	1.24
<b>Reconstituted Formula FT22#2</b> (permeation profile 100% - $C_{API} \approx 0.33$ mg/mL)	2.89	6.9	4638	1.23
<b>Reconstituted Formula FT22#3</b> (content 100% - $C_{API} \approx 0.20$ mg/mL)	2.89	3.4	4593	1.24
<b>Reconstituted Formula FT22#3</b> (permeation profile 100% - $C_{API} \approx 0.33$ mg/mL)	2.89	3.4	4639	1.24
<b>Reconstituted Formula FT22#4</b> - Content 100% - ( $C_{API} \approx 0.20$ mg/mL)	2.89	a)	4585	1.24
<b>Reconstituted Formula FT22#4</b> (permeation profile 100% - $C_{API} \approx 0.33$ mg/mL)	2.89	a)	4645	1.23
<b>Real Test Sample</b> (permeation content 100% - $C_{API} \approx 0.20$ mg/mL)	2.94	a)	6050	1.16
<b>Real Test Sample</b> (permeation profile ~ 90% - $C_{API} \approx 0.30$ mg/mL)	2.93	a)	5707	1.16
<b>Limits</b>	$\pm 10\%$	$\geq 1.5$	$\geq 2000$	$0.8 \leq S \leq 1.5$
<b>Evaluation</b>	COMPLIES	COMPLIES	COMPLIES	COMPLIES

a) First peak of the chromatogram

### 2.1.3.2. System precision

System precision is evaluated based on the closeness of agreement between 5-6 injections/measurements of the same standard solution in one day. Relative standard deviation (RSD) is usually investigated, and its evaluation dictates the precision of the method.

Precision of the HPLC system was demonstrated by performing 6 consecutive measurements in one day of one standard solution at 100% of theoretical content concentration ( $C_{API} \approx 0.20$  mg/mL) and one standard solution at 100% theoretical permeation profile concentration ( $C_{API} \approx 0.33$  mg/mL).



The concentration measured and results obtained for the system precision test at a theoretical content concentration ( $C_{API} \approx 0.20$  mg/mL) is expressed in Table 18.

**Table 18** - System precision results for API standard solution at 100% of the theoretical content concentration ( $C_{API} \approx 0.20$  mg/mL). Key: RF = response factor; RT = retention time; SD = standard deviation; RSD = Relative standard deviation.

<b>System precision (<math>C_{API} \approx 0.20</math> mg/mL)</b>	<b>RF</b>	<b>RT</b>
<b>Average (n=6)</b>	8.26E+06	2.85
<b>SD</b>	15601	0.003
<b>RSD (%)</b>	0.19	0.102

The concentration measured and results obtained for the system precision test at theoretical permeation concentration ( $C_{API} \approx 0.33$  mg/mL) are expressed in Table 19.

**Table 19** - System precision results for API standard solution at 100% of the theoretical permeation concentration ( $C_{API} \approx 0.33$  mg/mL). Key: RF = response factor; RT = retention time; SD = standard deviation; RSD= relative standard deviation.

<b>System precision (<math>C_{API} \approx 0.33</math> mg/mL)</b>	<b>RF</b>	<b>RT</b>
<b>Average (n=6)</b>	8.35E+06	2.85
<b>SD</b>	2707	0.004
<b>RSD (%)</b>	0.03	0.137

**Table 20** - System precision results evaluation. Key: RF = response factor; RSD = relative standard deviation.

	<b>RSD Results</b>	<b>Limits</b>	<b>Evaluation</b>
<b>API RF</b> ( $C_{API} \approx 0.20$ mg/mL)	0.19	$\leq 0.85\%$	COMPLIES
<b>API RF</b> ( $C_{API} \approx 0.33$ mg/mL)	0.03	$\leq 0.85\%$	COMPLIES

From the results obtained, it can be concluded that the system is precise for multiple measurements in the same standard solution.

### 2.1.3.3. Detection limit (DL) and quantitation limit (QL)

The detection limit (DL) is a statistical value that establishes the lowest amount or concentration of analyte that can be readily distinguished from zero. The presence of the analyte can be assessed but not necessarily quantified with reliable accuracy and precision.

As for the quantification limit (QL), it refers to the lowest amount of analyte in a sample which can be quantitatively determined with suitable precision and accuracy. The quantitation limit is a parameter of quantitative assays for low levels of compounds in sample matrices.

Several approaches are available to determine the detection and quantification limits. For this evaluation, a Signal-to-Noise approach was applied.

The maximum amplitude of the background noise (h) was evaluated in a chromatogram obtained from injection of a blank solution observed over a distance equal to 20 times the width at half-height of API in the chromatograms and situated equally around the place where these peaks would be found.

The signal-to-noise (S/N) was calculated as follows:

$$S/N = \frac{2H}{h} \quad (\text{Equation 5})$$

H = peak height (signal)

h = noise amplitude (noise)

For DL, the minimal concentration should provide a peak height three times the baseline noise ( $S/N \geq 3$ ). As for the QL, a peak height of ten times the baseline noise ( $S/N \geq 10$ ) should be given at the minimal concentration.

The QL was confirmed by performing a recovery test, analysing 3 independent test solutions containing API at QL concentration in a placebo formulation after the permeation test (using the receptor solution). The estimated DL and QL are expressed in Table 21.

**Table 21** - Detection Limit and Quantitation Limit by S/N ratio.

	Detection Limit			Quantitation Limit		
	Conc. Level (%)	Conc. Level (mg/mL)	S/N	Conc. Level (%)	Conc. Level (mg/mL)	S/N
API	0.03	0.0001	2.95	0.3	0.001	16.2

The QL of 0.3% was validated regarding the accuracy. Theoretical concentration, concentration measured, and results obtained are expressed in Table 22.

**Table 22** - API permeation accuracy results at 0.3%. Key: RSD = relative standard deviation; CI = confidence interval.

API Permeation Level	Area	Theoretical Conc. (mg/mL)	Obtained Conc. (mg/mL)	Recovery (%)	Average Recovery (%)	RSD (%)	95% CI (%)	
							Min.	Max.
0.3%	8311	9.27E-04	8.98E-04	96.81	98.13	1.51	94.39	101.9
	8553	9.26E-04	9.24E-04	99.72				
	8113	8.95E-04	8.76E-04	97.85				

The signal-to-noise (S/N) approach reveals the DL as 0.03% and QL as 0.3%.

The evaluation of QL regarding accuracy is expressed in Table 23.

**Table 23** - Evaluation of API accuracy at 0.3% (0.001 mg/mL). Key: RSD = relative standard deviation.

	Result	Limits	Evaluation
Recovery (%)	98.13	90% – 110%	COMPLIES
RSD (%)	1.51	≤ 7%	

#### 2.1.3.4. Linearity

The linearity of an analytical procedure is its ability (within a given range) to obtain test results that are directly proportional to the concentration (amount) of analyte in the sample.

For content: a set of 5 concentrations at 60%, 80%, 100%, 120% and 140% of theoretical content concentration ( $C_{API} \approx 0.20$  mg/mL) were prepared and analyzed. The set of solutions was prepared from 2 independent stock solutions of API. This test was performed for active ingredients alone. The final solutions obtained were analyzed according to the analytical procedure (single injection). Linear regression was computed from the data (concentration versus area units). The intercept of y-axis (related to the peak area of the solutions at 100% concentration level), slopes, residual sum of squares and correlation coefficient were calculated and evaluated. Linearity was evaluated in 1 day.

For permeation profile: a set of 14 concentrations at 0.3% (QL), 1.5%, 3.0%, 12% 24%, 36% 48%; 60%; 72%, 84%; 100%; 120%; 140% and 170% of the theoretical concentration of in Franz-cell were prepared and analyzed. The set of solutions was prepared from 2 independent stock solutions of API. This test was performed for API alone. The final solutions obtained were analyzed according to the analytical procedure (single injection). Linear regression was computed from the data (concentration versus area units). The intercept of y-axis (related to 100%), slope, residual sum of squares and correlation coefficient were calculated. Linearity was evaluated in 1 day.

The obtained results for API in theoretical content concentration ( $C_{API} \approx 0.20$  mg/mL) are expressed in Table 24 and Figure 23.

**Table 24** - Linearity results for API in theoretical content concentration ( $C_{API} \approx 0.20$  mg/mL). Key: RF = response factor.

Concentration Level (%)	Real concentration (mg/mL)	Area	RF (n= 1)
60	0.12	983232	8.21E+06
80	0.16	1327117	8.27E+06
100	0.20	1649604	8.26E+06
120	0.24	1999114	8.31E+06
140	0.28	2328479	8.33E+06

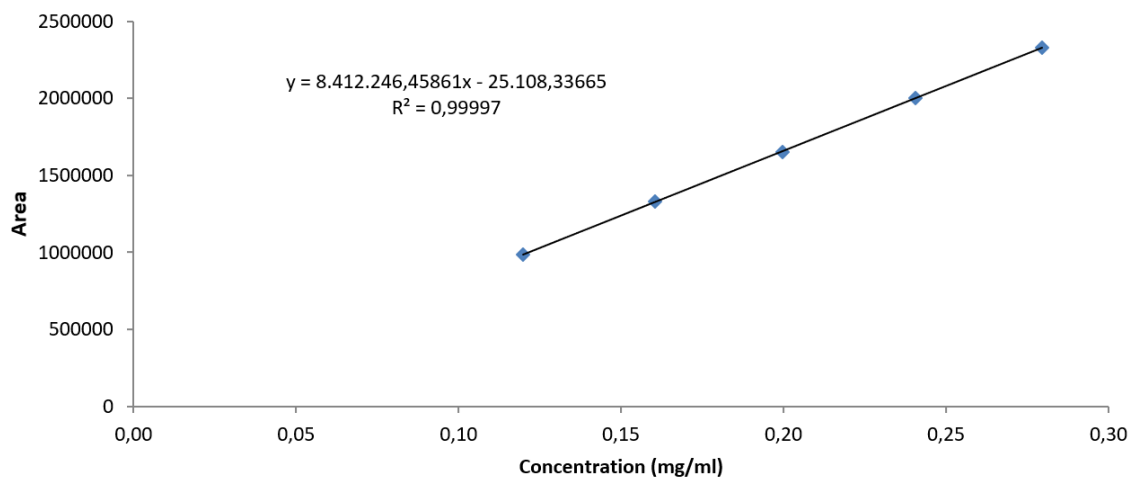


**Figure 23** - Linear regression for API in theoretical content concentration ( $C_{API} \approx 0.20$  mg/mL).

The obtained results for API in theoretical permeation concentration ( $C_{API} \approx 0.33$  mg/mL) are expressed in Table 25 and Figure 24.

**Table 25** - Linearity results for API in theoretical permeation concentration ( $C_{API} \approx 0.33$  mg/mL). Key: RF = response factor.

Concentration Level (%)	Real concentration (mg/mL)	Area	RF (n= 1)
0.30	0.0010	9309	9.29E+06
1.5	0.0050	41366	8.29E+06
3.0	0.0100	83480	8.33E+06
12	0.0399	327753	8.21E+06
24	0.0802	668113	8.33E+06
36	0.1198	983232	8.21E+06
48	0.1604	1327117	8.27E+06
60	0.1997	1649604	8.26E+06
72	0.2406	1999114	8.31E+06
84	0.2796	2328479	8.33E+06
100	0.3348	2791570	8.34E+06
120	0.3994	3334941	8.35E+06
140	0.4692	3905667	8.33E+06
170	0.5592	4592080	8.21E+06

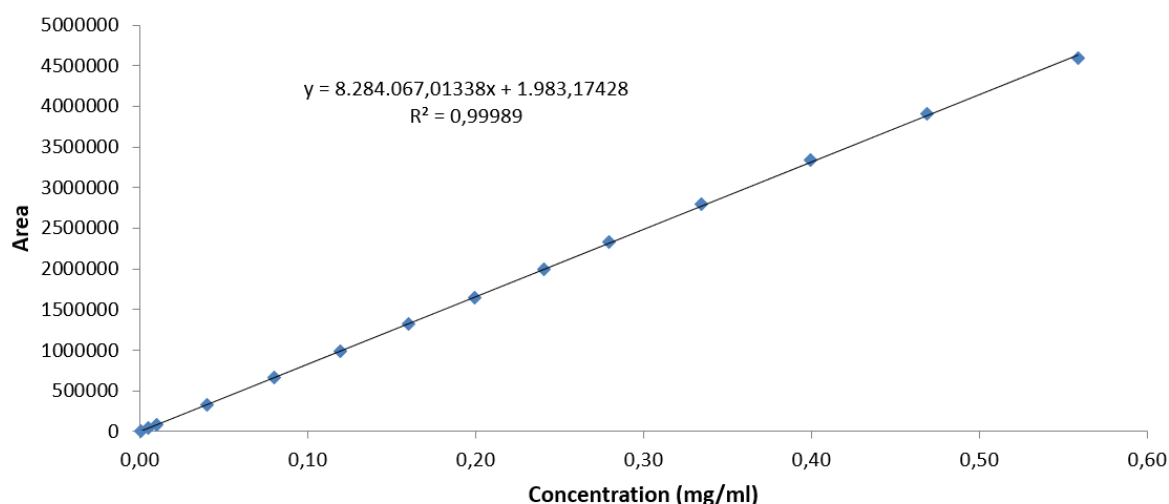


**Figure 24** - Linear regression for API in theoretical permeation concentration ( $C_{API} \approx 0.33$  mg/mL).

The evaluations of the method linearity results for API in theoretical content concentration ( $C_{API} \approx 0.20$  mg/mL) are expressed in Table 26.

**Table 26** - Linearity results evaluation for API in theoretical content concentration ( $C_{API} \approx 0.20$  mg/mL).

	Results	Limits	Evaluation
<b>y-intercept</b> (% rel. to $\approx 0.20$ mg/mL)	-1.52	$\leq \pm 3\%$	COMPLIES
<b>Correlation coefficient (r)</b>	1.000	$\geq 0.997$	COMPLIES
<b>Residual Sum of Squares</b>	3.87E+07	-	-
<b>Slope</b>	8.41E+06	-	-

The evaluations of the method linearity results for API in theoretical permeation concentration ( $C_{API} \approx 0.33$  mg/mL) are expressed in Table 27.

**Table 27** - Linearity results evaluation for API in theoretical content concentration ( $C_{API} \approx 0.33$  mg/mL).

	Results	Limits	Evaluation
<b>y-intercept</b> (% rel. to $\approx 0.33$ mg/mL)	0.07	$\leq \pm 10\%$	COMPLIES
<b>Correlation coefficient</b>	1.00	$\geq 0.99$	COMPLIES
<b>Residual Sum of Squares</b>	3.24E+09	-	-
<b>Slope</b>	8.28E+06	-	-

From the results obtained, it can be concluded that the method can generate results directly proportional to the concentration of API within the range of the analytical procedure (content and permeation profile).

### 2.1.3.5. Accuracy

Accuracy expresses the closeness of agreement between the value which is accepted either as a conventional true value or an accepted reference value and the value found in the analytical method. It is evaluated by calculation of recovery and is expressed as recovery percentage of the theoretical amount.

The analysis was performed as follows:

Three independent solutions of reconstituted formulas were prepared for the levels 60%, 100% and 140% of theoretical content concentration ( $C_{API} \approx 0.20$  mg/mL). They were analyzed according to the analytical procedure (single injection). Each test solution was prepared with independent weighing's.

Recovery percentage, RSD between recovery values and 95% confidence interval were calculated and evaluated from 3 measurements from each level.

The evaluation of the method accuracy is expressed in Table 28.

**Table 28** - Evaluation of accuracy results. Key: RSD = relative standard deviation; CI = confidence interval.

	Level			Limits (%)	Evaluation
	60%	100%	140%		
<b>Recovery (%)</b>	99.77	99.45	98.67	98 - 102	COMPLIES
<b>RSD (%)</b>	0.72	0.20	0.37	≤ 2	COMPLIES
<b>95% CI (%)</b>	97.98 – 101.6	98.96 – 99.93	97.75 – 99.60	-	Suitable

From the evaluation of results, it can be concluded that the analytical method is accurate in the range of 60 to 140%.

### 2.1.3.6. Stability

The stability is defined as the ability of a sample to preserve its physicochemical properties, and especially the concentration of the analyte, after several times of storage under specific conditions. Stability assays are important to estimate the maximum allowed period between standard preparation and analysis or between sample collection and analysis.

Standard Solutions:

Two API standard solutions at 100% ( $C_{API} \approx 0.20\text{mg/mL}$ ) were prepared from two independent weightings. Standard solutions were analyzed (single injection) at  $t=0\text{h}$ .

The standard solutions were kept:

- In vial inside the auto-sampler at  $20^{\circ}\text{C}$  and re-injected at approximately  $t=3\text{h}$ ,  $t=6\text{h}$ ,  $t=23\text{h}$ , and  $t=47\text{h}$ .

Standard solution stability was determined in the concentration change of API in each time tested. The results were also compared with t-student test (paired two samples for the mean), considering a confidence level of 95% ( $p\text{-value}>0.05$ ).

The evaluation of the method stability for the standard solution of API ( $C_{API} \approx 0.20\text{mg/mL}$ ) is expressed in Table 29.

**Table 29** - Results evaluation for  $C_{API}$  standard solution in vials kept inside the autosampler at  $20^{\circ}\text{C}$ .

	t = 3h	t = 6h	t = 23h	t = 47h	Limits	Evaluation
<b>Change in Average concentration (%)</b> (from t = 0h)	0.05	0.31	0.25	0.26	$\leq 2$	COMPLIES
<i>Student test for average concentration</i> <b>(p-value)</b>	0.41	0.10	0.14	0.21	$> 0.05$	STATISTICALLY SIMILAR

From the evaluation of results, it can be concluded that standard solutions are considered stable for, at least, 47 hours kept in vials at  $20^{\circ}\text{C}$  (inside the autosampler).

A summary from the assessment of results is presented in Table 30.

**Table 30** - Assessment of results from HPLC Method Pre-Validation. Key: RSD = relative standard deviation, CI = confidence interval; S/N = signal-to-noise.

Parameter	Result				
<b>Selectivity</b> (Content and Permeation profile)	<b>Parameter</b>		<b>Result</b>		
	Interference		Comply		
	Peak performance		Comply		
<b>System Precision</b> (Content and Permeation profile)	<b>Parameter</b>		<b>RSD (%)</b>		
	STD 100% Content		0.19		
	STD 100% Permeation		0.03		
<b>Detection and Quantification Limit</b> (Permeation profile)	<b>DL</b>		<b>QL</b>		
	<b>Level</b>	<b>S/N</b>	<b>Level</b>	<b>S/N</b>	
	0.03%	2.95	0.3%	16.2	
	<b>Level = 0.3% (QL)</b>				
	Average Recovery (%)		98.1		
	RSD (%)		1.51		
	CI_95% (%)		94.39-101.9		
<b>Linearity</b> (Content)	<b>Parameter</b>		<b>Result</b>		
	y-intercept (rel. 100% area)		-1.52		
	Correlation Coefficient		1.00		
	Residual Sum of Squares		3.87E+07		
<b>Linearity</b> (Permeation profile)	Slope		8.41E+06		
	y-intercept (rel. 100% area)		0.07		
	Correlation Coefficient		1.00		
	Residual Sum of Squares		3.24E+09		
<b>Accuracy</b> (Content)	<b>Parameter</b>		<b>Result</b>		
			<b>60%</b>	<b>100%</b>	<b>140%</b>
	Average recovery (%)		99.77	99.45	98.67
	RSD (%)		0.725	0.20	0.37
	CI 95%		97.98-101.6	98.96-99.93	97.75-99.60
<b>Stability</b> (Content)	<b>Standard Solution at 100%</b>				
	<b>Parameter</b>		<b>Autosampler 20°C</b>		
	Time (h)		47		
	% concentration change		0.26		
	p-value		0.21		

## 2.2. Franz Cell *in vitro* method development

### 2.2.1. Introduction

This section regards the development of a method to predict permeation of drug formulations through the buccal mucosa. An initial thorough comparison among the existing methodologies in what concerns *in vitro* membranes as well as compatible diffusion chambers was performed.



As previously described in **Section 1.7**, various membranes are mentioned as successful *in vitro* models. Amongst these, Permeapad<sup>®</sup> Barrier was selected as the model for this method based on applicability, ease to perform *in-house*, cost and purpose of the method. With the insight of achieving a method capable of distinguishing molecules with different characteristics as well as possible mechanisms, the fact that this biomimetic membrane is one of the very few *in vitro* models that includes paracellular transport besides transcellular is attractive. In addition, the time-consuming disadvantage of cell cultures; the higher cost of tissue-engineered mucosa and the reduced number of studies employing impregnated membranes reinforced this membrane choice.

As for the diffusion chamber, it was determined that the most used apparatus for *in vitro* buccal permeation studies with described compatibility for Permeapad<sup>®</sup> Barrier membranes included the Franz Cell, Flow through cell and Ussing Chamber. The definition of vertical Franz diffusion cell as the diffusion apparatus relied mostly on the *in-house* availability and the possibility to overcome the disadvantages often raised by authors.

In an *in vitro* permeation study, the experimental conditions including, amongst others, the temperature, buffer solutions, and dose of formulation, should be as close as possible to the *in vivo* conditions to obtain biorelevant results. On this matter, the donor chamber reflects the site of drug delivery, the buccal mucosa; whereas the receptor chamber simulates *in vivo* plasma, defined as PBS pH=7.4. As drug permeation occurs through the Permeapad<sup>®</sup> Barrier membrane, samples are taken periodically from the receptor chamber and replaced by fresh PBS pH=7.4.

Notwithstanding, these study conditions need to be optimized to provide reproducible and reliable results. To this end, risk assessment tools were applied based on the analytical quality by design approach.

### **Analytical Quality by Design**

Manufacturing industries, including pharmaceutical, chemical, food and others, share a common purpose in providing products with quality, efficacy and safety. To this end, the pharmaceutical industry has been embracing a more systematic and risk-based approach when developing pharmaceutical products, termed as Quality-by-Design (QbD). According to ICHQ8 R2 guideline (90), QbD can be defined as “a systematic approach to drug development, which begins with predefined objectives, and uses science and risk management approaches to gain product and process understanding and ultimately process control”, reducing the

number of out-of-specification results and enhancing product quality (91). These have been extended to the development of analytical methods and procedures, referred to as analytical quality by design (aQbD). aQbD workflow can be categorized into several steps: definition of an analytical target profile (ATP) and critical method attributes (CMAs); implementation of a risk assessment to identify and assess risks associated with critical method parameters (CMPs); method development and validation by the establishment of a design of experiments (DoE) and a method operable design region (MODR) (92).

### 2.2.2. Set-up development

According to prior knowledge as well as literature research, a cause-effect relationship and risk assessment approach was established to identify critical method variables (CMV), that is, the parameters that present potential risks for the method and may then be important to be evaluated regarding the method performance.

The Cause-and-Effect diagram, also referred to as Ishikawa diagram, is represented in Figure 29. In a “fishbone-like” structure, potentially critical factors are organized into categories related to the analyst, laboratory environment, equipment, materials, methods, amongst others.

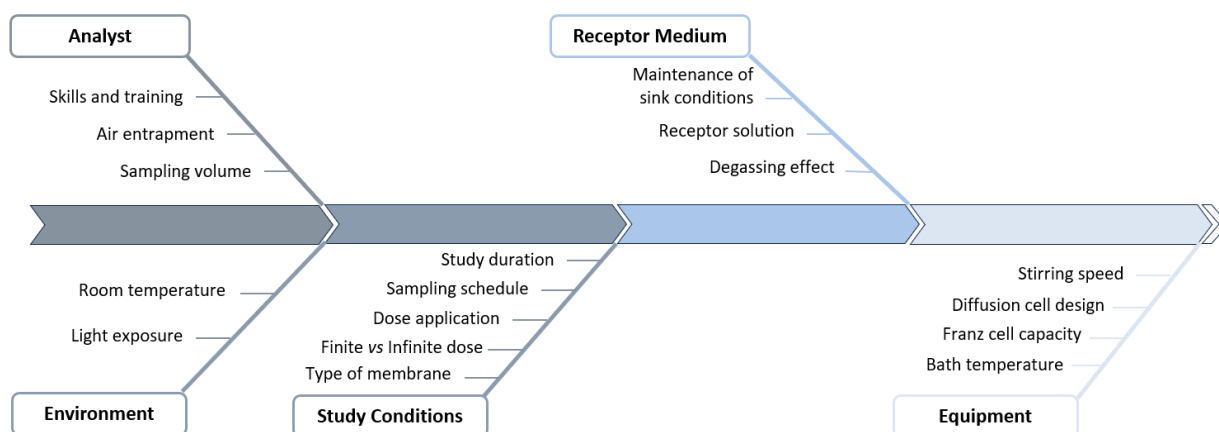


**Figure 25** - Representation of the Ishikawa diagram.

Based on the previous relationship and prior knowledge, the most prominent critical method variables (CMV) were categorized regarding criticality (low, medium, or high-risk variables) concerning the critical analytical attributes (CAAs) - permeability flux at steady state ( $J_{ss}$ ), apparent permeability ( $P_{app}$ ) and lag time - through the establishment of an initial risk estimation matrix, see Table 31.

**Table 31** - Initial risk assessment for IVPT method optimization. Criticality was assessed based on the impact of CMV on CAAs, i.e., permeability flux at steady state ( $J_{ss}$ ), apparent permeability ( $P_{app}$ ) and lag time.

Initial risk assessment for IVPT method optimization			
Critical method variables (CMV)		Criticality	Justification
Analyst	Skills and training	Medium	Compliance of this variable was established through laboratory qualification studies.
	Air entrapment	High	The presence of air bubbles reduces the contact area of the membrane with the receptor solution as well as the receptor volume of the diffusion cell, which leads to variability and bias results.
Measurement	Sampling volume accuracy	High	A reproducible sampling volume is required to attain an accurate determination of the cumulative drug amount in the receptor solution.
Equipment	Bath temperature	Medium	Mimic the temperature of <i>in vivo</i> environment (1).
	Diffusion cell design	Low	Vertical Franz Diffusion cells are extensively described as a suitable apparatus for permeation studies.
	Franz Cell capacity	Low	The volume capacity may influence the maintenance of sink conditions. If these are kept, the capacity is not a critical parameter.
	Stirring speed	Low	Stirring is critical for the maintenance of both the uniform drug distribution as well as temperature equilibrium (94). Poor stirring may be associated to an inefficient fluid mixing in the side arm; on the other hand, stirring should not cause vortex formation.
Study Conditions	Sampling Schedule	Medium	Frequently enough to allow steady state assessment.
	Finite dose vs Infinite dose	High	Finite dose reproduces 'in-use' conditions, applying a dose that may exhibit marked depletion which is reflected in the permeation profile by a plateauing effect. On the other hand, infinite-dose involves the application of a larger amount of formulation, desirable when the objective is the assessment of diffusional parameters.
	Dose application	Medium	The dose should be carefully applied to the donor chamber, and fulfill the mucosal surface area homogeneously.
	Type of membrane	Low	Membrane characteristics and its choice in the study may influence the resistance provided to the drug formulation. The membrane was previously selected.
Receptor Medium	Maintenance of sink conditions	High	Sink conditions have to be ensured in the receptor medium so that the drug permeation is not limited by the lack of solubility.
	Receptor solution	Low	Mimic body fluid conditions in terms of pH and salt content. The receiver pH was fixed at 7.4 to simulate <i>in vivo</i> plasma pH (93).

A set of experiments were then conducted to assess and validate the initial risk assessment to the end of establishing an updated risk assessment matrix based on the results.

### 2.2.2.1. Temperature evaluation test

The permeation test should be conducted with the set-up at a temperature of  $37\pm 0.5^{\circ}\text{C}$  to mimic the in vivo environment (1). To determine how much time the set-up takes to reach this temperature, the set-up was mounted by placing a PBS pH=7.4 cup within the water bath and each Franz Cell in the stirring system (600 rpm) connected to the circulator. The temperatures of the water bath, the PBS pH=7.4 cup and each of the 6 Franz Cell were registered every 5 minutes until a total of 40 minutes. The results obtained are shown in Table 8.

**Table 32** - Temperature ( $^{\circ}\text{C}$ ) of the *set-up* components.

Components	$T_{(t=0\text{min})}$	$T_{(t=5\text{min})}$	$T_{(t=10\text{min})}$	$T_{(t=15\text{min})}$	$T_{(t=20\text{min})}$	$T_{(t=25\text{min})}$	$T_{(t=30\text{min})}$	$T_{(t=35\text{min})}$	$T_{(t=40\text{min})}$
<b>Water-Bath</b>	15.5	25.3	33.2	36.9	37.0	37.0	37.1	37.0	37.1
<b>PBS 7.4 cup</b>	16.4	19.0	24.8	32.6	35.1	36.4	36.7	36.8	36.8
<b>Franz Cell 1</b>	18.4	25.0	33.0	36.6	36.7	36.7	36.7	36.7	36.7
<b>Franz Cell 2</b>	18.7	26.0	33.5	36.6	36.7	36.7	36.7	36.7	36.7
<b>Franz Cell 3</b>	17.9	26.0	33.6	36.6	36.7	36.7	36.7	36.7	36.7
<b>Franz Cell 4</b>	18.0	26.0	33.6	36.6	36.7	36.7	36.7	36.7	36.7
<b>Franz Cell 5</b>	18.1	26.0	33.8	36.6	36.7	36.7	36.7	36.7	36.7
<b>Franz Cell 6</b>	18.2	26.1	33.9	36.5	36.6	36.6	36.6	36.6	36.6

It was concluded that the *set-up* takes 30 minutes to reach the temperature of  $37\pm 0.5^{\circ}\text{C}$  and it stays stable for the next 10 minutes. The Franz Cells were left deliberately opened to mimic the worst-case scenario (heat losses), and the PBS pH=7.4 and water bath were deliberately cooled before starting the test to also simulate the worst-case scenario. The Franz Cell 6, despite complying with the test acceptance criteria ( $37\pm 0.5^{\circ}\text{C}$ ), reached a relatively minor temperature, which can be attributed to being the more distant Franz Cell on the stirring system from the circulator; moreover, the closest Franz Cell showed relatively greater temperature.

### 2.2.2.2. Filling procedure

According to *PermeGear, Inc.*, there are two possible filling procedures. Process number 1 refers to filling the Franz Cell with 12 mL using a syringe, and subsequently placing the membrane on top of the receptor chamber followed by the donor chamber, securing it with a clamp. The volume is then adjusted to be aligned with the calibration mark. Process number 2 refers to filling the Franz Cell with about 10 mL, place the membrane on top of the receptor chamber followed by the donor chamber, securing it with a clamp. The rest of the volume is filled after removal of the Franz Cell from the support system and while turning the Franz Cell at a  $\sim 90$  - degree angle using a replacement tip. The receptor chamber volume is then adjusted to be aligned with the calibration mark. The development carried on using the process number 2.

### 2.2.2.3. Air bubbles entrapment

One of the Franz Cell apparatus known limitations is the formation of air bubbles during the permeation test as the exposed surface area is diminished when bubbles are present, interfering with the permeation profile. On this matter, a test was conducted filling the Franz Cell with PBS pH=7.4 according to sub-chapter **2.2.2.2. Filling Procedure** process number 1, placing a dialysis membrane, and wrapping the top with a double layer of parafilm and the sampling port of the Franz Cell with a layer of parafilm. No air bubbles were visible at the start of the test, but along the study, bubbles were formed beneath the membrane and on the magnet.

To reduce the formation of air bubbles, the test was repeated previously degassing the PBS pH=7.4 for 10 minutes. The number of bubbles formed was reduced but were still present at both the magnet and below the membrane along with the study. Facing this issue, it was tested to previously touch the magnet with the micropipette tips while being stirred, so that the bubbles rise to the top; then lift the cell out of the support system and reverse it to turn it upside down so that the bubbles beneath the membrane are released out through the sampling port, as can be seen in Figure 30. The test was initiated with no air bubbles present but along the sampling process, bubbles were visibly formed. Therefore, it was included in the procedure to remove the air bubbles whenever necessary after each collection time point and subsequently align the receptor solution with the calibration mark. To facilitate this process, the tubes connecting the Franz Cell to the support system were switched to longer ones.

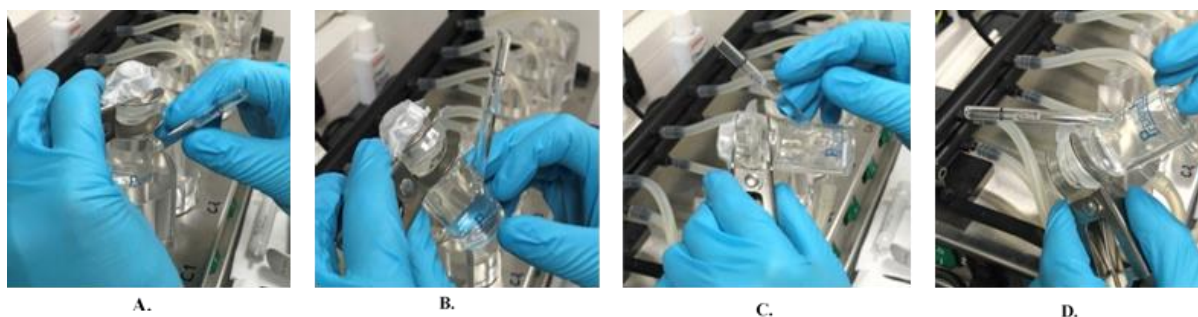


**Figure 26** - Sequence representation of air bubbles removal process. **A.** Franz Cell removal of the stirring system; **B.** Start of turning the Franz Cell; **C.** Franz Cell turned at a ~90-degree angle; **D.** Franz Cell turned at a ~100-degree angle, air bubbles being released through the sampling port while tapping on the bottom.

#### 2.2.2.4. Collection and replacement techniques

To collect the receptor solution from the Franz Cell, two techniques were studied regarding precision, accuracy and applicability. The first concerned a syringe with a tube connected to the respective needle, as it can be seen in Figure 27; and the second one can be described as a micropipette (200 $\mu$ L) plus a tip connected to a tube wrapped up in parafilm, as it can be seen in Figure 28. A series of 5 measurements of 100 $\mu$ L and 200 $\mu$ L were performed using water, consequently weighted, and the temperature ( $^{\circ}$ C) registered between measurements.



**Figure 27** - Needle plus a tube technique.



**Figure 28** - Micropipette plus a tube technique.

Table 33 resumes the results obtained from precision and accuracy tests.

**Table 33** - Collection techniques precision and accuracy results.

	100 $\mu$ L		200 $\mu$ L	
	Needle	Micropipette	Needle	Micropipette
<b>Average (mg)</b>	91.58	90.46	190.63	187.74
<b>SD (mg)</b>	2.55	0.14	3.79	1.47
<b>RSD (%)</b>	2.78	0.16	1.99	0.78
<b>H2O Vol. Average (<math>\mu</math>L)</b>	91.85	90.73	191.21	188.30
<b>Error (<math>\mu</math>L)</b>	-8.15	-9.27	-8.79	-11.70

The syringe technique (needle) showed higher variability between collections and although it demonstrated to have a relatively minor error, the need for a definition of volume at each collection by the analyst is less practical and can lead to analyst inter and intra-variability. For these reasons, the development proceeded with the more practical and more accurate micropipette technique.

After this initial analysis, the collection from the receptor solution using the micropipette tip was tested after filling a Franz Cell with about 12 mL of water. As the tube was introduced through the Franz Cell sampling port, water leaked from the apparatus due to the volume occupied by the tube. To surpass this issue, the tube used was replaced by a smaller caliber tube, maintaining the overall collection technique, as can be seen in Figure 29. No leakage or other problem was observed when introducing this micropipette tip into a Franz Cell filled with 12 mL of water. This statement was reinforced by pre-wrapping the top of the Franz Cell with parafilm, and by the introduction of a magnet.



**Figure 29** - Micropipette tip plus a small-caliber tube technique.

To have 1 micropipette tip associated with 1 Franz Cell when collecting the samples to avoid contamination, six similar micropipette tips were made and numbered, and their precision and accuracy were analyzed. The results are represented in Tables 34 and 35.

**Table 34** - Precision and accuracy of the micropipette tips collecting 100 $\mu$ L.

Micropipette	100 $\mu$ L					
	1	2	3	4	5	6
Average (mg) (n=5)	90.95	90.13	92.60	91.96	91.95	90.49
SD (mg)	0.22	2.07	0.50	1.28	0.53	1.00
RSD (%)	0.25	2.30	0.54	1.39	0.58	1.10
H <sub>2</sub> O Vol. Average ( $\mu$ L)	91.23	90.41	92.88	92.24	92.22	90.76
Error ( $\mu$ L)	-8.77	-9.59	-7.12	-7.76	-7.78	-9.24

**Table 35** - Precision and accuracy of the micropipette tips collecting 200 $\mu$ L.

Micropipette	200 $\mu$ L					
	1	2	3	4	5	6
Average (mg) (n=5)	191.20	191.60	193.25	191.64	191.23	190.63
SD (mg)	0.90	1.58	0.31	1.06	1.17	1.19
RSD (%)	0.47	0.82	0.16	0.55	0.61	0.63
H <sub>2</sub> O Vol. Average ( $\mu$ L)	191.77	192.18	193.83	192.21	191.81	191.20
Error ( $\mu$ L)	-8.23	-7.82	-6.17	-7.79	-8.19	-8.80

Based on the results obtained, the micropipette tips number 2 and number 6 were discarded for displaying superior RSD and error.

The replacement of the receptor solution is performed using a syringe where it is attached replacement tips that consist of a needle within a small-caliber tube wrapped in parafilm, as seen in Figure 30.



**Figure 30** - Receptor solution replacement tip.

After conducting some permeation tests, it was found that the RSD from the permeation profile was increased using this technique, which could be attributed to the micropipette tips starting to get deteriorated through usage and time. Precision and accuracy evaluations were performed, and the results are presented in Table 36.

**Table 36** - Precision and accuracy results of the micropipettes collecting 200 $\mu$ L from 19/10/2020 and 16/12/2020.

	200 $\mu$ L					
	Micropipette 1		Micropipette 3		Micropipette 4	
	19/out	16/dez	19/out	16/dez	19/out	16/dez
<b>Average (mg)</b>	191.20	191.43	193.25	191.54	191.64	188.61
<b>SD (mg)</b>	0.90	3.57	0.31	4.98	1.06	2.38
<b>RSD (%)</b>	0.47	1.86	0.16	2.60	0.55	1.26
<b>H<sub>2</sub>O Vol. Average (<math>\mu</math>L)</b>	191.77	192.00	193.83	192.12	192.21	189.18
<b>Error (<math>\mu</math>L)</b>	-8.23	-8.00	-6.17	-7.88	-7.79	-10.8

Although all 3 micropipette tips showed similar error compared to the initial evaluation, a significantly higher RSD is demonstrated. Furthermore, before the degradability issue and the impractical necessity of consistently building new micropipette tips, tips from Permegear<sup>®</sup> were acquired. Permegear<sup>®</sup> pipette tip assemblies are comprised of a 1 mL micropipette tip that gets attached to a longer tip, as illustrated in Figure 31.

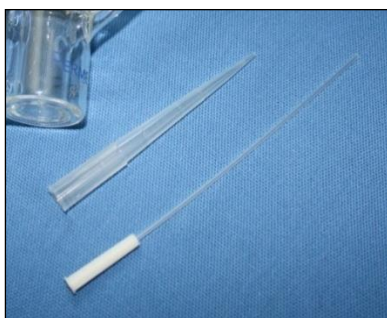


**Figure 31** - Permegear<sup>®</sup> micropipette tips assembly (94).



Precision and accuracy assessment tests were conducted comparing:

- A) Permegear® 1mL micropipette tip connected to the Permegear® pipette tip, and;
- B) 'in-house' 1mL micropipette tip connected to the Permegear® pipette tip.

The results from collecting 100µL and 200µL are presented in Tables 37 and 38, respectively.

**Table 37** - Precision and accuracy of the Permegear® micropipette tips collecting 100µL.

	100µL							
	A1	B1	A2	B2	A3	B3	A4	B4
<b>Average (mg) n=5</b>	77.16	74.35	76.11	76.29	76.63	76.58	76.38	76.46
<b>SD (mg)</b>	2.08	2.62	1.78	0.71	0.97	1.48	1.24	1.00
<b>RSD (%)</b>	2.69	3.53	2.34	0.93	1.26	1.94	1.62	1.31
<b>H<sub>2</sub>O Vol. Average (µL)</b>	77.28	74.47	76.34	76.51	76.77	76.72	76.51	76.60
<b>Error (µL)</b>	-22.72	-25.53	-23.66	-23.49	-23.23	-23.28	-23.49	-23.40

**Table 38** - Precision and accuracy of the Permegear® micropipette tips collecting 200µL.

	200µL							
	A1	B1	A2	B2	A3	B3	A4	B4
<b>Average (mg) n=5</b>	174.50	174.19	175.92	176.16	175.39	174.92	177.38	173.52
<b>SD (mg)</b>	2.69	3.89	1.80	2.16	1.89	1.87	2.50	3.48
<b>RSD (%)</b>	1.54	2.23	1.03	1.23	1.08	1.07	1.41	2.00
<b>H<sub>2</sub>O Vol. Average (µL)</b>	174.78	174.46	176.20	176.44	175.91	175.44	177.70	173.83
<b>Error (µL)</b>	-25.22	-25.54	-23.80	-23.56	-24.09	-24.56	-22.30	-26.17

Based on these results, to obtain an accurate volume during collection from the Franz Cell, an adjustment into the micropipette of plus 25µL to collection volumes of 100µL or 200µL is required.

Furthermore, precision and accuracy tests collecting 500µL were also performed, based on the necessity of increasing the volume collected from the receptor chamber. The results are presented in Table 39.

**Table 39** - Precision and accuracy of the Permegear® micropipette tips collecting 500µL.

Micropipette	500µL			535µL		
	1	2	3	4	5	6
<b>Average (mg) n=5</b>	468.22	466.62	464.26	494.93	502.94	506.95
<b>STD (mg)</b>	3.45	2.59	2.16	4.90	3.87	1.70
<b>RSD (%)</b>	0.74	0.55	0.47	0.99	0.77	0.33
<b>H<sub>2</sub>O Vol. Average (µL)</b>	469.49	467.88	465.52	496.27	504.30	508.33
<b>Error (µL)</b>	-30.51	-32.12	-34.48	-3.73	4.30	8.33

Based on these results, to obtain an accurate volume during collection from the Franz Cell, an adjustment into the micropipette of plus 35µL to a collection volume of 500µL is required.

### 2.2.2.5. Study conditions

#### ***Finite Dose vs Infinite Dose***

The applied dose of formulation on the donor chamber may vary according to the study purpose. Finite dose conditions reproduce 'in-use' conditions, by the application of a small amount (up to 10 mg/cm<sup>2</sup> (OECD, 2004)), mimicking *in vivo* conditions as the dose exhibits depletion as the study is carried out (95). Under finite dose conditions, the dose should be carefully applied on the donor chamber and homogeneously distributed through the membrane surface as the uneven surface area leads to biased results. This is usually prevented, in our case, by leaning the Franz Cell from side to side. On the other hand, studies can be conducted under infinite-dose conditions involving the application of a larger amount of formulation (more than 10 mg/cm<sup>2</sup> of formulation (OECD, 2004)) when the aim is the evaluation of diffusional parameters or investigation of mechanisms of permeation enhancement.

#### ***Maintenance of sink conditions***

The receptor medium can have an impact on compound solubility and consequently limit drug permeation as the drug must easily dissolve in the receptor medium. This is guaranteed by the establishment of sink conditions. On this matter, in order for sink conditions to be maintained, the maximum concentration of the sample in the receptor medium is required to be 3 times less the saturation solubility; which in certain cases can be challenging to maintain, for example, in poorly soluble drugs. Some modifications can be made to improve solubility, such as reduction in drug concentration; inclusion of solubility modifiers in the receptor medium; or modification of pH in the receptor medium, which on the other hand, may lead to loss of bio relevancy.

Moreover, under infinite dose conditions, there is a higher possibility of loss at sink conditions, since a larger amount of formulation is placed in the donor chamber. One strategy to overcome this circumstance is to increase the collection volume, increase the number of collections timepoints (or both) to avoid the concentration in the receptor solution exceeding its target for sink conditions (3x), since a higher amount of API mass is removed from the receptor chamber with the collection process.

Furthermore, in a permeation study, it is fundamental that sink conditions are kept during the steady-state phase of the permeation profile as the posterior time points are not required to measure permeability coefficients.

To this end, the concentration saturation of the API in PBS pH=7.4 was determined. The results are shown in Table 40.

**Table 40** - API concentration saturation in the receptor medium (PBS pH=7.4).

	<b>pH</b>	<b>Concentration (mg/mL)</b>
<b>#1</b>	7.441	0.55
<b>#2</b>	7.445	0.56
<b>#3</b>	7.442	0.62
<b>Average (mg/mL)</b>		0.58
<b>Target for sink conditions (3x) (mg/mL)</b>		0.193

Based on these results, the concentration in the receptor chamber should be kept inferior to 0.193 mg/mL to maintain sink conditions.

#### **2.2.2.6. Final risk assessment matrix**

In the Table 41, it is presented the final risk assessment matrix constructed based on the studies conducted and the knowledge acquired.

**Table 41** - Final risk assessment for IVPT method optimization. Criticality was assessed on the basis of the impact of CMV on CAA i.e., permeability flux at steady state ( $J_{ss}$ ), apparent permeability ( $P_{app}$ ) and lag time.

Final risk assessment for IVPT method optimization			
Critical method variables (CMV)		Criticality	Adjustments made
Analyst	Skills and training	Medium	Compliance of this variable was established through laboratory qualification studies.
	Air entrapment	Medium	Receptor medium degassing was included as well as the periodical removal of air bubbles.
Measurement	Sampling volume accuracy	High	Assessment of pipettes' precision and accuracy was performed. Micropipette's volume was adjusted, accordingly.
Equipment	Bath temperature	Medium	Study of <i>set-up</i> 37°C temperature achievement.
	Diffusion cell design	Low	Fixed parameter.
	Franz Cell capacity	Low	Fixed parameter.
	Stirring speed	Low	Fixed parameter.
Study Conditions	Sampling Schedule	Medium	Collection time points are narrower in the phases exhibiting higher variability, and longer as it reaches plateau phase.
	Finite Dose vs Infinite Dose	High	The dose will influence permeation profile and it depends on the objective of the study.
	Dose application	Medium	Possible losses are accounted by weighing the device before and after the formulation application. The formulation is homogenized by leaning the Franz Cell.
	Type of membrane	Low	Fixed parameter.
Receptor Medium	Maintenance of sink conditions	High	Sink conditions were calculated and an increase in collection volume was performed.

### 2.2.3. Evaluation of permeation profile of artificial membranes

#### **Permeation profile phases**

Through the permeation profile curve, three different phases can be defined and distinguished (see Figure 41). As the study begins with the insertion of the formulation on the donor chamber, the drug only starts to permeate when the membrane is saturated; this “saturation process” can be seen in the permeation profile and is termed lag time. The lag time is determined from the intercept of the extrapolated linear portion of the permeation profile with the X-axis.

This linear part of the plot corresponds to the steady-state. During this phase, the donor concentration is superior to the receptor concentration and permeation occurs, being the membrane capacity the main limiting factor for permeation.

As the donor chamber concentration gradually reduces, the variation between both chambers consequently keeps decreasing, eventually reaching a plateau, corresponding to the third phase.

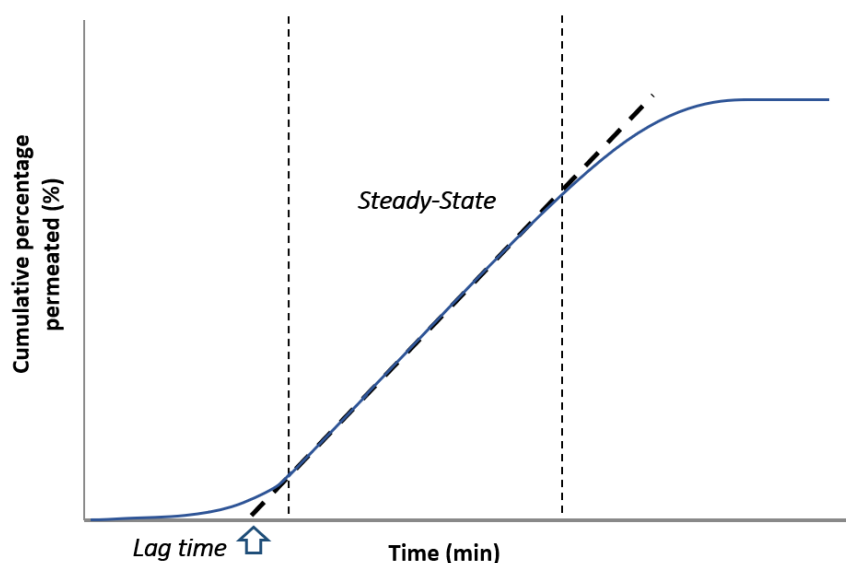


**Figure 32** - Permeation profile phases: Lag time, Steady-State and 'plateau' phase.

Permeation studies were conducted using several artificial membranes in order to compare the respective permeation profiles and permeability coefficients. The barriers placed between the donor and receptor chamber regarded two filter membranes, a dialysis membrane and the Permeapad Barrier® membrane.

### 2.2.3.1. Study conditions

Samples of 200 $\mu$ L were collected at 5, 10, 15, 20, 25, 30, 40, 50, 60, 90, 120, 180, 240, 300 and 360 minutes using Permeagear<sup>®</sup> micropipette tips from 3 Franz-Cell apparatus.

The steady-state flux was calculated as follows:

$$J_{ss} = \left( \frac{\Delta Q_t}{\Delta t} \right)_{ss} \cdot \frac{1}{A}, \quad (\text{Equation 6})$$

Where Q is the cumulative amount of drug permeated through the buccal mucosa membrane, t is the diffusion time and A is the diffusional area.

The permeability coefficient was calculated as follows:

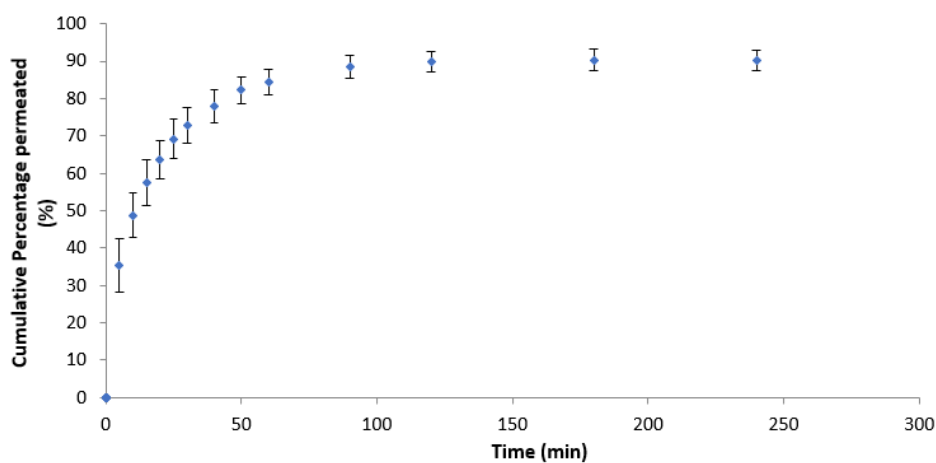
$$P = \frac{dQ/dt}{AC_d}, \quad (\text{Equation 7})$$

Where A is the surface area of diffusion, dQ/dt is the amount of drug permeated per unit time at steady-state and C<sub>d</sub> is the donor drug concentration.

### 2.2.3.2. Filters

The permeation profile of two different filter membranes regarding material, pore size and thickness was assessed. These consisted in a polypropylene filter, pore size of 0.2  $\mu$ m; as well as a Nylon Net Filter with a pore size of 80  $\mu$ m; both with 47mm diameter surface. The permeation profile using 0.2  $\mu$ m polypropylene filters and 80 $\mu$ m Nylon filters are presented in Figure 33 a) and b), respectively.

a)



b)

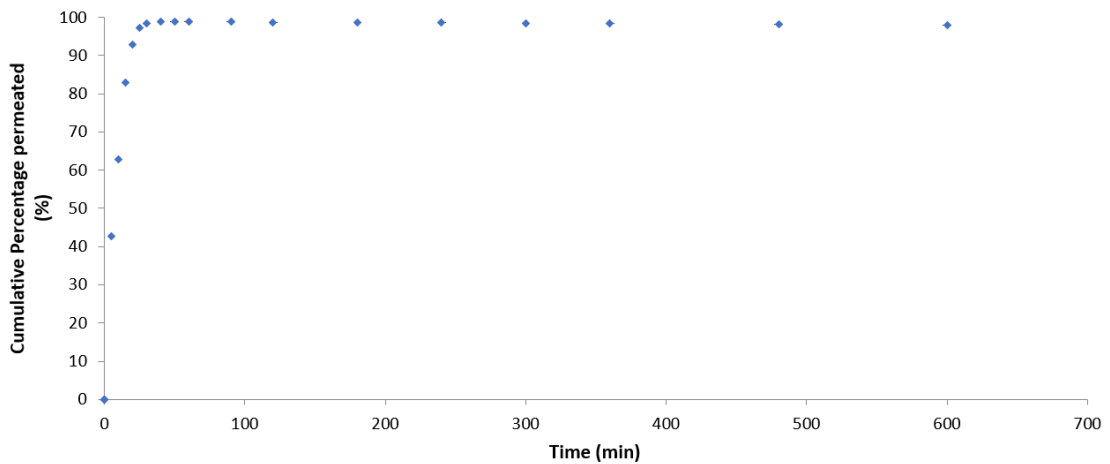


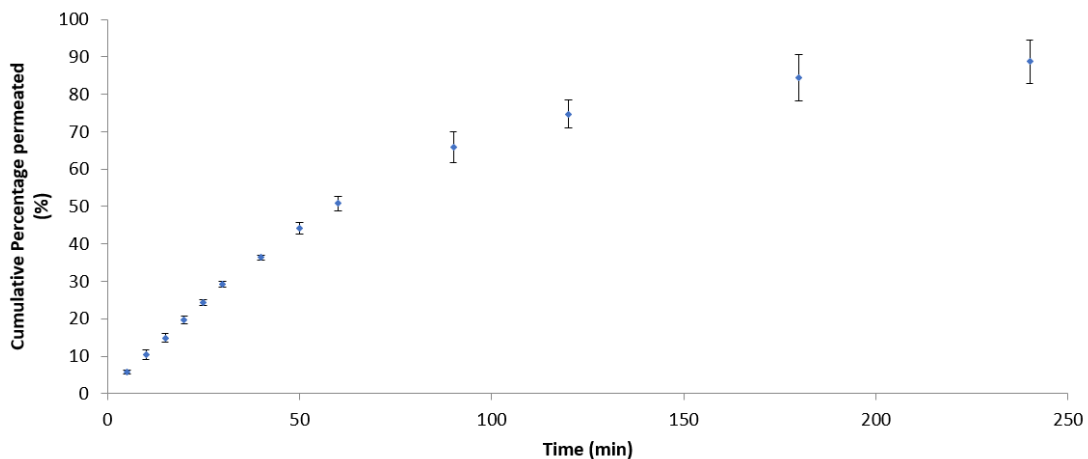
**Figure 33** - Permeation profile using (a) 0.2 µm polypropylene filters and (b) 80 µm nylon filters.

As expected, no permeation resistance was enforced by the filters and thus 100% cumulative drug content is achieved in a relatively short time, slightly earlier for the 80µm nylon filter. Consequently, the permeation profile not only reflects an absence of lag time phase as the membrane is readily permeable, but also the inability to determine the steady state slope as the number of time points is not narrower enough to track rapid permeation. Moreover, it can be concluded that no factors other than the membrane barrier affect diffusion.

### 2.2.3.3. Dialysis membrane

An in vitro permeation study was conducted using a dialysis membrane of 3500 Daltons molecular weight. These regenerated cellulose membranes were acquired *in-house* and its permeation profile as a membrane was assessed. The permeation profile is presented in Figure 34 a). Based on this profile, the steady-state slope was determined considering  $t_{\text{initial}}$  (min) =5 and  $t_{\text{final}}$  (min) =50 and is presented in Figure 34 b).

a)



b)

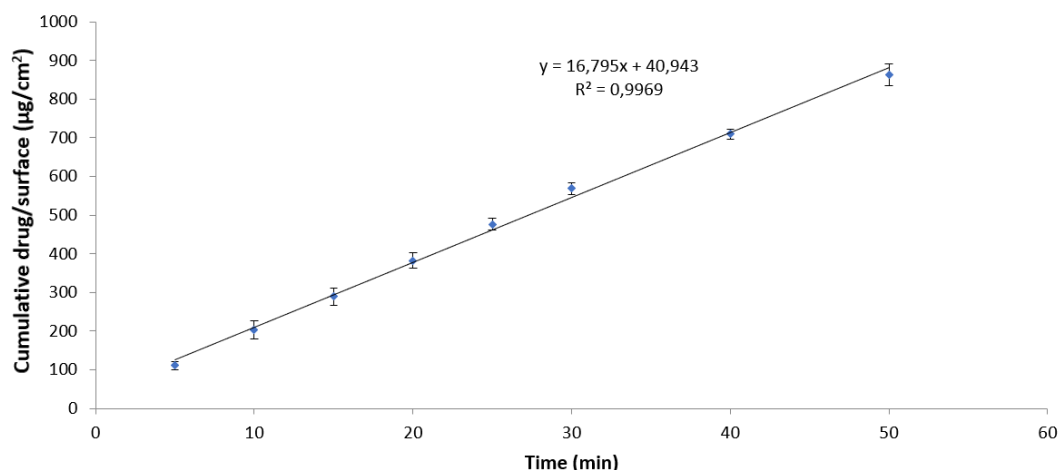


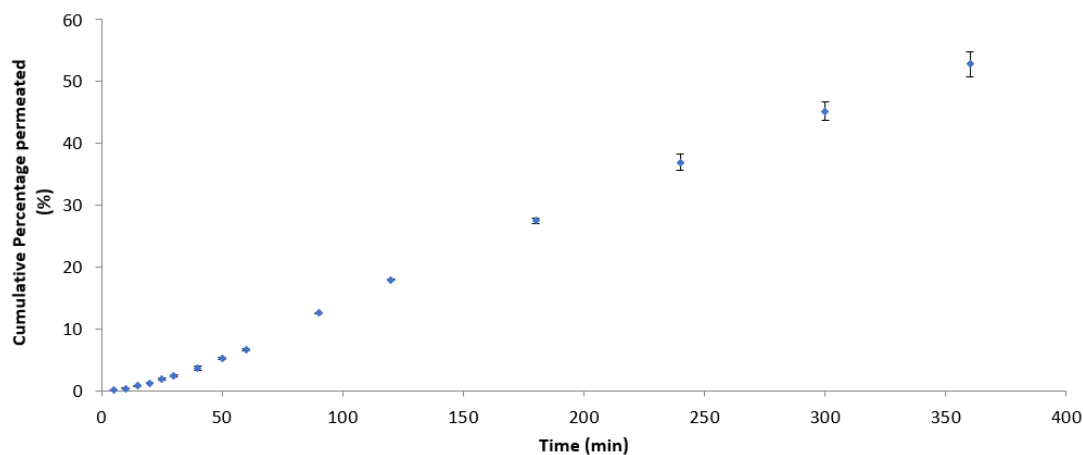
**Figure 34** - Representation of the (a) Permeation profile and (b) Steady-State slope from the permeation study using a dialysis membrane.

According to the permeation profile, the permeation parameters yielded a permeability flux ( $J_{ss}$ ) of  $16.79 \mu\text{g}/(\text{cm}^2 \cdot \text{min})$ , and an apparent permeability ( $P_{app}$ ) of  $45.32 \times 10^{-5} \text{ cm}/\text{min}$ . Regenerated cellulose membranes do not have any biomimetic properties as they are discriminatory based solely on the compounds molecular size. For this reason, the membrane is readily permeable, and no lag time phase is observed on the permeation profile.

#### 2.2.3.4. PermeaPad® Barrier membrane

For the *in vitro* permeation study employing a PermeaPad® Barrier membrane, it was verified that the more appropriate filling procedure is process number 2 (see **sub-section 2.2.2.2.**), because it maintains the membrane composition layers stable and viable. The permeation profile is presented in Figure 35 a). Based on this profile, the steady-state slope was determined considering  $t_{\text{initial}}$  (min) =40 and  $t_{\text{final}}$  (min) =240 and is presented in Figure 35 b).

a)





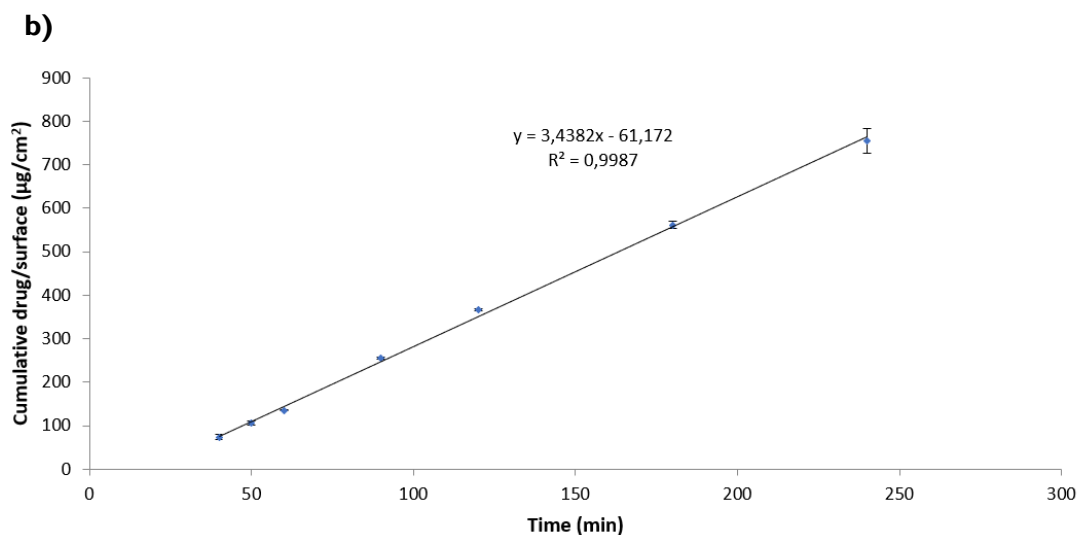
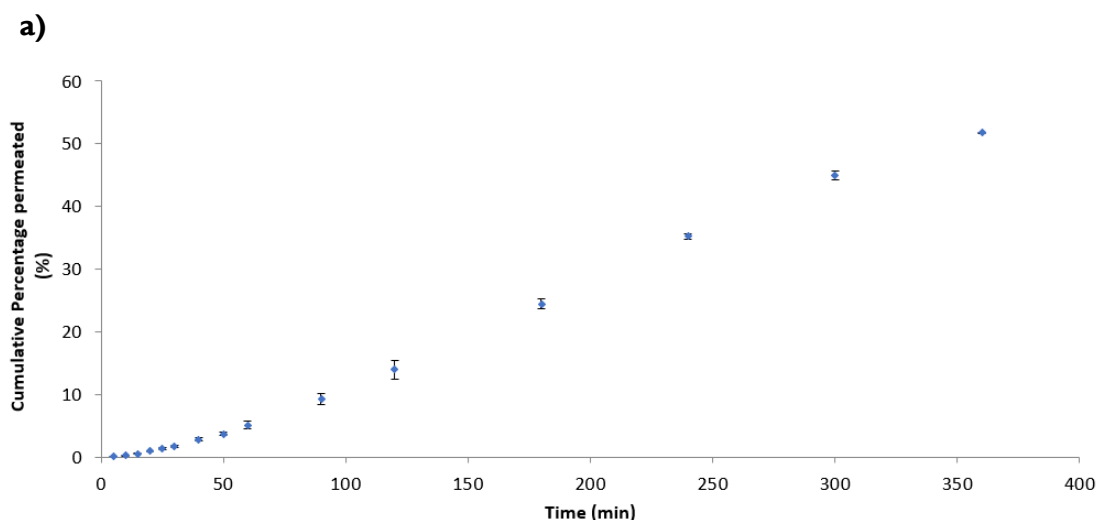


**Figure 35** - Representation of the **(a)** Permeation profile and **(b)** Steady-State slope from the permeation study using a PermeaPad® Barrier membrane.

According to permeation profile the permeation parameters rendered a permeability flux ( $J_{ss}$ ) of  $3.438 \mu\text{g}/(\text{cm}^2 \cdot \text{min})$ ; an apparent permeability ( $P_{app}$ ) of  $9.236 \times 10^{-5} \text{ cm}/\text{min}$ , and a lag time of 17.80 min. In contrast to regenerated cellulose membranes, the permeation profile obtained with the Permeapad® Barrier is, on the other hand, quite different: a lag time phase is clearly visible as well as a longer and more easily determined steady state slope. Moreover, more time point studies would be needed in order to obtain a complete permeation profile, since 360min is not sufficient to certainly define the *plateau* phase.

To validate the results obtained from the first permeation study with the PermeaPad® Barrier membrane, the same test was repeated. The permeation profile is presented in Figure 36 a). The steady-state slope was determined considering  $t_{\text{initial}}$  (min) = 50 and  $t_{\text{final}}$  (min) = 300, based on the permeation profile, and is presented in Figure 36 b).



b)

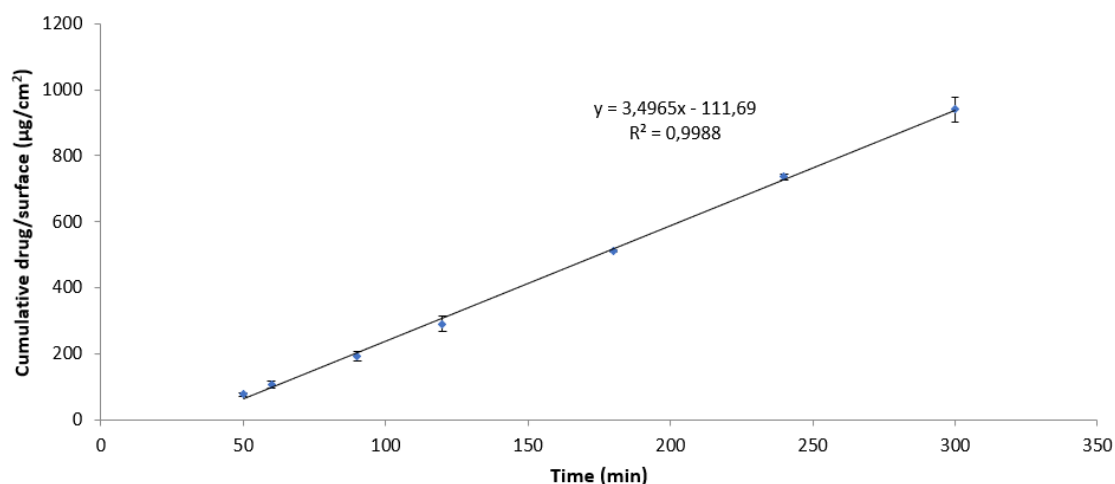


**Figure 36** - Representation of the (a) Permeation profile and (b) Steady-State slope from the permeation study (#2) using a PermeaPad® Barrier membrane.

According to permeation profile the permeation parameters showed the values of: permeability flux ( $J_{ss}$ ,  $\mu\text{g}/(\text{cm}^2 \cdot \text{min}) = 3.497$ ; apparent permeability ( $P_{app}$ ,  $\text{cm}/\text{min} (\times 10^{-5}) = 9.500$  and a lag time of 31.94.

Table 43 resumes the permeation studies using the prototype and different artificial membranes.

**Table 43** - Permeation Studies summary using different artificial membranes.

Formulation	Membrane	Steady-State (min)		$J_{ss}$ $\mu\text{g}/(\text{cm}^2 \cdot \text{min})$	$P_{app}$ $(\times 10^{-5} \text{ cm}/\text{min})$	Lag Time (min)
		$t_{initial}$	$t_{final}$			
Prototype	Filters	a)	a)	a)	a)	a)
	Dialysis	5	50	16.79	45.32	b)
	PermeaPad® Test #1	40	240	3.438	9.236	17.80
	PermeaPad® Test #2	50	300	3.497	9.500	31.94

a) Not possible to clearly determine the steady-state and permeation coefficients as the drug permeation was very fast.

b) Absence of lag time.

This evaluation allowed for the comprehension of the permeation profile and validation of our method to discriminate amongst distinct membranes.

The permeation coefficients through filters were not measurable due to the faster diffusion as no barrier is offered to drug permeation. As for the dialysis membrane and Permeapad®, the dialysis membrane demonstrated higher apparent permeability than Permeapad® Barrier

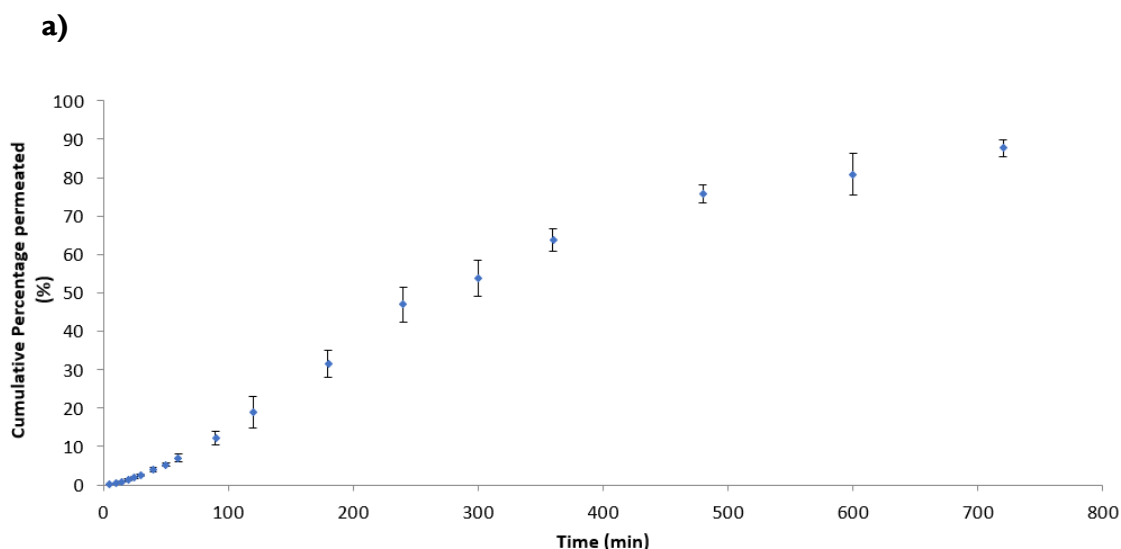
membrane as it creates a barrier based on the molecular size whereas Permeapad® biomimetic properties reflects its role as a good barrier to use in permeability studies. In the case of Permeapad®, no plateau was achieved; however, although it is fundamental to recognize the beginning and end of the steady-state phase in the permeation profile to determine permeability coefficients and steady-state flux, it is not necessary to reach 100% of the drug amount permeated. Moreover, the two permeation tests using Permeapad® Barrier membrane reflected similar permeability coefficients and permeation profiles to each other, reinforcing the method reproducibility.

## 2.2.4. Permeation studies using Permeapad® Barrier membrane

### 2.2.4.1. Finite Dose vs Infinite Dose conditions

A permeation study under finite conditions was conducted in order to assess drug formulation application under 'in-use' conditions. Samples of 200µL of the receptor solution were collected at 5, 10, 15, 20, 25, 30, 40, 50, 60, 90, 120, 180, 240, 300, 360, 480, 600, 720 minutes (time points).

The permeation profile is presented in Figure 37 a). Based on this profile, the steady-state slope was determined considering  $t_{\text{initial}}$  (min) =50 and  $t_{\text{final}}$  (min) =240 and is presented in Figure 37 b).



b)

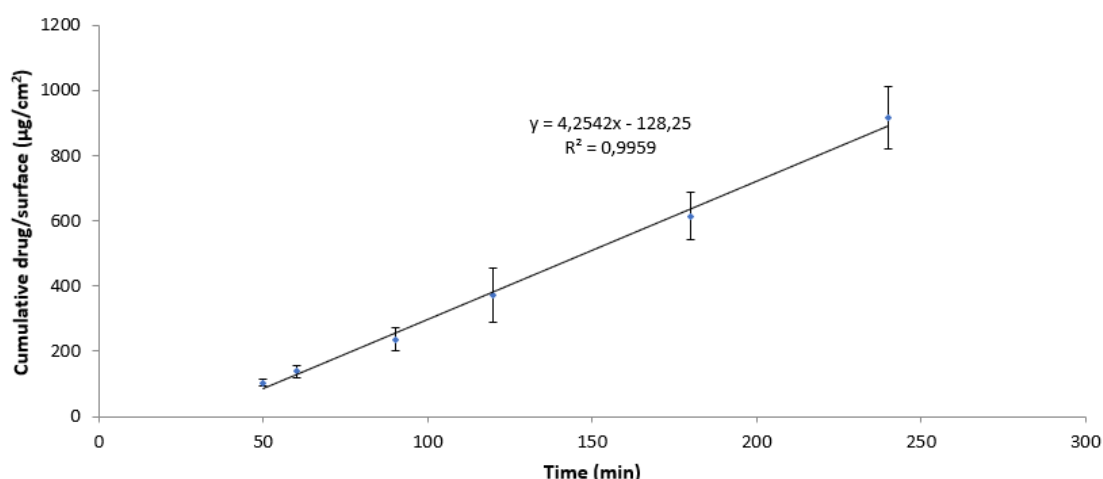


**Figure 37** - Representation of the (a) Permeation profile and (b) Steady-State slope from the permeation study using a PermeaPad® Barrier membrane under finite dose conditions.

The maintenance of sink conditions along the permeation profile was assessed. According to the results shown in Table 44, at the last time point contemplating the steady state phase ( $t_{\text{final}}$  (min) = 240) the experiment is still being conducted under sink conditions. Only when reaching 480min collection time point is that the drug concentration in the receptor solution falls higher than the limit defined previously (Concentration (mg/mL) = 0.193).

**Table 44** - Assessment of sink conditions at time points 240min, 360min and 480min from collecting 200µL of the receptor solution under Finite dose conditions. Key: SS = steady-state.

Permeation Profile	Time points		Target for sink conditions: 0.193 mg/mL	
			Concentration (mg/mL)	Evaluation
SS $t_{\text{final}}$ (min)	240min	FC1	0.146	<b>Complies</b>
		FC2	0.120	
		FC3	0.127	
Plateau Phase	360min	FC1	0.182	<b>Complies</b>
		FC2	0.165	
		FC3	0.176	
	480min	FC1	0.210	<b>Does not comply</b>
		FC2	0.198	
		FC3	0.209	

With the aim of performing a more thorough assessment of permeability coefficients, the permeation study was performed under infinite dose conditions, where a higher amount of dose formulation is applied. For this reason, sink conditions are more easily lost, and therefore, to prevent this situation, an increase in the collection volume was made (500µL).

Based on the precision and accuracy results presented in Table 39, the volume in the micropipette was adjusted to 535 $\mu$ L.

The permeation profile of permeation study under infinite dose conditions collecting 500 $\mu$ L is presented in Figure 38 a). Based on the profile, the steady-state slope was determined considering  $t_{\text{initial}}$  (min) =60 and  $t_{\text{final}}$  (min) =360, which is presented in Figure 38 b).

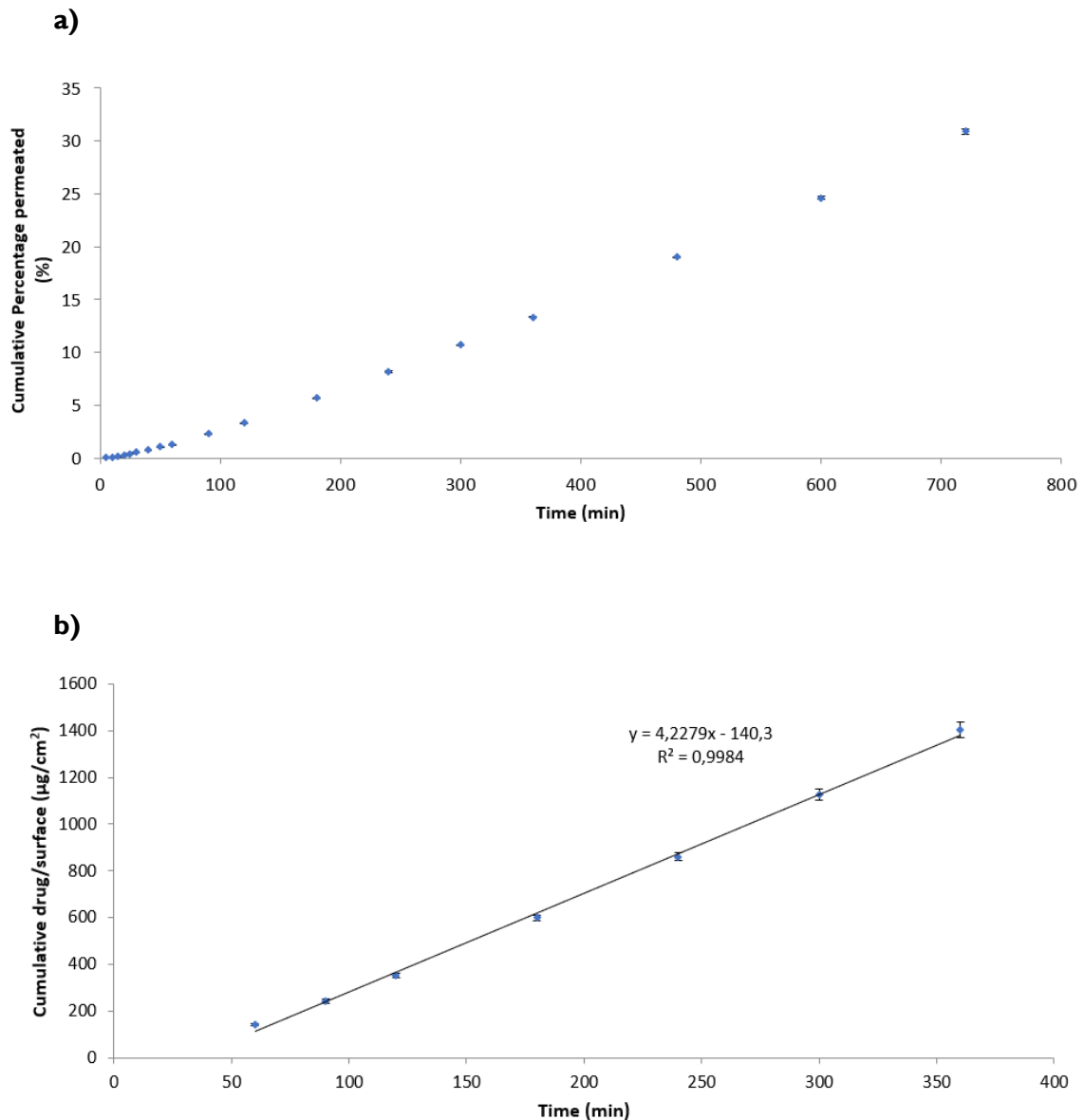


**Figure 38** - Representation of the **(a)** Permeation profile and **(b)** Steady-State slope from the permeation study using a PermeaPad<sup>®</sup> Barrier membrane under infinite dose conditions, collecting 500 $\mu$ L of receptor solution.

According to Table 45, sink conditions were maintained under infinite dose conditions during 360min throughout the permeation test.

**Table 45** - Assessment of sink conditions at time points 240min, 360min and 480min from collecting 500µL of the receptor solution under infinite dose conditions.

Permeation Profile	Time points		Target for sink conditions: 0.193 mg/mL	
			Concentration (mg/mL)	Evaluation
SS $t_{final}$ (min)	240min	FC1	0.116	<b>Complies</b>
		FC2	0.119	
Plateau Phase	360min	FC1	0.183	<b>Complies</b>
		FC2	0.189	
	480min	FC1	0.216	<b>Does not comply</b>
		FC2	0.209	

Figure 39 shows the permeation profile (a) and steady state slope (b) respectively, prior to plotting the permeation results from finite dose conditions collecting 200µL and infinite dose conditions collecting 500µL.

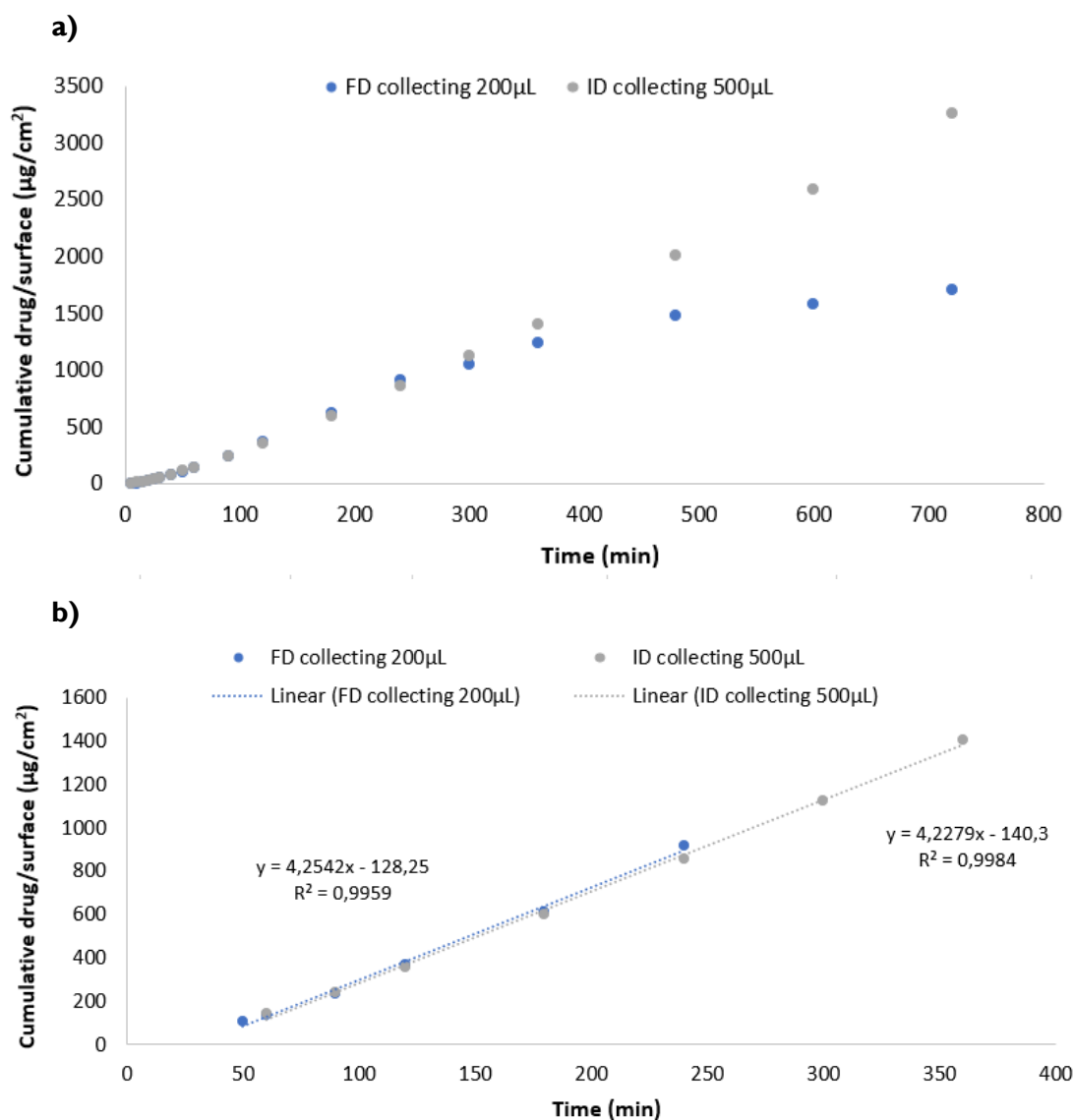


**Figure 39** - Representation of the (a) Permeation profile and (b) Steady-State slope from the permeation study using a PermeaPad® Barrier membrane under FD conditions collecting 0.2mL and ID conditions collecting 500uL of receptor solution.

Comparing finite dose conditions study with infinite dose conditions study, a lag time phase is equally noticeable, as well as a similar steady state phase. Moreover, the identical permeation profile from both the permeation studies demonstrated a non-implication from the alteration of the collection volume. From the time point of 480 minutes, the finite dose application approaches the plateau phase, as the variation between donor and receptor chamber keeps reducing, owing to donor drug depletion. On the other hand, the study under infinite dose conditions carries on with the steady state phase, as the high amount of drug present in the donor chamber leads to a constant drug concentration in the donor chamber i.e., no change in the thermodynamic activity exists.

Sink conditions are not maintained from the time point 480 minutes; nonetheless, the linear profile presented reflect no impact from the higher concentration on the compound solubility i.e., permeation.

In Table 46, it is presented the permeability coefficients results from the previous reported permeation profiles.

**Table 46** - Permeability coefficients results from Finite Dose (FD) conditions collecting 200 $\mu$ L; Infinite Dose (ID) conditions collecting 500 $\mu$ L.

Dose Conditions	Collection Volume ( $\mu$ L)	Average
		Papp ( $\times 10^{-5}$ cm/min)
FD	200	10.63
ID	500	10.52
	<b>Average</b>	10.58
	<b>STD</b>	0.08
	<b>RSD (%)</b>	0.01

From these results, it can be concluded that permeability coefficients between the two permeation studies were not significantly different.

### 2.2.5. Inclusion of permeation enhancer

The inclusion of permeation enhancers in drug formulations are a very common strategy to improve the API permeation, which will depend on its physicochemical properties. The permeation enhancer used to assess its impact on our drug formulations as well as our method selectivity is, according to the literature, described to act by disruption of the phospholipidic layer i.e., integrity of the epithelium.

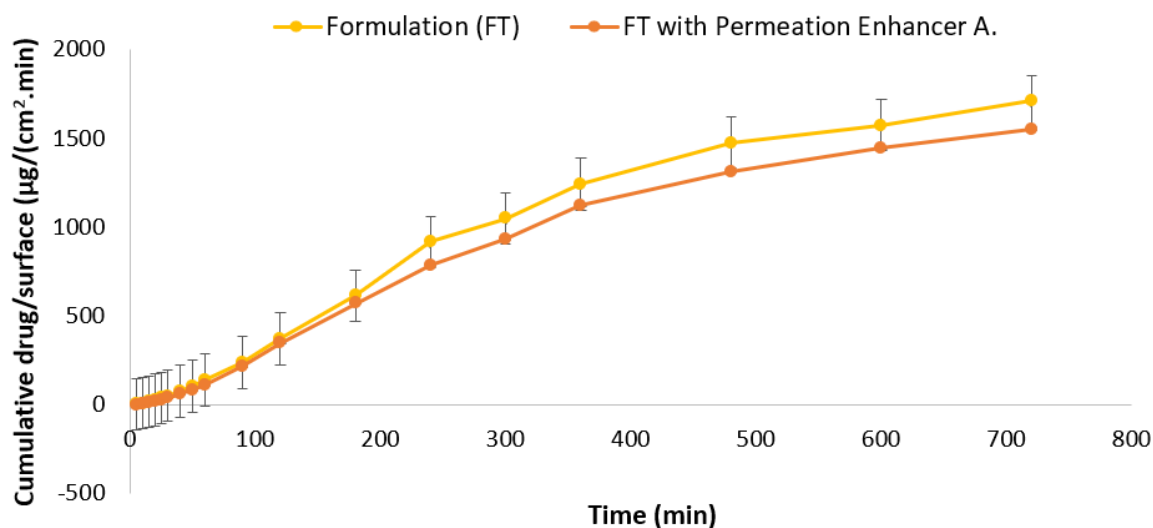
A permeation study was conducted under finite dose conditions for the assessment of *formulation (FT) + permeation enhancer A*. Samples of 200 $\mu$ L of the receptor solution were collected at 5, 10, 15, 20, 25, 30, 40, 50, 60, 90, 120, 180, 240, 300, 360, 480, 600 and 720 minutes (time points).

For the purpose of comparison, the results are summarized in Table 47, and the permeation profile and apparent permeability chart are shown in Figure 40 a) and b), respectively.

**Table 47** - Permeability coefficients results from the permeation study with **i)** formulation and **ii)** formulation including permeation enhancer A.; under finite dose conditions. Results are expressed as mean  $\pm$  standard deviation,  $n=2^*$  and  $n=3^{**}$ .

Drug formulation	$J_{ss}$ ( $\mu\text{g}/(\text{cm}^2 \cdot \text{min})$ )	$P_{app}$ ( $\times 10^{-5}$ cm/min)	Lag Time (min)
Formulation	$3.4 \pm 0.2^*$	$8.5 \pm 0.5^*$	$19 \pm 3^*$
FT with permeation enhancer A.	$3.57 \pm 0.02^{**}$	$8.82 \pm 0.05^{**}$	$24 \pm 7^{**}$

a)





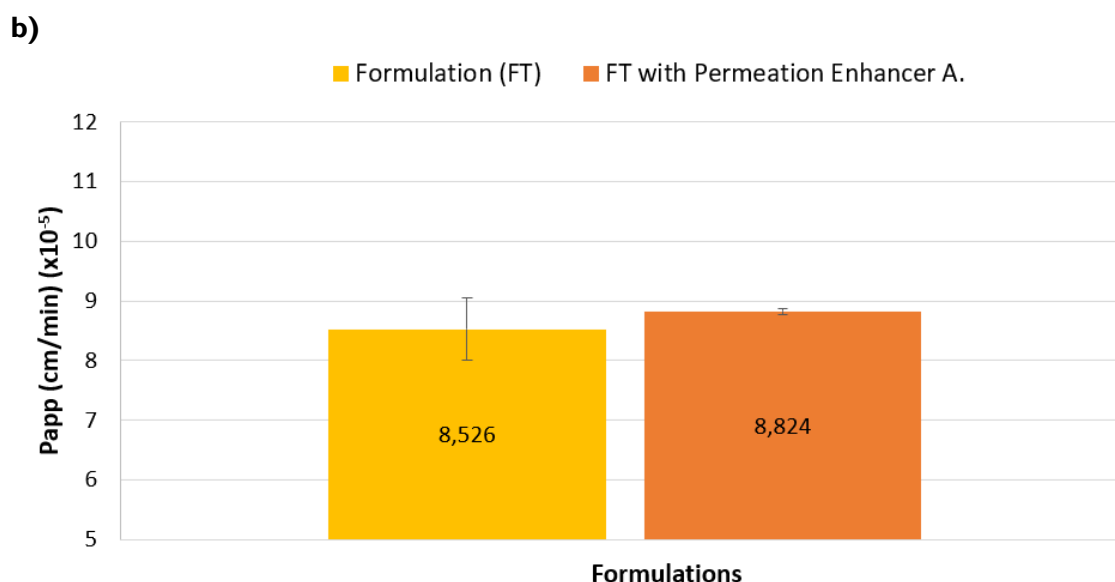


**Figure 40** - Representation of (a) permeation profile and (b) apparent permeability ( $P_{app}$ ) from the permeation study applying the formulation without permeation enhancer (FT) and upon the inclusion of permeation enhancer A. (FT with Permeation Enhancer A.); under FD conditions collecting 200 $\mu$ L of receptor solution. Results are expressed as mean  $\pm$  standard deviation.

Analyzing the results shown previously, it can be noticed that under finite dose conditions, only a slight increase in the apparent permeability is observed for the formulation with the permeation enhancer A. On the other hand, a plateauing region is denoted after the steady-state phase, which may prevent a significant time-dependent permeation increase to be reflected.

To substantiate such findings, a study under infinite dose conditions is needed, where the steady-state phase would be prolonged and consequently, a more insight on the permeability coefficients as well as a more accurate and robust conclusion would be possible.

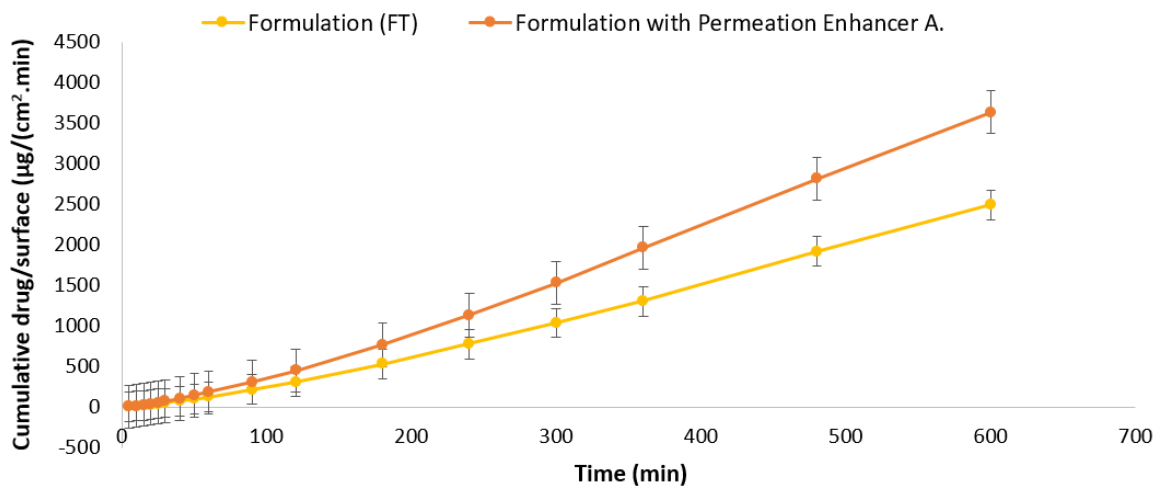
Following this rational, a permeation study was conducted under infinite dose conditions for the assessment of *formulation (FT) + permeation enhancer A*. Samples of 500 $\mu$ L of the receptor solution were collected at 5, 10, 15, 20, 25, 30, 40, 50, 60, 90, 120, 180, 240, 300, 360, 480, 600 minutes (time points). The results are summarized in Table 48, and the permeation profile and apparent permeability chart are shown in Figure 41 a) and b), respectively.

**Table 48** - Permeability coefficients results from the permeation study with **i)** formulation and **ii)** formulation including permeation enhancer A, under infinite dose conditions. Results are expressed as mean  $\pm$  standard deviation, n=6.

Drug formulation	$J_{ss}$ $\mu\text{g}/(\text{cm}^2 \cdot \text{min})$	$P_{app}$ $(\times 10^{-5} \text{ cm}/\text{min})$	Lag Time (min)
Formulation	$4.0 \pm 0.6$	$10 \pm 1$	$41 \pm 15$
FT + permeation enhancer A.	$5.9 \pm 0.3^*$	$14.5 \pm 0.8^*$	$42 \pm 11^*$

\* Statistical analysis from Student's *t*-tests between formulation and formulation with permeation enhancer A.  $J_{ss}$  and  $P_{app}$  values were considered significantly different ( $p < 0.05$ ), and lag time not significantly different ( $p > 0.05$ ).

a)



b)

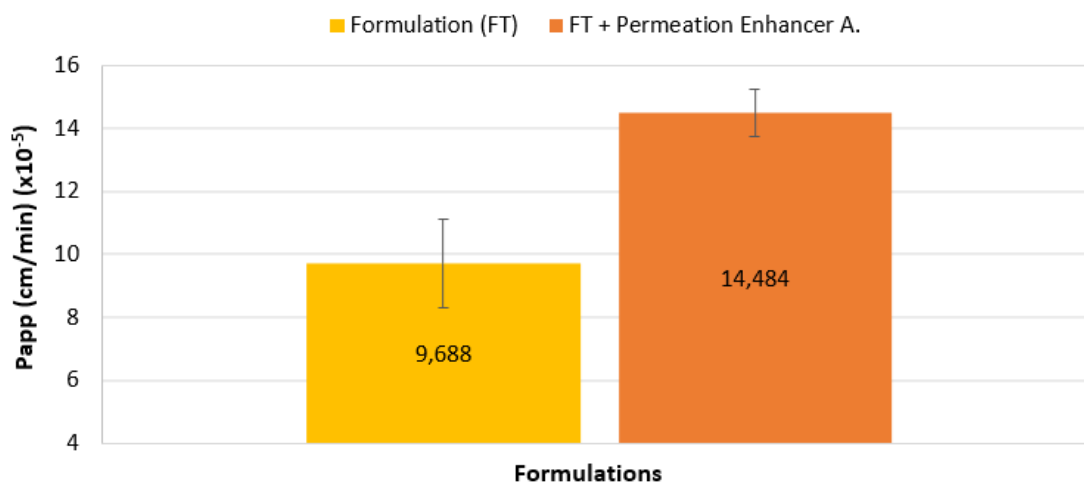


**Figure 41** - Representation of **(a)** permeation profile and **(b)** apparent permeability ( $P_{app}$ ) chart from the permeation study applying the formulation without permeation enhancers (FT) and upon the inclusion of permeation enhancer A. (FT with Permeation Enhancer A.); under ID conditions collecting 500  $\mu\text{L}$  of receptor solution. Results are expressed as mean  $\pm$  standard deviation, n=6. Apparent permeability ( $P_{app}$ ) values were considered significantly different ( $p < 0.05$ ) based on a Student's *t*-test analysis.

Under infinite dose conditions, a significant increase in permeation flux and apparent permeability is observed after incorporation of the permeation enhancer into the drug formulation, supporting the relevance of the applied dose for better discrimination of permeation outcomes. Also, it should be noted that a similar lag time is obtained between the permeation profiles of the two formulations.



# *Chapter 3.*

## *Concluding Remarks and Future Perspectives*



The work reported in this Dissertation reflects the successful development of a reproducible *in-vitro* method to assess the buccal permeation of drug formulations. This permeation method may be divided into: i) method *set-up*, which comprised a Franz Diffusion Cell apparatus and a biomimetic membrane - Permeapad® Barrier - where tests were performed regarding air bubbles formation, temperature, collection techniques, filling procedure and study dose conditions; in order to achieve an optimum and biorelevant procedure; ii) analytical HPLC based method with the purpose of quantifying the total amount of drug in the formulation - Content - and the amount of drug permeated through the permeation profile - Permeation Profile. These methods were then implemented in Bluepharma with the purpose of optimization of internal in-development formulations.

Based on the significant permeation improvement shown in the studies regarding the inclusion of an permeation enhancer into the drug formulation, our method is apparently able to discriminate the effect of permeation enhancers effect on the permeation behavior of drugs. Nevertheless, replication of the previous permeation enhancement studies will be necessary to validate the results.

In terms of future work, investigating permeation enhancers that act through distinct mechanisms than those tested in this work and at different concentrations would also provide further insight into whether this biomimetic membrane - Permeapad® Barrier - is sensitive to other enhancement mechanisms and its response to the influence of their concentration in the drug formulation. Further steps would include the study of other APIs with distinct physicochemical properties from the one exploited in this work.

Moreover, the development of an *ex vivo* method is already taking place with the aim of obtaining an *in vitro* - *ex vivo* correlation, and, in addition, to verify the response of membranes from animal tissue to the effect of permeation enhancers. Porcine buccal membrane was selected as it is the most suitable tissue model for the assessment of buccal drug delivery, resembling the human buccal tissue in structure, morphology, thickness, and composition. Complementary findings are thus expected to obtain, so that a more a more robust model could be established.





## References

- (1) PINTO, Soraia; PINTADO, Manuela E.; SARMENTO, Bruno - In vivo, ex vivo and in vitro assessment of buccal permeation of drugs from delivery systems. *Expert Opinion on Drug Delivery*. ISSN 17447593. 17:1 (2020) 33–48.
- (2) HERRERA, Jorge L.; LYONS, Michael F.; JOHNSON, Lawrence F. - Saliva: Its role in health and disease. *Journal of Clinical Gastroenterology*. ISSN 15392031. 10:5 (1988) 569–578.
- (3) BALIGA, Sharmila; MUGLIKAR, Sangeeta; KALE, Rahul - Salivary pH: A diagnostic biomarker. *Journal of Indian Society of Periodontology*. ISSN 0972124X. 17:4 (2013) 461–465.
- (4) HUMPHREY, Sue P.; WILLIAMSON, Russell T. - A review of saliva: Normal composition, flow, and function. *Journal of Prosthetic Dentistry*. ISSN 00223913. 85:2 (2001) 162–169.
- (5) MACEDO, Ana S. et al. - Novel and revisited approaches in nanoparticle systems for buccal drug delivery. *Journal of Controlled Release*. ISSN 18734995. 320: October 2019 (2020) 125–141.
- (6) CAMPISI, G. et al. - Human Buccal Mucosa as an Innovative Site of Drug Delivery. *Current Pharmaceutical Design*. ISSN 13816128. 16:6 (2010) 641–652.7.
- (7) Hao J, Heng PWS. Buccal delivery systems. *Drug Dev Ind Pharm*. (2003);29(8):821–32.
- (8) VEUILLEZ, F. et al. - Factors and strategies for improving buccal absorption of peptides. *European Journal of Pharmaceutics and Biopharmaceutics*. ISSN 09396411. 51:2 (2001) 93–109
- (9) HARRIS, David; ROBINSON, Joseph R. - Drug delivery via the mucous membranes of the oral cavity. *Journal of Pharmaceutical Sciences*. ISSN 15206017. 81:1 (1992) 1–10.
- (10) SQUIER, C. A.; KREMER, M. J. - Biology of oral mucosa and esophagus. *Journal of the National Cancer Institute*. Monographs. ISSN 10526773. 52242:29 (2001) 7–15. 11.
- (11) Sattar M, Sayed OM, Lane ME. Oral transmucosal drug delivery - Current status and future prospects. *Int J Pharm*. (2014);471(1–2):498-506.
- (12) TOLO, K. J. - STUDY OF EPITHELIUM PERMEABILITY OF GINGIVAL POCKET TO ALBUMIN IN GUINEA PIGS AND NORWEGIAN PIGS. *Archives of Oral Biology*. 16 (1971) 881–888.
- (13) STEPHENS, P.; GENEVER, P. - Non-epithelial oral mucosal progenitor cell populations. 44: March 2006 (2007) 1–10. 14.
- (14) SOHI, Harmik et al. - Critical evaluation of permeation enhancers for oral mucosal drug delivery. *Drug Development and Industrial Pharmacy*. ISSN 15205762. 36:3 (2010) 254–282.
- (15) SQUIER, C. A.; NANNY, D. - Measurement of blood flow in the oral mucosa and skin of the rhesus monkey using radiolabelled microspheres. *Archives of Oral Biology*. ISSN 00039969. 30:4 (1985) 313–318.
- (16) COLLINS, L. M. C.; DAWES, C. - The Surface Area of the Adult Human Mouth and Thickness of the Salivary Film Covering the Teeth and Oral Mucosa. *Journal of Dental Research*. ISSN 15440591. 66:8 (1987) 1300–1302.
- (17) MASHRU, Rajashree et al. - Transbuccal delivery of lamotrigine across porcine buccal mucosa: In vitro determination of routes of buccal transport. *Journal of Pharmacy and Pharmaceutical Sciences*. ISSN 14821826. 8:1 (2005) 54–62.

- (18) MASHRU, Rajashree et al. - Transbuccal delivery of lamotrigine across porcine buccal mucosa: In vitro determination of routes of buccal transport. *Journal of Pharmacy and Pharmaceutical Sciences*. ISSN 14821826. 8:1 (2005) 54–62.
- (19) SATHEESH MADHAV, Nookala Venkala et al. - Recent trends in oral transmucosal drug delivery systems: An emphasis on the soft palatal route. *Expert Opinion on Drug Delivery*. ISSN 17425247. 9:6 (2012) 629–647.
- (20) SQUIER, C. A. - The permeability of oral mucosa. *Critical Reviews in Oral Biology and Medicine*. ISSN 10454411. 2:1 (1991) 13–32.
- (21) RADHA, Bhati; RAJA, Nagrajan - A detailed review on oral mucosa drug delivery system. *International Journal of Pharmaceutical Sciences and Research*. 3:03 (2012) 659–681.
- (22) ROSSI, Silvia; SANDRI, Giuseppina; CAMELLA, Carla M. - Buccal drug delivery: A challenge already won? *Drug Discovery Today: Technologies*. . ISSN 17406749. 2:1 (2005) 59–65
- (23) ATHBONE, Michael J.; TUCKER, Ian G. - Mechanisms, barriers and pathways of oral mucosal drug permeation. *Advanced Drug Delivery Reviews*. . ISSN 0169409X. 12:1–2 (1993) 41–60.
- (24) MASHRU, Rajashree et al. - Transbuccal delivery of lamotrigine across porcine buccal mucosa: In vitro determination of routes of buccal transport. *Journal of Pharmacy and Pharmaceutical Sciences*. . ISSN 14821826. 8:1 (2005) 54–62.
- (25) SALAMAT-MILLER, Nazila; CHITTCHANG, Montakarn; JOHNSTON, Thomas P. - The use of mucoadhesive polymers in buccal drug delivery. *Advanced Drug Delivery Reviews*. ISSN 0169409X. 57:11 (2005) 1666–1691.
- (26) DAVIS, Belinda J.; JOHNSTON, A.; TURNER, P. - Buccal absorption of verapamil- evidence for membrane storage. *British Psychological Society*. (1979) 434–435.
- (27) NICOLAZZO, Joseph A.; REED, Barry L.; FINNIN, Barrie C. - Buccal penetration enhancers - How do they really work? *Journal of Controlled Release*. ISSN 01683659. 105:1–2 (2005) 1–15.
- (28) HENRY, J. A. et al. - Drug recovery following buccal absorption of propranolol. *Br. J. clin. Pharmacol.* 10 (1980) 61–65.
- (29) MANNING, A. S.; EVERED, D. F. - The absorption of sugars from the human buccal cavity. *Clinical Science and Molecular Medicine*. ISSN 03010538. 51:2 (1976) 127–132.
- (30) OYAMA, Yujiro et al. - Carrier-mediated transport systems for glucose in mucosal cells of the human oral cavity. *Journal of Pharmaceutical Sciences*. ISSN 00223549. 88:8 (1999) 830–834.
- (31) UTOGUCHI, Naoki et al. - Carrier-mediated absorption of salicylic acid from hamster cheek pouch mucosa. *Journal of Pharmaceutical Sciences*. ISSN 00223549. 88:1 (1999) 142–146.
- (32) KUROSAKI, Yuji et al. - Existence of a specialized absorption mechanism for cefadroxil, an aminocephalosporin antibiotic, in the human oral cavity. *International Journal of Pharmaceutics*. ISSN 03785173. 82:3 (1992) 165–169.
- (33) SADOOGH-ABASIAN, F.; EVERED, D. F. - Absorption of vitamin C from the human buccal cavity. *British Journal of Nutrition*. ISSN 0007-1145. 42:1 (1979) 15–20.

- (34) D.F. EVERED, F. SADOOH-ABASIAN, P. Patel - Absorption of nicotinic acid and nicotinamide across human buccal mucosa in vivo. *Em Life Sciences*, (1980) Vol. 27. p. 1649–1651.
- (35) NARANG, Neha; SHARMA, Jyoti - Sublingual mucosa as a route for systemic drug delivery. *International Journal of Pharmacy and Pharmaceutical Sciences*. ISSN 09751491. 3: SUPPL. 2 (2011) 18–22.
- (36) BHAL, Sanjivanjit K. - Application Note Lipophilicity Descriptors: Understanding When to Use Log P & Log D Application of Lipophilicity Descriptors in Drug. ACD/Labs - Advanced Chemistry Development, Inc. Toronto, Canada. (2019) 3–6.
- (37) KOKATE, Amit et al. - In silico prediction of drug permeability across buccal mucosa. *Pharmaceutical Research*. ISSN 07248741. 26:5 (2009) 1130–1139.
- (38) DENEER, V. H. M. et al. - Buccal transport of flecainide and sotalol: Effect of a bile salt and ionization state. *International Journal of Pharmaceutics*. ISSN 03785173. 241:1 (2002) 127–134.
- (39) ŞENEL, S. et al. - In vitro studies on enhancing effect of sodium glycocholate on transbuccal permeation of morphine hydrochloride. *Journal of Controlled Release*. ISSN 01683659. 51:2–3 (1998) 107–113.
- (40) DIAZ-DEL CONSUELO, Isabel et al. - Comparison of the lipid composition of porcine buccal and esophageal permeability barriers. *Archives of Oral Biology*. ISSN 00039969. 50:12 (2005) 981–987.
- (41) JACOBSEN, Jette et al. - TR146 cells grown on filters as a model for human buccal epithelium: I. Morphology, growth, barrier properties, and permeability. *International Journal of Pharmaceutics*. . ISSN 03785173. 125:2 (1995) 165–184.
- (42) MØRCK NIELSEN, Hanne; RØMER RASSING, Margrethe - TR 146 cells grown on filters as a model of human buccal epithelium: V. Enzyme activity of the TR146 cell culture model, human buccal epithelium and porcine buccal epithelium, and permeability of leu-enkephalin. *International Journal of Pharmaceutics*. ISSN 03785173. 200:2 (2000) 261–270.
- (43) PADERNI, Carlo et al. - Oral local drug delivery and new perspectives in oral drug formulation. *Oral Surgery, Oral Medicine, Oral Pathology and Oral Radiology*. ISSN 22124403. 114:3 (2012).
- (44) SQUIER, C. A.; ROONEY, Lynn - The Permeability of Keratinized and Nonkeratinized Oral Epithelium to Lanthanum In Vivo - *Journal of Ultrastructure Research*. 295 (1976) 286–295.
- (45) SQUIER, C. A. - The permeability of keratinized and nonkeratinized oral epithelium to horseradish peroxidase. *Journal of Ultrastructure Research*. ISSN 00225320. 43:1–2 (1973) 160–177.
- (46) ALFANO, Michael C.; DRUMMOND, James F.; MILLER, Sanford A. - Localization of Rate-Limiting Barrier to Penetration of Endotoxin Through Nonkeratinized Oral Mucosa In Vitro. *Journal of Dental Research* (1975).
- (47) HAUGEN, Ellen; JOHANSEN, Jan R. - Penetration of the oral mucosa by radiolabelled chlorhexidine in guinea pigs. *Acta Odontologica Scandinavica*. ISSN 00016357. 33:6 (1975) 365–372.
- (48) JACOBSEN, Jette - Buccal iontophoretic delivery of atenolol HCl employing a new in vitro three-chamber permeation cell. *Journal of Controlled Release*. ISSN 01683659. 70:1–2 (2001) 83–95.
- (49) PATEL, Mangala P. et al. - Electrically induced transport of macromolecules through oral buccal mucosa. *Dental Materials*. ISSN 01095641. 29:6 (2013) 674–681.

- (50) CHINNA REDDY, P.; CHAITANYA, K. S. C.; MADHUSUDAN RAO, Y. - A review on bioadhesive buccal drug delivery systems: Current status of formulation and evaluation methods. *DARU, Journal of Pharmaceutical Sciences*. ISSN 15608115. 19:6 (2011) 385–403.
- (51) SHARMA, S.; KULKARNI, J.; PAWAR, A. P. - Permeation enhancers in the transmucosal delivery of macromolecules. *Pharmazie*. ISSN 00317144. 61:6 (2006) 495–504.
- (52) HASSAN, Nisreen et al. - Chemical permeation enhancers for transbuccal drug delivery. *Expert Opinion on Drug Delivery*. ISSN 17425247. 7:1 (2010) 97–112.
- (53) SCHOLZ, Oliver A. et al. - Drug delivery from the oral cavity: focus on a novel mechatronic delivery device. *Drug Discovery Today*. ISSN 13596446. 13:5–6 (2008) 247–253.
- (54) MANOHAR, Shinkar Dattatraya; SRIDHAR, Dhake Avinash; MALLIKARJUNA, Setty Chitral - Drug delivery from the oral cavity: A focus on mucoadhesive buccal drug delivery systems. *PDA Journal of Pharmaceutical Science and Technology*. ISSN 19482124. 66:5 (2012) 466–500.
- (55) WEI, Ran et al. - Effects of iontophoresis and chemical enhancers on the transport of lidocaine and nicotine across the oral mucosa. *Pharmaceutical Research*. ISSN 07248741. 29:4 (2012) 961–971.
- (56) OH, Dong Ho et al. - Enhanced transbuccal salmon calcitonin (sCT) delivery: Effect of chemical enhancers and electrical assistance on in vitro sCT buccal permeation. *European Journal of Pharmaceutics and Biopharmaceutics*. ISSN 18733441. 79:2 (2011) 357–363.
- (57) NICOLAZZO, Joseph A.; FINNIN, Barrie C. - In vivo and in vitro models for assessing drug absorption across the buccal mucosa. Em Ehrhardt C., Kim KJ. (eds) *Drug Absorption Studies. Biotechnology: Pharmaceutical Aspects*, vol. VII (2008).
- (58) PUDNEY, Paul D. A. et al. - A new in vivo Raman probe for enhanced applicability to the body. *Applied Spectroscopy*. ISSN 00037028. 66:8 (2012) 882–891.
- (59) NAIR, Anroop B. et al. - In vitro techniques to evaluate buccal films. *Journal of Controlled Release*. ISSN 01683659. 166:1 (2013) 10–21.
- (60) WANG, Shuangqing; ZUO, Along; GUO, Jianpeng - Types and evaluation of in vitro penetration models for buccal mucosal delivery. *Journal of Drug Delivery Science and Technology*. ISSN 17732247. 61 (2021).
- (61) SHOJAEI, Amir H. - Buccal mucosa as a route for systemic drug delivery: A review. *Journal of pharmaceutical sciences*. ISSN 09759344. (1998) 15-30.
- (62) CASTRO, Pedro et al. - Tissue-based in vitro and ex vivo models for buccal permeability studies. *Em Concepts and Models for Drug Permeability Studies: Cell and Tissue based In Vitro Culture Models*. [S.l.]: Elsevier Ltd (2016) ISBN 9780081001141. p. 189–202.
- (63) FRANZ-MONTAN, Michelle et al. - Evaluation of different pig oral mucosa sites as permeability barrier models for drug permeation studies. *European Journal of Pharmaceutical Sciences*. ISSN 18790720. 81(2016) 52–59.
- (64) KULKARNI, Upendra et al. - Porcine buccal mucosa as in vitro model: Effect of biological and experimental variables. *Journal of Pharmaceutical Sciences*. ISSN 00223549. 99:3 (2010) 1265–1277.
- (65) BRUN, P. P. H. LE et al. - In vitro penetration of some  $\beta$ -adrenoreceptor blocking drugs through porcine buccal mucosa. *International Journal of Pharmaceutics*. ISSN 03785173. 49:2 (1989) 141–145.

- (66) SQUIER, C. A.; LESCH, C. A. - Penetration pathways of different compounds through epidermis and oral epithelia. *Journal of Oral Pathology & Medicine*. ISSN 16000714. 17:9–10 (1988) 512–516.
- (67) VRIES, Monique E. DE et al. - Localization of the permeability barrier inside porcine buccal mucosa: a combined in vitro study of drug permeability, electrical resistance and tissue morphology. *International Journal of Pharmaceutics*. ISSN 03785173. 76:1–2 (1991) 25–35.
- (68) AMORES, Sonia et al. - A comparative ex vivo drug permeation study of beta-blockers through porcine buccal mucosa. *International Journal of Pharmaceutics*. ISSN 18733476. 468:1–2 (2014) 50–54.
- (69) SHRESTHA, Neha et al. - Cell-based in vitro models for buccal permeability studies. *Concepts and Models for Drug Permeability Studies: Cell and Tissue based In Vitro Culture Models*. (2016) 31–40.
- (70) NIELSEN, Hanne Mørck; RASSING, Margrethe Romer - Nicotine permeability across the buccal TR146 cell culture model and porcine buccal mucosa in vitro: Effect of pH and concentration. *European Journal of Pharmaceutical Sciences*. ISSN 09280987. 16:3 (2002) 151–157.
- (71) HOLM, René et al. - In vitro, ex vivo and in vivo examination of buccal absorption of metoprolol with varying pH in TR146 cell culture, porcine buccal mucosa and Göttingen minipigs. *European Journal of Pharmaceutical Sciences*. ISSN 09280987. 49:2 (2013) 117–124.
- (72) NIELSEN, Hanne Mørck; RASSING, Margrethe Rømer - TR146 cells grown on filters as a model of human buccal epithelium: IV. Permeability of water, mannitol, testosterone and  $\beta$ -adrenoceptor antagonists. Comparison to human, monkey and porcine buccal mucosa. *International Journal of Pharmaceutics*. ISSN 03785173. 194:2 (2000) 155–167.
- (73) MOHARAMZADEH, K. et al. - Tissue-engineered Oral Mucosa: a Review of the Scientific Literature. *Journal of Dental Research*. 86 (2007) 115–24.
- (74) BRANDL, Martin; BAUER-BRANDL, Annette - Oromucosal drug delivery: Trends in in-vitro biopharmaceutical assessment of new chemical entities and formulations. *European Journal of Pharmaceutical Sciences*. ISSN 18790720. 128: November 2018 (2019) 112–117.
- (75) RAI, Vishwas; TAN, Hock S.; MICHNIAK-KOHN, Bozena - Effect of surfactants and pH on naltrexone (NTX) permeation across buccal mucosa. *International Journal of Pharmaceutics*. ISSN 03785173. 411:1–2 (2011) 92–97.
- (76) GIOVINO, Concetta et al. - An integrated buccal delivery system combining chitosan films impregnated with peptide loaded PEG-b-PLA nanoparticles. *Colloids and Surfaces B: Biointerfaces*. ISSN 09277765. 112 (2013) 9–15.
- (77) KOSCHIER, Francis et al. - In vitro effects of ethanol and mouthrinse on permeability in an oral buccal mucosal tissue construct. *Food and Chemical Toxicology*. ISSN 02786915. 49:10 (2011) 2524–2529.
- (78) SCIENCES, MatTek Life - MatTek – Products, atual. 2021. [Accessed on 20 Feb 2021]. Available in: <https://www.mattek.com/products/epioral-epigingival/>.
- (79) PIO, Massimiliano - In vitro tools for predicting biopharmaceutical performance of drugs in vivo. *Eur J Pharm Sci*. (2014) 342–66.

- (80) BIBI, Hanady Ajine; HOLM, René; BAUER-BRANDL, Annette - Use of Permeapad® for prediction of buccal absorption: A comparison to in vitro, ex vivo and in vivo method. *European Journal of Pharmaceutical Sciences*. ISSN 18790720. 93 (2016) 399–404.
- (81) BIBI, Hanady Ajine et al. - Permeapad™ for investigation of passive drug permeability: The effect of surfactants, co-solvents and simulated intestinal fluids (FaSSIF and FeSSIF). *International Journal of Pharmaceutics*. ISSN 18733476. 493:1–2 (2015) 192–197.
- (82) FARIAS, Smirna; BOATENG, Joshua S. - In vitro, ex vivo and in vivo evaluation of taste masked low dose acetylsalicylic acid loaded composite wafers as platforms for buccal administration in geriatric patients with dysphagia. *International Journal of Pharmaceutics*. ISSN 18733476. May (2020).
- (83) KHDAIR, A. et al. - In vitro artificial membrane-natural mucosa correlation of carvedilol buccal delivery. *Journal of Drug Delivery Science and Technology*. ISSN 17732247. 23:6 (2013) 603–609.
- (84) MURA, Paola et al. - A preliminary study for the development and optimization by experimental design of an in vitro method for prediction of drug buccal absorption. *International Journal of Pharmaceutics*. ISSN 18733476. 547:1-2 (2018) 530-536.
- (85) TANOJO, Hanafi et al. - New design of a flow-through permeation cell for studying in vitro permeation studies across biological membranes. *Journal of Controlled Release*. ISSN 01683659. 45:1 (1997) 41-47.
- (86) VERHOECKX, Kitty et al. - The impact of food bioactives on health: In vitro and Ex Vivo models. *The Impact of Food Bioactives on Health: In Vitro and Ex Vivo Models* (2015) 1–327.
- (87) NICOLAZZO, Joseph A.; REED, Barry L.; FINNIN, Barrie C. - The Effect of Various in Vitro Conditions on the Permeability Characteristics of the Buccal Mucosa. *Journal of Pharmaceutical Sciences*. ISSN 00223549. 92:12 (2003) 2399–2410.
- (88) SCIENTIFIC INSTRUMENTS - Scientific Instruments – Products, atual. 2021. [Accessed on 16 Apr 2021]. Available in: <https://ussing-chamber.com/systems-products/ussing-chambers>.
- (89) GUY, R. C. - International Conference on Harmonisation. *Encyclopedia of Toxicology: Third Edition*. 2: November 1994 (2014) 1070–1072.
- (90) FDA - ICH Guideline Q8 on pharmaceutical development. 8: September (2004). [Accessed on 16 Apr 2021]. Available in: <https://www.ema.europa.eu/en/ich-q8-r2-pharmaceutical-development>.
- (91) PERAMAN, Ramalingam; BHADRAYA, Kalva; REDDY, Yiragamreddy Padmanabha - Analytical Quality by Design: A Tool for Regulatory Flexibility and Robust Analytics. *International Journal of Analytical Chemistry* (2015).
- (92) MURA, Paola et al. - A preliminary study for the development and optimization by experimental design of an in vitro method for prediction of drug buccal absorption. *International Journal of Pharmaceutics*. ISSN 18733476. 547:1–2 (2018) 530–536.
- (93) KOKATE, Amit; LI, Xiaoling; JASTI, Bhaskara - Effect of drug lipophilicity and ionization on permeability across the buccal mucosa: A technical note. *AAPS PharmSciTech*. ISSN 15309932. 9:2 (2008) 501–504.
- (94) PERMEGEAR INC. - Permegear-Products, atual. 2019. [Accessed on 18 Mar 2021]. Available in: <https://permegear.com/side-bi-side-cells>.

(95) LAU, Wing Man; NG, Keng Wooi - Finite and Infinite Dosing. In: Dragicevic N, Maibach HI (eds). Em Percutaneous Penetration Enhancers Drug Penetration Into/Through the Skin: Methodology and General Considerations. ISBN 9783662532706. p. 1-414.